Sea urchin sperm chemotaxis: individual effects and fertilization success

Yasmeen H. Hussain

A dissertation

submitted in partial fulfillment of the

requirements for the degree of

Doctor of Philosophy

University of Washington

2016

Reading Committee:

Jeffrey A. Riffell, Chair

Barbara T. Wakimoto

Charles H. Muller

Program Authorized to Offer Degree:

Department of Biology

i

University of Washington

Abstract

Sea urchin sperm chemotaxis: individual effects and fertilization success

Yasmeen H. Hussain

Chair of the Supervisory Committee:
Jeffrey A. Riffell
Department of Biology

Egg chemoattraction of conspecific sperm mediates fertilization, a critical juncture in

reproduction, especially in broadcast-spawning organisms like sea urchins. In the century that

sea urchin sperm chemotaxis was studied before I started my work, many discoveries were made

about the variety of peptide attractants that sea urchin eggs release into the ocean environment

and the molecular mechanisms of the sperm chemotactic response. However, many questions

were left unanswered. Particularly, previous work has focused on the patterns that persist across

populations - it is well-known that chemotaxis generally changes sperm behavior and increases

recruitment to eggs. In contrast, the differences between female and male sea urchin individuals

and how those differences affect the dynamics of chemoattraction and chemotaxis has not been

well-studied.

In this dissertation, I studied not only average behavior but also individual differences. I (i)

investigated whether differences in sperm chemotactic ability between individual males

translated to differences in fertilization success, (ii) measured the chemoattractant release from

individual females in the framework of their ability to attract sperm, and (iii) studied the behavior and physiology of sperm in specific chemoattractant gradients to understand their threshold of recruitment and fertilization-relevant response.

I used an enzyme to digest chemoattractant and measured the resulting difference in the percent of eggs fertilized, then used novel chemotaxis assays in microfluidic channels to compare individual male chemotactic performance to fertilization success. Through this study, I found that chemotaxis can explain differences in individual male fertilization success. I then used high-performance liquid chromatography to determine the amount of chemoattractant released by eggs of individual females, computational models to investigate the resulting gradients, and microfluidic chemotaxis assays to assess how variable gradients affect sperm behavior. Through this work, I found that individual females vary significantly in their attractant release, which can in turn significantly affect sperm's ability to detect their chemoattractant gradients. Lastly, I used microfluidic chemotaxis assays coupled with calcium imaging tools to record concurrent sperm behavioral and physiologic responses to gradients of chemoattractant and applied data analytics methodologies to determine the amount of attractant needed to recruit sperm, and found a surprising amount of variation in individual sperm behavior.

In summary, my dissertation is an investigation of sperm chemotaxis in the frame of the individual: how individual male fertilization success correlates with their sperm chemotactic ability, how differences between females in egg chemoattractant release change their surrounding chemoattractant gradients, and how variable chemoattractant gradients affect the behavior and physiology of aggregate and individual sperm.

TABLE OF CONTENTS

4

LIST OF FIGURES AND TABLES

Acknowledgements

A version of Chapter III will be submitted for publication imminently. Important contributions to this work have come from Jonathan Wilkey, who made huge strides in data analysis, Shukri Salad, who assisted in writing and tracked dozens of sperm, Jeffrey Guasto, who co-designed the microfluidic device, ran experiments, provided data, wrote the sperm tracking algorithm, and added many ideas to the work, Roman Stocker, who provided ideas and co-designed the microfluidic device, Richard Zimmer, who added ideas and ran experiments, Nathan Kutz, who drove the clustering and machine learning data analysis, and Jeff Riffell, who contributed ideas for experimentation and analysis. Funding for this chapter was provided by the National Science Foundation through my Graduate Research Fellowship Program (DGE-1256082) and their grant to Jeffrey Riffell and collaborators (IOS-1121692, IOS-1354159), as well as the University of Washington and the ARCS Foundation.

I am extremely grateful to my thesis committee for their constant support, both as people and as scientists. Kathleen O'Connor, Barbara Wakimoto, Chip Muller, and Willie Swanson have provided invaluable feedback as I've transitioned from a first-year graduate student to the scientist I am today. Barbara has been involved and available throughout my graduate school career, encouraging me to pursue topics and career paths that interest me and making it clear that her help and advice was just one floor away. Kathleen is the best GSR I could have ever asked for – she has consistently been my advocate and a source of inspiration and wisdom and encouraged me to not only cultivate my academic career but also explore creativity and nature. I am so glad to have had Chip on board for my graduate work, with his wealth of knowledge about comparative reproduction and the translational aspects of basic science. Willie is a great committee member and resource, providing insight about the world of fertilization ecology and asking excellent, necessary questions throughout. I've been told that your committee can define your graduate career, and I feel like this is absolutely true. My thesis committee has been stellar, and I am very grateful to them for the time and heart they have put into the role.

I would like to thank my advisor, Jeff Riffell, whose mentorship and advising has helped me become the independent, resourceful scientist I am today. I'm grateful that he took a chance on me, a prospective student with minimal lab experience – he has been generous with his time and feedback on my work. I have learned so much about academia from working with Jeff, and I am

immensely appreciative of his support of my own career, wherever that may take me. I started graduate school just a year after Jeff started as a professor – the Riffell lab has grown quite a bit since then, and I have had the honor to work closely with an incredible group of colleagues.

My labmates Kelsey, Marie, Clément, Chloé, Gabriella, Winnie, Binh, Claire, Eleanor, Ryo, and Jeremy have given me an inordinate amount of their time and support – they made my day-to-day brighter and I'm not sure where I'd be without them. Many thanks to the undergraduate researchers who have contributed to my work and helped me learn how to be a better mentor: Shukri, Amelia, Lianne, Jennifer, Yinghe, Joshua, and Katie. I would like to express my appreciation for our neighbors in the Daniel and Moody labs, who have been generous with their time and resources, especially Sweta, Eatai, Dave, Octavio, Tanvi, Thomas, Brad, and Sharri.

I am fortunate to have had excellent mentors within the Biology faculty: Carl Bergstrom, Tom Daniel, Ray Huey, Ben Kerr, Alan Kohn, Jennifer Nemhauser, and Liz van Volkenburgh, in the UW faculty: Kelly Edwards and Dorothy Bullitt, and in the Seattle community: Beth Etscheid and Ron Howell, who have all been extremely supportive in my academic and personal endeavors. Scott Freeman, Eileen O'Connor, and Ben Wiggins have been integral in my development as a teacher, and the Biology staff, especially Judy Farrow, Marissa Adamcyzk, Sarah O'Hara, Brianna Divine, Yen Lai, Karen Peterson, Gretchen Shirley-Bellande, Pang Chan, Bruce Godfrey, Dave Hurley, Alex Chun, Alex Hansen, Ron Killman, Robert Goff, and Kristian Haapa-Aho have helped me through the logistics of this graduate degree.

I would like to extend my extreme gratitude to the many people who lent their time and expertise to my questions. Some were experts in sea urchins and marine systems: Emily, Eliza, Hilary, Lauren, Alex, Jason, Colette, Joshua, Scott, Don, Gary, Andy, Linda, Marti, and Vic. Some helped me understand peptide analysis: Martin, Kalkena, Priska, Jimmy, Vagisha, Brandon, Katherine, Damien, Brian, Sam, and Fang-Yi. Others helped me work through tricky data analysis and coding problems: Jonathan, Marie, Nathan, Clément, Lisa, Ian, Janneke, Leander, Melanie, Steve, Jenn, the UW Biostatistics Consulting Center, and the many contributors to Stack Exchange/Overflow. The communities of researchers at the Gordon Seminar and Conference on Fertilization and Activation of Development and the Society for Integrative and

Comparative Biology have been invaluable to the development of my dissertation and its context in the field.

A cadre of incredible women have blazed the path before me, offering their time and advice and showing me how to finish a PhD: Kelsey B, Tracy LP, Jodi S, Jessica L, Jessica H, Nicole H, Judy L, Melanie R, Kylee P, Emily G, and Hilary H. I owe a great deal to the graduate students and postdocs in the Biology department and GEMS, fellow students in GPSS and other campus committees, the greenhouse staff, and the friends and families of the abovementioned for being incredible colleagues and friends, including: Lauren, Katrina, Marcus, Jared, Heather, Peter, Elisha, Sweta, Daril, Frazer, Emily, Jessica, Jeanette, Nile, Terry, Takuo, Emily, Marie, Hilary, Luis, Katie, Greg, Myles, Rory, Melissa, Jessica, David, John, Octavio, Audrey, Eddie, Dustin, Evan, Caroline, Laura, Karlie, Ada, Alex, Jennifer, Justin, Carolyn, Sonia, Alma, Alicia, Stephanie, Aric, Amy, Arshiya, Jamie, Naomi, Michelle, Brian, Kerstin, Alex, Alice, Brian, Carrie, Hannah, Stephanie, Kory, Elloise, Carly, Erin, Elli, Susan, Ted, Alison, Andy, and others. These past 5.25 years in Seattle with you have been more fun than I imagined.

My pre-graduate school friends have been an incredible source of support, especially Rebecca, Kelsey, Sabrina, and Claire. This work is dedicated to my grandmother Suad and grandfather-in-law Larry, who both recently passed away, and the friends who left us too soon, Laurel, Nick and D.J. – I wish I could share this celebration with you.

To my family, who has always been there for me, who have never given up on me, and who have kept the "when are you graduating" questions to a minimum: thank you. I couldn't have asked for a more supportive and loving bunch. To my husband, Jon: thank you for everything – I've tried writing this sentence dozens of ways and can't find the right words to express how grateful I am for you.

To the reader: thank you for reading my dissertation! I sincerely hope you enjoy it.

Chapter I:
Sperm chemotaxis promotes individual fertilization success in sea urchins

Reproductive success fundamentally shapes an organism's ecology and evolution, and gamete traits mediate fertilization, which is a critical juncture in reproduction. Individual male fertilization success is dependent on the ability of sperm from one male to outcompete the sperm of other males when searching for a conspecific egg. Sperm chemotaxis, the ability of sperm to navigate towards eggs using chemical signals, has been studied for over a century, but such studies have long assumed that this phenomenon improves individual male fitness without explicit evidence to support this claim. Here, we assess fertilization changes upon use of a chemoattractant-digesting peptidase and use a microfluidic device coupled with a fertilization assay to determine the effect of sperm chemotaxis on individual male fertilization success in the sea urchin *Lytechinus pictus*. We show that removing chemoattractant from the gametic environment decreases fertilization success. We further find that individual male differences in chemotaxis to a well-defined gradient of attractant correlate with individual male differences in fertilization success. These results demonstrate that sperm chemotaxis is an important contributor to individual reproductive success.

INTRODUCTION

Sperm competition is a significant force in the evolution of male reproductive traits and critically important in individual male reproductive success (Birkhead and Moller, 1998; Engqvist, 2013). In particular, gamete characteristics operating at the scale of a single cell have been shown to mediate population- and individual-level differences in reproduction (Fitzpatrick et al., 2012;

Fitzpatrick and Lüpold, 2014; Levitan, 2000; Simmons and Fitzpatrick, 2012; Simpson et al., 2014; Snook, 2005; van der Horst and Maree, 2013). Sea urchin males with faster sperm have greater fertilization success (Levitan, 2000) and, in low-sperm-concentration situations, marine tube worm sperm head length correlates with relative fitness (Johnson et al., 2013). Gamete recognition factors are also known to play a role in sperm competition and fertilization success (Palumbi, 1999; Swanson and Vacquier, 2002; Zigler et al., 2005). For example, within the same species, sea urchin eggs are far more likely to be fertilized by sperm with closely-related alleles for the recognition protein bindin than by sperm with divergent bindin alleles (Palumbi, 1999), and gamete compatibility between different sea urchin species can be explained by bindin relatedness (Zigler et al., 2005). The interplay between sperm traits, behavior, and chemosensory processes is fundamental in regulating gamete interactions and fertilization. While sperm motility, morphology, and biochemical factors have been shown to influence fertilization success, a direct link between chemotactic navigation abilities of sperm and fertilization success remains elusive.

Chemical communication is suspected to be one of the many prezygotic forces operating to affect successful fertilization (Evans and Sherman, 2013; Riffell et al., 2004). Increasing evidence from a wide variety of taxa, ranging from marine invertebrate broadcast spawners to terrestrial internal fertilizers and plants, suggests that sperm chemotaxis to conspecific eggs is a common phenomenon (Brokaw, 1957; Eisenbach, 1999; Spehr et al., 2003; Yoshida et al., 2008). Recent studies have suggested that egg-derived chemoattractants specifically increase interaction and fertilization with compatible sperm (Fitzpatrick et al., 2012; Oliver and Evans, 2014; Riffell et al., 2004). For instance, abalone sperm chemotactically respond only to conspecific eggs, and

the presence of chemoattractant gradients originating from abalone eggs increases fertilization success (Riffell et al., 2004). Individual male mussels have sperm that preferentially orient towards the particular females with which they are most genetically compatible (Evans et al., 2012). Preferential chemoattraction of sperm to conspecific eggs suggests that sperm chemoattractant responses may have a role in the evolution of gamete traits in broadcast spawners (Evans and Sherman, 2013; Oliver and Evans, 2014), but the effect of sperm chemoattraction on individual fertilization success has remained unknown.

Broadcast-spawning marine invertebrates, particularly sea urchins, are excellent models for testing the correlation between sperm chemotactic behavior and individual male fertilization success. The sea urchin *Arbacia punctulata* has been used in studies of fertilization and embryo development since the late 1800s, due to the large numbers of gametes each animal produces and their ease of manipulation in a laboratory (Harvey, 1956). The first published experiments on animal sperm accumulation to conspecific eggs were conducted in *A. punctulata* in 1912 (Lillie, 1912). The attractants for the species *Strongylocentrotus purpuratus* (Watkins et al., 1978), *Lytechinus pictus* (Hansbrough and Garbers, 1981; Kopf et al., 1979), and *A. punctulata* (Suzuki et al., 1984; Ward et al., 1985) were identified decades later, and the physiology and molecular mechanisms of sea urchin sperm chemotaxis have been well-studied since then (Darszon et al., 2008; Kaupp et al., 2006; Yoshida and Yoshida, 2011). Other factors affecting fertilization success in sea urchins have also been explored: gamete recognition proteins have been identified and their effects on fertilization were characterized in *A. punctulata* (Schmell et al., 1977), *S. purpuratus* (Vacquier and Moy, 1977), and related species (Lessios et al., 2012; Levitan, 2012; Metz et al., 1998; Palumbi, 1999; Zigler et al., 2005). The large body of research on fertilization

12

and chemoattraction in sea urchins makes this an excellent model system to study the effects of chemoattraction on individual fertilization success.

Identifying the links between sperm chemoattraction and male fitness requires fine-scale control of the attractant conditions in parallel with the ability to identify differential male reproductive success. In this study, we used microfluidic devices and video microscopy of sperm chemotactic behavior to well-defined, spatiotemporal attractant gradients in combination with experimental manipulations of chemoattractant gradients around live eggs in fertilization bioassays. The results of our experiments demonstrate that individual fertilization success is an important contributor to sperm chemotactic ability.

MATERIALS AND METHODS

We investigated the effect of sperm chemoattraction on male fertilization success using two approaches: first by removing sperm chemoattractant from eggs and measuring the resulting difference in fertilization (Fig. 1A), then by comparing sperm navigation towards the chemoattractant gradient generated in a microfluidic device to individual male fertilization success (Fig. 1B,C).

Sea urchin gamete collection

Lytechinus pictus sea urchins were purchased during their gravid season of May-October (South Coast Bio-Marine, San Pedro, CA) and held in a dedicated seawater room (8-10°C, 75 L tanks) for up to two months, during which time they were supplied with kelp (*Nereocystis luetkeana*) and sea lettuce (*Ulva spp.*) collected from Shilshole Bay, WA. Both male and female gametes

were collected using standard protocols; 0.5-1.0 mL of 0.5 M KCl was injected into the coelomic cavity (Harvey, 1956; Strathmann, 1987). Sperm was collected dry and stored on ice for use within 8 hours. Eggs were spawned by female inversion onto a beaker containing 35 mL artificial seawater (ASW) made as described by Guerrero and coworkers (Guerrero et al., 2010). Eggs from 2-4 females were pooled together in equal ratios to minimize individual female variability.

Fertilization assays

In all experiments we examined the fertilization success between individual males as the initial step towards determining the correlation between sperm chemotaxis and fertilization. Prior to fertilization experiments, gamete concentrations were quantified in a hemacytometer, and the measured concentrations were used to control sperm:egg ratios in the fertilization bioassays (Lillie, 1915; Riffell et al., 2004; Schmell et al., 1977). Sperm:egg ratios of 100:1, 300:1, and 1000:1 (number of eggs = 1513 ± 356; number of sperm = $2\times10^5 \pm 3.3\times10^4$ at 100:1, $7.2\times10^5 \pm 1.6\times10^5$ at 300:1, $1.8\times10^6 \pm 2.3\times10^5$ at 1000:1) were added to each well of a 24-well plate (Falcon Clear Polystyrene Sterile Tissue Culture Multiwell Plate, BD Biosciences, San Jose, CA), yielding 8 replicates for each treatment and male at each sperm:egg ratio. To control for contact time, 1 mL 0.5 M KCl solution was added to stop sperm motility (Levitan, 2000) 3 minutes after exposure. This contact time yielded a consistent fertilization curve in preliminary experiments and is appropriate for *L. pictus* (Rosman et al., 2007). Embryos were allowed to develop for 1.5 hours, after which they were fixed with 4% formaldehyde in ASW and washed twice with fresh ASW. At least 100 embryos from each replicate were scored for percentage fertilization based on the number of cells showing cleavage. A total of 18 males were used, but

one male was excluded from analyses due to extremely low fertilization ($< 5\%$). To compare

male performance within each trial, relative male fertilization success was calculated as (mean %

eggs fertilized by male 1 / mean % eggs fertilized by male 2) for each pair of males within a

single trial (Tvedt et al., 2001).

Lytechinus pictus eggs contain speract, a well-studied peptide that acts as a sperm attractant

(Garbers et al., 1982; Guerrero et al., 2010; Shimomura et al., 1986b). Elastase (>99% purity;

Promega Corporation, Madison, WI), an enzyme which cleaves at the C-terminus of the amino

acids valine, glycine, and leucine (Narayanan and Anwar, 1969), was utilized to selectively

digest the speract (Gly-Phe-Asp-Leu-Asn-Gly-Gly-Gly-Val-Gly (Garbers et al., 1982)) attractant

around live eggs (Fig. 1A). Elastase was diluted to 10^{-7} M in ASW for use in trials, and was also

denatured by heating 5 mL of the diluted enzyme to a boil and used as a control for the effects of

adding the denatured enzyme to eggs. Eggs used for enzyme assays were spawned directly into

beakers containing 5×10^{-2} M Tris in ASW. Eggs from 2-4 females were pooled together in equal

ratios to minimize individual female variability, and 10 mL was put into each of three 40-mL

conical tubes. One tube received 0.5 mL of elastase, one tube received 0.5 mL of denatured

elastase, and the control tube received 0.5 mL of ASW. The eggs were incubated for 1.5 hours

before being used in a fertilization assay. The change in fertilization percent between treatments

was determined using a random-intercepts mixed effects model (Zuur et al., 2009) with

individual males as a random effect and sperm:egg ratio and treatment as fixed effects (package

lme4 (Bates et al., 2014), R (R Core Team, 2013), Vienna, Austria). Percent change in

fertilization is calculated as [(% eggs fertilized in control condition - % eggs fertilized in

treatment condition) / (% eggs fertilized in control condition)]. Prior to testing, the effects of

elastase on the chemoattractant speract and the viability of the gametes were examined. High

performance liquid chromatography and mass spectrometry confirmed that elastase digests both

synthetic and egg-associated speract (Fig. 2), and sperm exposed to a gradient of speract plus

elastase had a distribution in the microfluidic device that was not significantly different from the

ASW control (Student's t-test, all p > 0.1, Fig. 3A). In addition, to determine if elastase

influenced sperm motility, sperm were exposed to elastase or ASW in the microfluidic device

and the linear velocity of the cells were quantified. Results showed that cell velocities were not

significantly different between the ASW and elastase treatments (Student's t-test, n = 52 sperm,

p > 0.10; Fig 3B). The effects of elastase on egg viability and embryo development was

determined by incubating eggs in elastase or ASW, adding sperm to a gamete ratio of 300

sperm/egg, and examining the plutei larvae 69 h post-fertilization; no morphological differences

were found (Fig. 3C).

Microfluidics and imaging

We designed a microfluidic device which enabled us to expose sperm from different males to the

same precisely-controlled chemoattractant gradient (Fig. 1C) and compare sperm behavior

between males. As previously described (Ahmed and Stocker, 2008), polydimethylsiloxane

(PDMS) channels were designed using CAD software (Autodesk, San Rafael, CA), printed onto

transparency film with a high-resolution image setter (Fineline Imaging, Colorado Springs, CO),

and patterned onto a 4-inch silicon wafer, which was spin-coated with 60-µm-thick negative

photoresist (SU8-2100; Microchem, Newton, MA), by exposure to ultraviolet light. The

patterned channel structure had three input branch channels that met in a single 'test' channel

that was 4 cm long, 99 µm deep, and 1020 µm wide. PDMS (Dow Corning, Midland, MI) was

molded against the silicon master, cured at 22°C for 24 hours, peeled off of the silicon mold, and cut to the size of a standard glass slide (25 mm × 75 mm). Inlets and outlets were punched into the channel using a 1 mm Harris micro-punch (Ted Pella, Redding, CA) and attached to a glass slide. A covalent bond between the PDMS channel and glass slide was established by pretreating both with oxygen plasma and baking the bonded channel at 60°C for 1 hour.

The microfluidic device was placed on an inverted microscope (Nikon TE2000; Nikon Instruments, Melville, NY) equipped with a 10× Nikon Plan Fluor objective. Non-toxic polyethylene tubing (BD Intramedic[TM], Franklin Lakes, New Jersey) was inserted into input channels and attached to 1 mL gastight syringes (Hamilton Company, Reno, NV) containing ASW, sperm diluted 1000× (~1×10^7-5×10^7 sperm/mL) in ASW, or the attractant speract (Phoenix Pharmaceuticals, Burlingame, CA) diluted to 1.39×10^{-9} M in ASW. Experiments began an average of 5 minutes after sperm dilution. Bubbles were removed from the syringes and tubing prior to each experiment. A syringe pump (Harvard Apparatus, Holliston, MA) was used to apply a flow rate of 10 µL min^{-1} for 60 seconds to keep the cells and attractant stratified. Stopping the flow allowed the attractant gradient to develop by diffusion, and video recording began simultaneously. Sperm were imaged mid-depth in the channel using phase contrast microscopy by recording sequences of 1980 frames at 33 frames per second with a 512×512-pixel (field of view: 8.2×8.2 mm) CCD camera (iXon Ultra 897; Andor Technology, Belfast, UK). Image analysis software (Nikon-NIS Elements; Nikon Instruments) and Matlab (MathWorks, Natick, MA) were used to quantify sperm chemosensory behavior (detailed below). The concentration field of speract C(x,t) was obtained from the solution of the advection-diffusion equation (Ahmed et al., 2010a) and verified using epifluorescence images of

10^{-4} M fluorescein (Fluka), which was used as a proxy for the attractant in the microfluidic channels. To account for the difference in diffusion coefficients between fluorescein ($D = 5 \times 10^{-10}$ $m^2\,s^{-1}$ (Qasaimeh et al., 2011)) and speract ($D = 3\times 10^{-10}$ $m^2\,s^{-1}$ (Guerrero et al., 2013)), time was scaled by the ratio of their diffusion coefficients.

Chemotaxis assays and analysis

Microfluidic chemotaxis assays were performed by injecting sperm into the middle input port, ASW into a side input port, and speract in ASW (1.39×10^{-9} M) into the opposite side's input port (Fig 1C). No-speract controls were conducted in a similar manner, except ASW was injected into both side input ports. After video collection, custom scripts in Matlab (MathWorks) and R (R Foundation for Statistical Computing, Vienna, Austria (R Core Team, 2013)) were used to analyze the trajectories of the sperm tracks. Analyses included distribution of sperm within the channel, as well as track orientation with respect to the attractant gradient direction ($0°$). In *L. pictus* sea urchins the relationship of chemokinesis and chemotaxis is unclear (Chang et al., 2013; Shiba et al., 2008). We thus conducted a preliminary analysis of sperm from 10/18 males; results showed no evidence for speract influencing cell velocities compared to the ASW control (paired t-test, $p = 0.92$; mean $\pm$ s.e.m. for the speract treatment: 167.7 ± 70.7 $\mu m\,s^{-1}$; ASW treatment: 166.5 ± 58.7 $\mu m\,s^{-1}$).

For sperm distribution analysis, the locations of all visible sperm were marked at 10, 30, and 60 seconds after stopping flow, and cells stuck to the bottom of the channel were excluded from analysis. The proportion of sperm in the attractant (or control) location at each time point was calculated by dividing the number of sperm in the attractant side (1/3) of the channel by the total

number of sperm in the channel. To compare paired male performance within the same trial, the proportion of sperm in the attractant stream for male 2 was subtracted from that of male 1 (Gage et al., 2004).

For orientation analysis, the trajectories of 6–28 sperm per treatment per male were digitized and the first and last points of each track were used to determine the vector length, calculated as r $=\sqrt{(\Delta x)^2 + (\Delta y)^2}$, and orientation, calculated as $\theta_s = \tan^{-1}(\Delta y/\Delta x)$, of the full trajectory. The orientation of all sperm tracks in each treatment, reflected about the x-axis to yield a range of 0-180°, were pooled and used to test the difference between sperm orientation under control and attractant conditions. The mean orientation (θ) and mean resultant vector length (ρ) of all sperm from each male were calculated using the CircStats (Jammalamadaka and Gupta, 2001; Lund and Agostinelli, 2002) package in R (R Core Team, 2013). The mean orientation of sperm in the attractant treatment (θ_a) was used to compare sperm orientation between males. To compare paired male performance within the same trial, relative orientation was calculated as $\theta_{a\_male1} - \theta_{a\_male2}$. We also computed a preference index (PI) for each male, in which PI = [(number of sperm oriented towards the attractant ($\theta_a < 90°$) – number of sperm oriented away from the attractant ($\theta_a > 90°$))/(total number of sperm)] (Vinauger et al., 2014). The index takes a value of PI = 1 when all sperm are oriented towards the attractant and PI = -1 when all sperm are oriented away from the attractant.

RESULTS

Contribution of the sperm chemoattractant speract and inter-male variation to fertilization success

To identify the degree to which sperm chemotactic abilities may influence fertilization, we manipulated the attractant plumes around live eggs by exposing eggs to an enzyme (elastase) that selectively digests the chemoattractant (Fig. 2). As a control, we determined that elastase had no effect on gamete viability and embryo development (Fig. 3). Using a range of sperm:egg ratios that spans from sperm-limiting (100:1 sperm:egg) to saturating (1000:1 sperm:egg) conditions, we measured the difference in fertilization success between treatments for each male and for all males in the experiment. For one representative male (Fig. 4A), the percent of eggs fertilized in artificial seawater (ASW; first control) was 13.5% higher than in the elastase treatment (CI [-19.2, -7.9], ANCOVA, Tukey post-hoc test, $p < 0.001$) and the percent of eggs fertilized after incubation in denatured elastase (second control) was not significantly different from the ASW treatment (ANCOVA, Tukey test, $p = 0.47$). For another representative male (Fig. 4B), the fertilization percent for eggs in ASW was 4.6% higher (CI [-9.0, -0.28]) than eggs incubated in elastase (ANCOVA, Tukey test, $p < 0.05$) and fertilization percentages of controls (ASW, denatured elastase) were not significantly different from each other (ANCOVA, Tukey test, $p = 0.47$). Individual male differences have a significant effect on fertilization (ANOVA for male effect, $p < 0.001$). Therefore, we analyzed the data from all 8 males with a random-intercepts mixed-effects model (Zuur et al., 2009) with male as the random effect and sperm:egg ratio and treatment as fixed effects.

We found that, for all individual males combined (Fig. 4C), elastase lowered fertilization by 5.1% (CI [-7.76,-2.51], $n = 532$, $p < 0.001$), a 22.4% change in fertilization from the seawater control. Using the same model, we found that denatured elastase did not affect fertilization (CI [-2.43, 2.82], $n = 532$ trials, $p = 0.88$). We tested adding an interaction between sperm:egg ratio

and treatment to the model and found no significant interaction (ANOVA of models with and without interaction, p = 0.26). However, we see that the treatment effect at the sperm:egg ratio of 300 sperm per egg is larger than the model average, as elastase lowers fertilization by 8.5%, which is a 37.5% change in fertilization from the seawater control (student's t-test, p = 0.05, Bonferroni-corrected p-values, n = 8 males with 8 fertilization replicates/treatment/male (for 3 males, 3 replicates/treatment/male)). At the sperm-limited gamete ratio of 100 sperm per egg and at the sperm-saturated gamete ratio of 1000 sperm per egg, there is no statistically significant difference between fertilization in control and elastase conditions (p = 1.0 and 0.63, respectively). Our data show that removing chemoattractant from live eggs decreases fertilization success, especially at intermediate sperm/egg concentrations.

Relationship between individual fertility and sperm chemotactic behavior

In order to determine the effect of sperm chemotactic behavior on individual male fertilization success, we compared the fertilization success of males paired with the same group of eggs to the chemotactic ability of sperm from the same males. Sperm chemotactic ability was measured for a subpopulation of sperm from individual males using a microfluidic chemotaxis assay. A chemoattractant gradient was formed by stopping a controlled, laminar flow within a microfluidic device and allowing diffusion to occur (see Materials and Methods for details). To identify how the entire sperm population from a male responds to the attractant gradient, we examined the spatial distribution of sperm within the channel at 10, 30, and 60 seconds after the gradient was initiated. The distribution of sperm in the channel differed significantly between the control and attractant conditions where sperm aggregate in the high-attractant-concentration region of the channel (Fig. 5). For individual males, the number of cells in the attractant side of

the channel was higher than control experiments where the attractant is replaced with ASW (e.g., Fig. 5A). For all males combined, the proportion of sperm in the attractant side of the channel was significantly higher than in the control channel, at all time points (e.g. at 10 s, proportion in attractant = 0.16, in control = 0.09; t-tests, n = 17 males, all $p < 0.05$) (Fig. 5B). Due to differences in baseline fertilization ability for trials completed during different times in the gravid season, we investigated the impact of sperm behavior on fertilization differences within trials of paired males. Differences in fertilization between males were significantly correlated with sperm distribution in the attractant stream (linear regression, slope = 1.28, n = 8 pairs (16 males), $R^2 = 0.62$, $p < 0.05$) (Fig. 6A).

To quantify single-sperm behavior, we considered the orientation of sperm tracks towards the attractant source. We verified that the mean whole-track sperm orientation θ (0°-180°), calculated by CircStats (Lund and Agostinelli, 2002) in R (R Core Team, 2013), became closer to 0° (the direction of the attractant source) in response to the application of a chemoattractant gradient (Fig. 7A,B) (Wilcoxon test, $p < 0.001$, n = 345 sperm tracks in attractant and 316 sperm in control from 17 males). Sperm exposed to the attractant oriented and exhibited a higher preference index than sperm exposed to the ASW control (PI attractant = 0.34 ± 0.06, PI control = 0.04 ± 0.07, paired t-test, n = 17 males, $p < 0.01$) (Fig. 7D). Individual males differed in their mean sperm orientation θ_a (Fig. 7C), but these differences were not statistically significant (ANOVA of θ_a with male as the factor, $p = 0.17$). We then examined the relationship of the relative fertilization success of males paired by trial with the relative mean orientation of sperm towards the attractant source (0°). Differences in fertilization ability had an inverse relationship with sperm orientation towards the attractant θ_a (Fig. 6B), but this effect was not statistically

22

significant (linear regression, slope = -0.02, n = 8 pairs (16 males), $R^2 = 0.30$, p = 0.16). Our data show that sperm movement towards the chemoattractant source partially explains differences in male fertilization success.

DISCUSSION

In this study, we investigated the effect of sperm chemotaxis on fertilization success using two distinct approaches. In the first approach, we compared fertilization ability with and without an enzyme that digests the sperm chemoattractant speract. In the second approach, we coupled fertilization assays with a novel chemotaxis assay in a microfluidic device (Fig. 1) to compare the fertilization success and chemotactic performance of paired males fertilizing the same group of eggs. We found that removing the sperm chemoattractant decreased fertilization success (Fig. 4) and that sperm movement towards the chemoattractant correlated with relative male fertilization success (Fig. 6).

Removing speract from live eggs led to an overall percent decrease in fertilization of 22.4%. This difference is significant, and may compound with other selection mechanisms in sperm competition, such as sperm longevity (Levitan, 2000) and gamete recognition proteins (Evans and Sherman, 2013; Levitan, 2012; Palumbi, 1999; Swanson and Vacquier, 2002). Gamete recognition proteins are a particularly important prezygotic mediator of fertilization success. The gamete recognition proteins bindin (Vacquier and Moy, 1977) (on sperm) and EBR1 (Foltz and Lennarz, 1990) (on eggs) mediate both interspecies and intraspecies gamete compatibility (Palumbi, 1999; Zigler et al., 2005). This known influence on fertilization, coupled with extensive evidence that gamete recognition factors evolve more quickly than other proteins

(Swanson and Vacquier, 2002), implies that gamete recognition proteins are a crucial component of fertilization success, operating downstream of water-borne sperm attractants. Our current study provides impetus towards determining the relative contributions of gamete recognition proteins and sperm chemotaxis on individual male fitness.

Digestion of the chemoattractant around eggs had the greatest effect when sperm:egg ratios were at the intermediate (300:1) gamete ratio, where we found a 37.5% change in fertilization; when sperm are limiting (100:1) or saturating (1000:1), loss of chemoattractant had less of an effect. These results are similar to previous work where Riffell et al found that chemoattraction did not affect fertilization under sperm-limiting and sperm-saturating conditions (Riffell et al., 2004). We also recognize that the overall 5% decrease in fertilization success is relatively low, which suggests that these fertilization assays with sperm and eggs in an enclosed space may increase random encounters and reduce the impact of chemotaxis. Nonetheless, our data show that the chemoattractant speract is an important factor mediating *L. pictus* gamete interactions and fertilization success.

As a result, we considered differences in sperm chemotactic ability and their effect on individual male fitness. Microfluidics allowed us to reproducibly control the spatial and temporal gradient of speract chemoattractant that sperm were experiencing and simultaneously visualize sperm population dynamics and individual sperm behavior (Ahmed et al., 2010a). Microfluidic chemotaxis assays showed that more sperm oriented to and migrated towards the chemoattractant than to seawater. The population-level indicator of cell accumulation and the single-cell indicator

of swimming orientation demonstrate that sperm chemotaxis can be robustly measured in our microfluidic device.

The proportion of sperm migrating to the attractant stream correlated significantly with the relative fertilization success of paired males, indicating that the ability of sperm to move towards their chemoattractant reflects their ability to fertilize eggs. This result reveals a direct connection between sperm chemotactic behavior and male reproductive success, and builds upon previous studies which found that chemoattraction increases gamete encounters (Riffell et al., 2004) and connected sperm preference for particular eggs to gamete compatibility and conspecific recognition (Evans et al., 2012; Oliver and Evans, 2014). The present study is the first to demonstrate that differences in individual male fertilization success are correlated with differences in sperm chemotaxis.

Interestingly, we did not find a significant correlation between mean orientation of sperm towards the attractant and relative fertilization success of paired males. Sperm orientation may be a weaker indicator of chemotactic ability than sperm distribution because sperm traveling at any angle between 0° and 90° will reach the attractant source. We also may not have captured the full extent of sperm recruitment towards the attractant, as the approximately 3-sec delay between stopping flow and the cessation of fluid motion may have been enough time for sperm to adapt to the attractant before being captured in our tracking algorithm. Nonetheless, the relationship between sperm distribution and male fertilization success and the change in orientation by sperm in the presence of the attractant indicates that sperm chemoattraction is an important contributor to fertilization success.

Sperm competition and chemoattraction

Once gametes from broadcast-spawning invertebrates such as sea urchins are released into the ocean, their variable fertilization success leads directly to differences in reproductive success between males (Evans et al., 2012; Fitzpatrick and Lüpold, 2014). The large scale of the ocean environment, which dilutes gametes, and its frequently turbulent nature, which can affect motility, creates strong selective pressure on gamete traits. Sperm traits are thus vital in promoting gamete encounters in the water column, and there is evidence that traits such as sperm motility and morphology often correlate with male reproductive success (Fitzpatrick and Lüpold, 2014; Simmons and Fitzpatrick, 2012; Snook, 2005). Evidence from multiple marine organisms, including broadcast-spawning mussels and internally- and externally-fertilizing fish, suggests that sperm chemoattraction is under selective pressure (Evans and Sherman, 2013). Previous studies found a correlation between sperm chemoattraction to specific eggs and the ability of the eggs to be fertilized, both in broadcast-spawning marine invertebrates (Evans et al., 2012; Krug et al., 2009) and humans (Ralt et al., 1991), providing evidence for chemoattraction as a signal of gamete viability and compatibility. In this study, the significant effect of chemoattraction on fertilization success reinforces our understanding of chemotaxis as a trait with potential for selection. The ubiquity of sperm chemoattraction in divergent taxa and the species-specificity of chemoattractant signaling molecules (Miller, 1997; Riffell et al., 2004; Yoshida et al., 2013) suggests a role for chemoattraction in reproductive isolation and species evolution.

Summary

Using a chemoattractant-digesting peptidase and a microfluidic device coupled with fertilization assays, we show that sperm chemotactic ability affects individual male fertilization success in the sea urchin *L. pictus*. Removing chemoattractant from a group of eggs leads to a decrease in the percent of eggs that are fertilized. Sperm change their distribution and orientation in response to the application of a chemoattractant gradient generated within a microfluidic device. Individual male sperm distribution in the channel at 10 seconds post-attractant-exposure correlates with fertilization success, results which are particularly important for broadcast-spawning marine invertebrates where fertilization is rapid. Sperm chemotaxis is common throughout sexually-reproducing organisms (Eisenbach, 1999; Sawada et al., 2014), including humans, and our results indicate that microfluidic chemotaxis assays could be used to test male fitness. Our study demonstrates for the first time that sperm chemotaxis influences individual fertilization success, implying that sperm chemoattraction is a trait under selection and providing impetus for investigating the relative contributions of sperm chemotaxis and other gamete traits to fertilization.

FIGURES

Figure 1: Experimental methods and microfluidic device used in chemotaxis assays (A) The effect of chemoattraction for fertilization was determined by digesting attractant with elastase and comparing fertilization success. The performance of elastase-exposed eggs was compared to eggs incubated in denatured elastase, as well as artificial seawater (ASW). **(B)** The relationship between chemotaxis and fertilization success was determined by comparing sperm performance in a microfluidic-based chemotaxis assay (depicted in C) to the percent of eggs fertilized by the corresponding males. **(C)** Microfluidic channel used in chemotaxis assay. (C, *left*) The microfluidic channel was 1020 µm wide and 99 µm deep. Sperm diluted 1000× in ASW was injected into the middle input port, ASW was injected into a side input port, and $1.39{\times}10^{-9}$ M speract in ASW was injected into the opposite side input port. No-speract controls were run in parallel, with ASW injected into both side input ports. Video images of sperm in the channel were recorded 5 mm from the inlet. (C, *right*) The microfluidic channel allowed precise experimental and computational determination of the speract concentration in the channel. **(D)** The starting speract concentration used for the chemotaxis assay was $c_0 = 1.39{\times}10^{-9}$ M, and speract diffusion in the channel was determined by the advection-diffusion equation and confirmed experimentally with measurements of diffusion of 10^{-4} M fluorescein used in place of attractant (C, *left*). To account for the difference in diffusion coefficients between fluorescein (D $= 5 \times 10^{-10}$ m^2/s) and speract (D $= 3{\times} 10^{-10}$ m^2/s), time was scaled by the ratio of the diffusion coefficients.
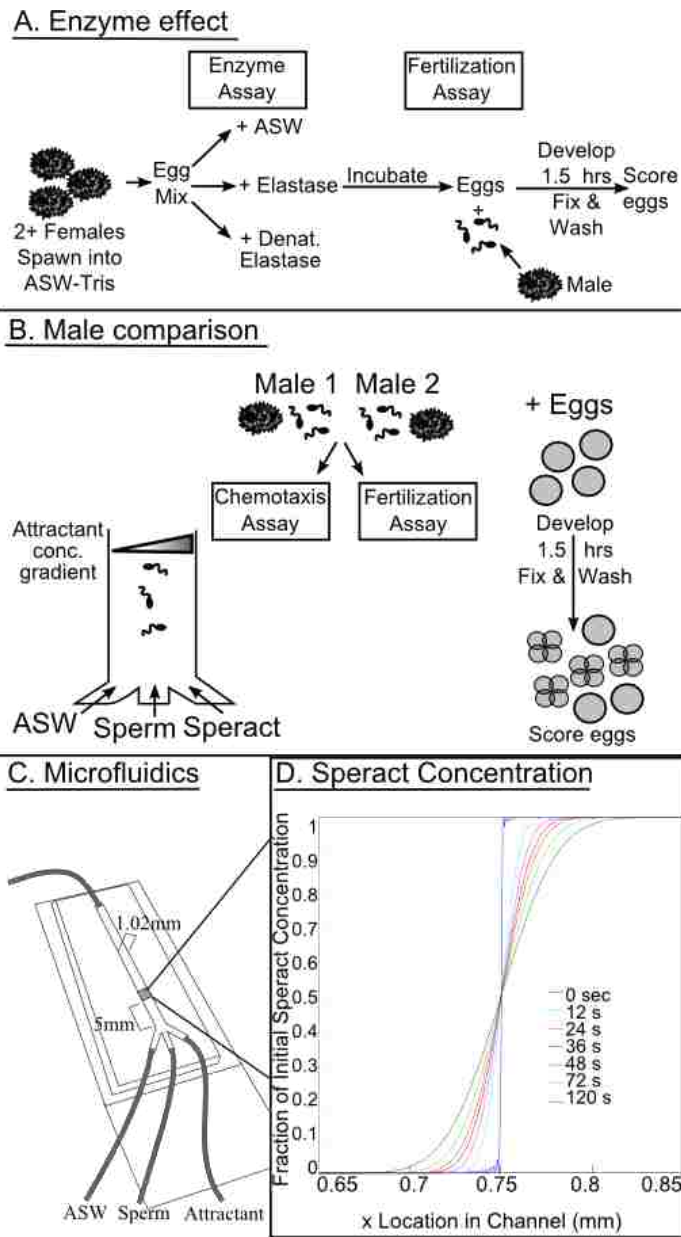
Figure 2: HPLC-MS data shows purified and native speract is digested by the enzyme elastase while the peptide resact, used as an internal standard, remains. Red denotes data from the control condition (without elastase) and blue denotes data from the elastase-incubated solution. **(A)** Extracted ion chromatogram for 622-623 m/z, corresponding with the primary peak of the internal standard resact, which is retained between the control and elastase-incubated conditions. **(B)** Mass spectrum of the retention time corresponding with the primary peak of the

internal standard resact. The mass fragmentation of resact is identical in the control and elastase conditions. **(C)** Extracted ion chromatogram for 893-894 m/z, corresponding with the primary peak of the sperm chemoattractant speract, which is digested in the elastase-incubated (red) condition. **(D)** Mass spectrum of the retention time corresponding with the primary peak of speract, showing that speract is no longer present in the elastase-incubated (red) condition. **(E)** Eggs from two *Lytechinus pictus* females were incubated in artificial seawater with elastase (red) or without elastase (blue). The eggs were centrifuged and the egg-conditioned seawater was desalted using Sep-Pak C18 columns, lyophilized, and reconstituted in Milli-Q water. Speract appears in the control condition and does not appear in the elastase-incubated solution, indicating that native speract is digested by elastase. **(F)** Mass spectrum of the retention time corresponding with the primary peak of speract in egg-conditioned seawater, showing that speract is no longer present around eggs incubated in elastase.
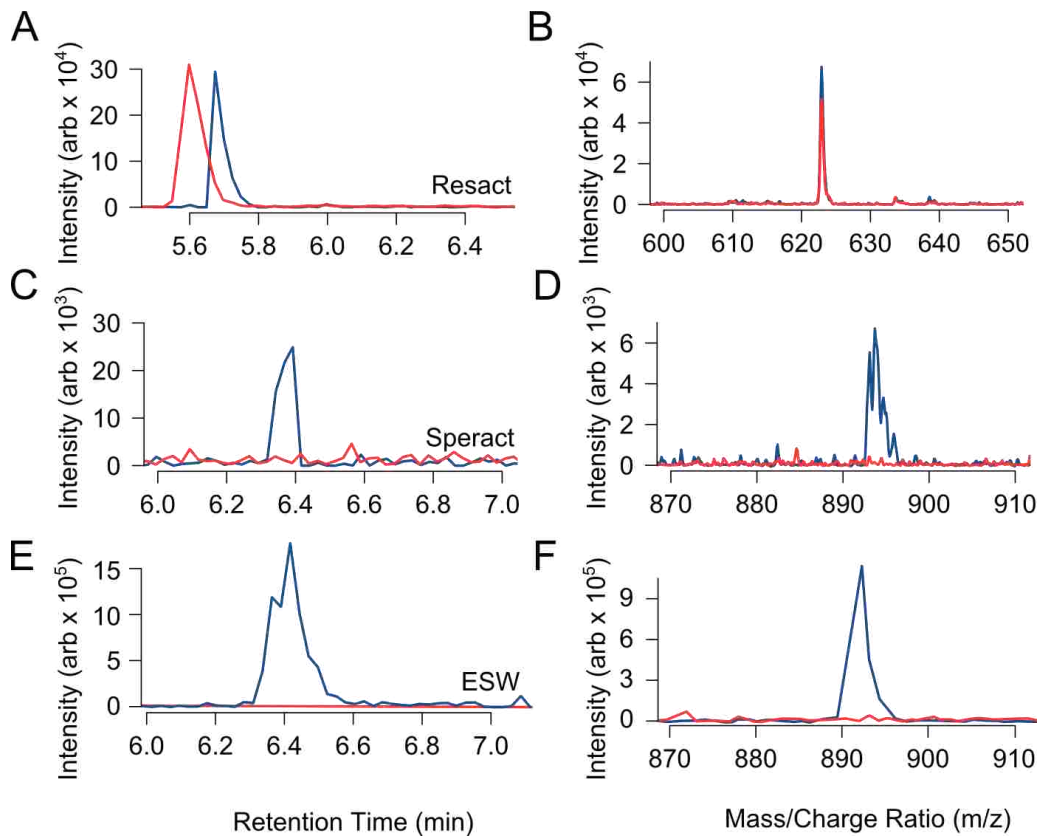
Figure 3: Elastase negates the effect of speract on sperm distribution, and does not affect sperm motility or embryo development. (A) The distribution of sperm in ASW does not significantly differ from the distribution of sperm in a speract-elastase mixture (Student's t-test, all p > 0.1). **(B)** Sperm motility does not change in seawater with elastase, as compared to sperm motility in a seawater control. The mean velocity of sperm in the control and elastase treatments are not significantly different (Student's t-test, n = 52 sperm (26 per treatment), p = 0.104). **(C)** Eggs incubated in seawater with elastase develop to the pluteus larval stage identically to eggs incubated in seawater without elastase. (*i*) Pluteus larva from egg in seawater control, 69 hours post-fertilization. (*ii*) Pluteus larva from egg in elastase condition, 69 hours post-fertilization.
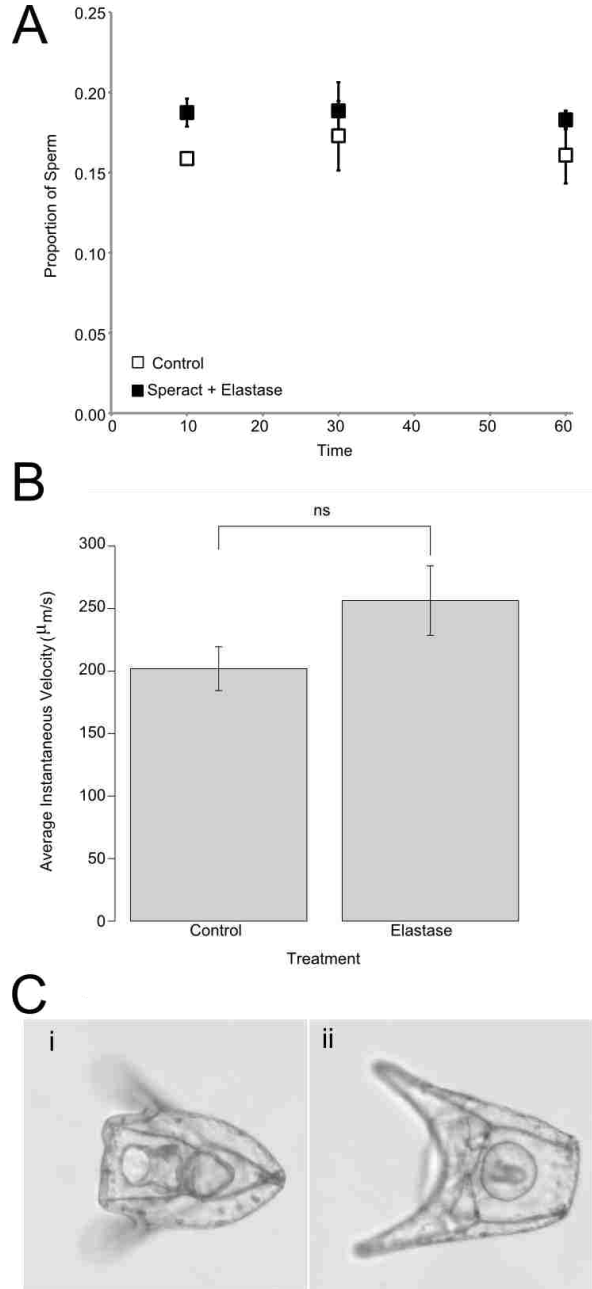
Figure 4: Effect of elastase on fertilization rates (A) Fertilization curve for one male crossed with eggs incubated with artificial seawater (control), elastase (peptidase treatment), or denatured elastase (second control). **(B)** Fertilization curve for another representative male crossed with eggs in artificial seawater, elastase, or denatured elastase. **(B)** Combined mean fertilization curves of all males fertilizing eggs incubated with artificial seawater, elastase, or denatured elastase. Elastase yielded a change in fertilization of 22.35% (n = 532, p < 0.001) and denatured elastase did not affect fertilization (p = 0.88). At a log sperm:egg ratio of 2.5, elastase yields a percent change of fertilization of 37.5% (n = 113, p = 0.05). At the log sperm:egg ratios of 2.0 and 3.0, there is no statistically significant difference between control and elastase fertilization rates (p=1.0 and 0.63). Error bars indicate ± s.e.m.
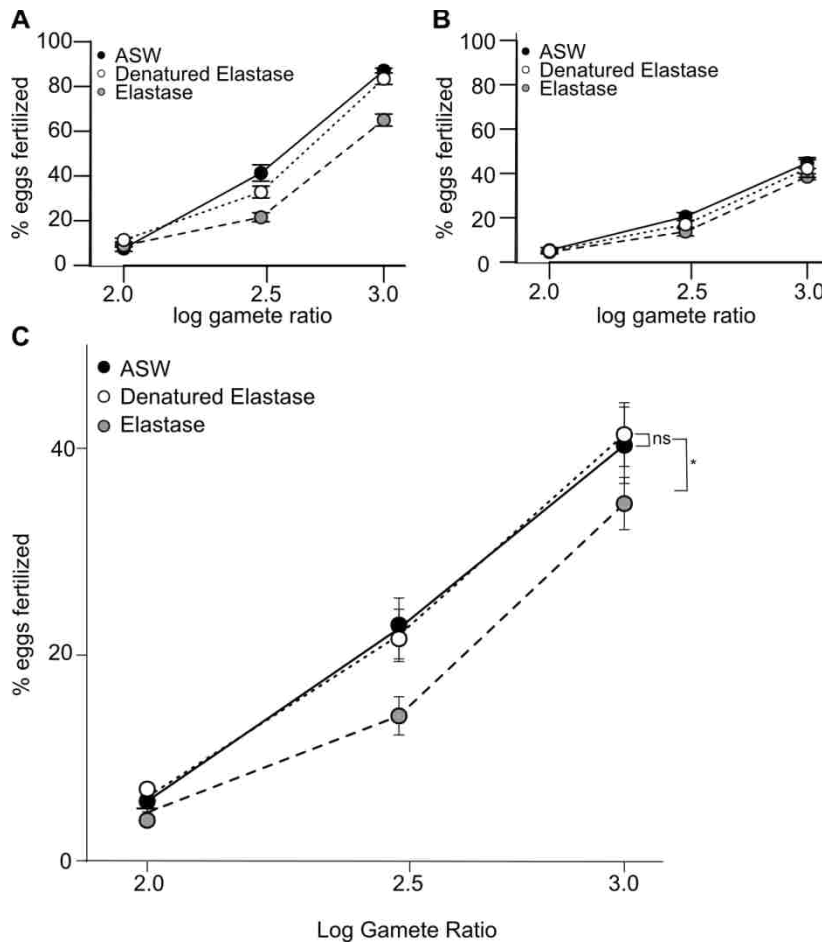
Figure 5: Changes in sperm distribution between control and attractant conditions (A) In a representative experiment, significantly more sperm move into the attractant side of the channel than when attractant is replaced with seawater (control). **(B)** In all trials, at 10, 30, and 60 seconds after flow is stopped in the microfluidic channel, the ratio of sperm in the attractant side of the channel to the ASW side is higher than when no attractant is present (Student's t-tests, n=17 males, all $p < 0.05$). Error bars indicate $\pm$ s.e.m.
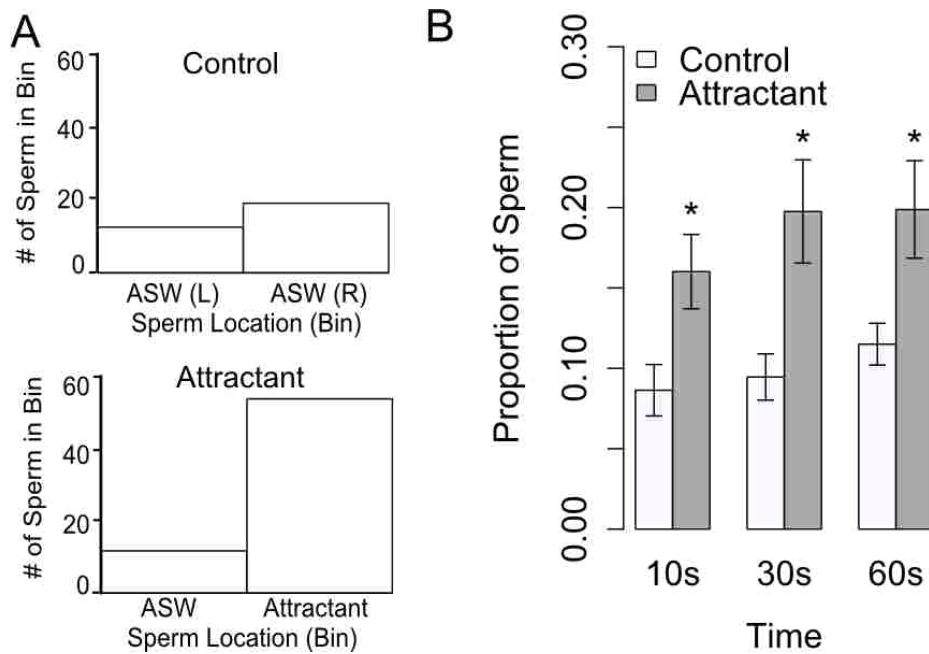
Figure 6: Relative fertilization success related to sperm chemotactic parameters (A)
Relative fertilization success of individual males paired by trial, varying by the relative
proportion of sperm in the attractant stream at 10 seconds post-attractant-exposure. Differences
in fertilization rates are explained by sperm distribution in the attractant stream (linear
regression, slope = 1.28, n = 8 pairs (16 males), R^2 = 0.62, p < 0.05). **(B)** Relative fertilization
success of individual males paired by trial, varying by the relative mean orientation of sperm
towards the attractant source. We expect an inverse relationship, as 0° is the direction of the
attractant source. Differences in fertilization rates seem to be explained by sperm orientation
towards the attractant, but the relationship is not statistically significant (linear regression, slope
= -0.02, n = 8 pairs (16 males), R^2 = 0.30, p = 0.16).
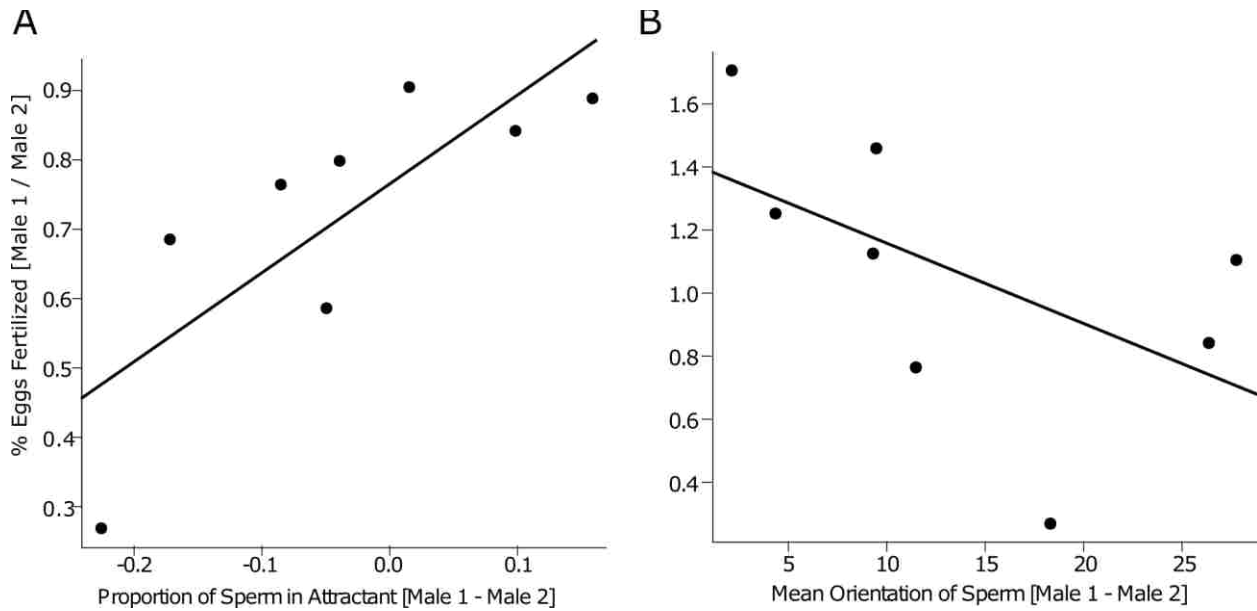
Figure 7: Sperm orientation in the microfluidic channel, where the angle (θ) 0° is the direction of the attractant source (A) In the no-speract control, the mean sperm direction θ is 88.3° and the mean resultant vector length ρ is 0.82 (scaled to maximum count), n = 316 sperm from 17 males **(B)** The mean sperm orientation to attractant θ_a is 72.7° and the mean resultant vector length ρ is 0.74 (scaled to maximum count), n = 345 sperm from 17 males. **(C)** Mean resultant vectors (ρ) of mean sperm orientation of each male to the attractant. **(D)** Preference index (PI) of sperm in the control and attractant conditions, where positive preference index indicates a higher proportion of sperm moving towards the attractant side of the channel. Sperm have a higher preference index towards attractant than a seawater control (PI attractant = 0.34, PI control = 0.04, paired t-test, n = 17 males, p < 0.01).

REFERENCES

Aguirre, J.D., Blows, M.W., Marshall, D.J., 2016. Genetic Compatibility Underlies Benefits of Mate Choice in an External Fertilizer. Am. Nat. 187, 000–000. doi:10.1086/685892

Ahmed, T., Shimizu, T.S., Stocker, R., 2010a. Microfluidics for bacterial chemotaxis. Integr. Biol. 2, 604–629. doi:10.1039/c0ib00049c

Ahmed, T., Shimizu, T.S., Stocker, R., 2010b. Bacterial Chemotaxis in Linear and Nonlinear Steady Microfluidic Gradients. Nano Lett. 10, 3379–3385. doi:10.1021/nl101204e

Ahmed, T., Stocker, R., 2008. Experimental verification of the behavioral foundation of bacterial transport parameters using microfluidics. Biophys. J. 95, 4481–4493.

Alvarez, L., Dai, L., Friedrich, B.M., Kashikar, N.D., Gregor, I., Pascal, R., Kaupp, U.B., 2012. The rate of change in Ca 2+ concentration controls sperm chemotaxis. J. Cell Biol. 196, 653–663. doi:10.1083/jcb.201106096

Asmar, N.H., 2004. Partial Differential Equations, 2nd ed. Pearson.

Bates, D., Maechler, M., Bolker, B., Walker, S., 2014. lme4: Linear mixed-effects models using Eigen and S4.

Bell, A.F., Crimaldi, J.P., 2015. Effect of steady and unsteady flow on chemoattractant plume formation and sperm taxis. J. Mar. Syst. 148, 236–248. doi:10.1016/j.jmarsys.2015.03.008

Beltrán, C., Galindo, B.E., Rodríguez-Miranda, E., Sánchez, D., 2007. Signal transduction mechanisms regulating ion fluxes in the sea urchin sperm. Signal Transduct. 7, 103–117. doi:10.1002/sita.200600129

Bentley, J.K., Shimomura, H., Garbers, D.L., 1986. Retention of a Functional Resact Receptor in Isolated Sperm Plasma Membranes. Cell 45, 281–288.

Birkhead, T., Moller, A. (Eds.), 1998. External Fertilizers, in: Sperm Competition and Sexual Selection. Academic Press, San Diego, California, pp. 177–191.

Böhmer, M., Van, Q., Weyand, I., Hagen, V., Beyermann, M., Matsumoto, M., Hoshi, M., Hildebrand, E., Kaupp, U.B., 2005. Ca2+ spikes in the flagellum control chemotactic behavior of sperm. EMBO J. 24, 2741–52. doi:10.1038/sj.emboj.7600744

Brokaw, C.J., 1957. Chemotaxis of bracken spermatozoids. J. Exp. Biol. 35, 192–196.

Brown, D.A., Berg, H.C., 1974. Temporal stimulation of chemotaxis in Escherichia coli. Proc. Natl. Acad. Sci. 71, 1388–92.

Burnett, L.A., Anderson, D.M., Rawls, A., Bieber, A.L., Chandler, D.E., 2011. Mouse sperm exhibit chemotaxis to allurin, a truncated member of the cysteine-rich secretory protein family. Dev. Biol. 360, 318–328. doi:10.1016/j.ydbio.2011.09.028

Chang, H., Kim, B.J., Kim, Y.S., Suarez, S.S., Wu, M., 2013. Different migration patterns of sea urchin and mouse sperm revealed by a microfluidic chemotaxis device. PLoS One 8, e60587. doi:10.1371/journal.pone.0060587

Clark, N.L., Aagaard, J.E., Swanson, W.J., 2006. Evolution of reproductive proteins from animals and plants. Reproduction 131, 11–22. doi:10.1530/rep.1.00357

Clark, N.L., Gasper, J., Sekino, M., Springer, S.A., Aquadro, C.F., Swanson, W.J., 2009. Coevolution of interacting fertilization proteins. PLoS Genet. 5, e1000570. doi:10.1371/journal.pgen.1000570

Clifton, A., 2015. WindRose [WWW Document]. Stack Overflow. URL http://stackoverflow.com/questions/17266780/wind-rose-with-ggplot-r

Cook, S.P., Brokaw, C.J., Muller, C.H., Babcock, D.F., 1994. Sperm Chemotaxis: Egg Peptides Control Cytosolic Calcium to Regulate Flagellar Responses. Dev. Biol. 165, 10–19.

Crean, A.J., Marshall, D.J., 2015. Eggs with larger accessory structures are more likely to be fertilized in both low and high sperm concentrations in Styela plicata (Ascidiaceae). Mar. Biol. 162, 2251–2256. doi:10.1007/s00227-015-2755-0

Crean, A.J., Marshall, D.J., 2008. Gamete plasticity in a broadcast spawning marine invertebrate. Proc. Natl. Acad. Sci. U. S. A. 105, 13508–13513. doi:10.1073/pnas.0806590105

Crimaldi, J.P., Zimmer, R.K., 2014. The physics of broadcast spawning in benthic invertebrates. Ann. Rev. Mar. Sci. 6, 141–65. doi:10.1146/annurev-marine-010213-135119

Darszon, A., Guerrero, A., Galindo, B.E., Nishigaki, T., Wood, C.D., 2008. Sperm-activating peptides in the regulation of ion fluxes, signal transduction and motility. Int. J. Dev. Biol. 52, 595–606. doi:10.1387/ijdb.072550ad

De Lisa, E., Salzano, A.M., Moccia, F., Scaloni, A., Di Cosmo, A., 2013. Sperm-attractant peptide influences the spermatozoa swimming behavior in internal fertilization in Octopus vulgaris. J. Exp. Biol. 216, 2229–37.

doi:10.1242/jeb.081885

Eisenbach, M., 1999. Sperm chemotaxis. Rev. Reprod. 4, 56–66.

Engqvist, L., 2013. A general description of additive and nonadditive elements of sperm competitiveness and their relation to male fertilization success. Evolution 67, 1396–1405. doi:10.1111/evo.12024

Evans, J.P., Garcia-Gonzalez, F., Almbro, M., Robinson, O., Fitzpatrick, J.L., 2012. Assessing the potential for egg chemoattractants to mediate sexual selection in a broadcast spawning marine invertebrate. Proc. R. Soc. 279, 2855–2861. doi:10.1098/rspb.2012.0181

Evans, J.P., Sherman, C.D.H., 2013. Sexual selection and the evolution of egg-sperm interactions in broadcast-spawning invertebrates. Biol. Bull. 224, 166–183.

Farley, G.S., Levitan, D.R., 2001. The role of jelly coats in sperm-egg encounters, fertilization success, and selection on egg size in broadcast spawners. Am. Nat. 157, 626–636. doi:10.1086/320619

Fitzpatrick, J.L., Lüpold, S., 2014. Sexual selection and the evolution of sperm quality. Mol. Hum. Reprod. 20, 1180–1189. doi:10.1093/molehr/gau067

Fitzpatrick, J.L., Simmons, L.W., Evans, J.P., 2012. Complex patterns of multivariate selection on the ejaculate of a broadcast spawning marine invertebrate. Evolution (N. Y). 66, 2451–2460. doi:10.5061/dryad.307c3n10

Foltz, K.R., Lennarz, W.J., 1990. Purification and characterization of an extracellular fragment of the sea urchin egg receptor for sperm. J. Cell Biol. 111, 2951–2959. doi:10.1083/jcb.111.6.2951

Franke, E.S., Babcock, R.C., Styan, C.A., 2002. Sexual conflict and polyspermy under sperm-limited conditions: in situ evidence from field simulations with the free-spawning marine echinoid Evechinus chloroticus. Am. Nat. 160, 485–96. doi:10.1086/342075

Friedrich, B.M., Julicher, F., 2007. Chemotaxis of sperm cells. Proc. Natl. Acad. Sci. 104, 13256–13261. doi:10.1073/pnas.0703530104

Gage, M.J.G., Macfarlane, C.P., Yeates, S., Ward, R.G., Searle, J.B., Parker, G. a., 2004. Spermatozoal traits and sperm competition in Atlantic salmon. Curr. Biol. 14, 44–47. doi:10.1016/j.cub.2003.12.028

Garbers, D.L., Hardman, J.G., 1976. Effects of egg factors on cyclic nucleotide metabolism in sea urchins. J. Cyclic Nucleotide Res. 2, 59–70.

Garbers, D.L., Watkins, H.D., Hansbrough, J.R., Smith, A., Misono, K.S., 1982. The amino acid sequence and chemical synthesis of speract and of speract analogues. J. Biol. Chem. 257, 2734–2737.

Gray, J., 1928. The Effect of Egg-Secretions on the Activity of Spermatozoa. BJEB 362–365.

Guerrero, A., Espinal, J.J., Wood, C.D., Rendon, J.M., Carneiro, J., Martínez-Mekler, G., Darszon, A., Rendón, J.M., Carneiro, J., Martínez-Mekler, G., Darszon, A., 2013. Niflumic acid disrupts marine spermatozoan chemotaxis without impairing the spatiotemporal detection of chemoattractant gradients. J. Cell Sci. 126, 1477–1487. doi:10.1242/jcs.121442

Guerrero, A., Nishigaki, T., Carneiro, J., Tatsu, Y., Wood, C.D., Darszon, A., 2010. Tuning sperm chemotaxis by calcium burst timing. Dev. Biol. 344, 52–65.

Hansbrough, J.R., Garbers, D.L., 1981. Speract: purification and characterization of a peptide associated with eggs that activates spermatozoa. J. Biol. Chem. 256, 1447–1452.

Harvey, E.B., 1956. The American Arbacia and Other Sea Urchins. Princeton University Press, Princeton, NJ.

Heck, D.E., Laskin, J.D., 2003. Ryanodine-Sensitive Calcium Flux Regulates Motility of Arbacia punctulata Sperm. Biol. Bull. 205, 185–186.

Hellberg, M.E., Dennis, A.B., Arbour-Reily, P., Aagaard, J.E., Swanson, W.J., 2012. the Tegula Tango: a Coevolutionary Dance of Interacting, Positively Selected Sperm and Egg Proteins. Evolution (N. Y). 66, 1681–94. doi:10.1111/j.1558-5646.2011.01530.x

Holt, W. V., Fazeli, a., 2015. Do sperm possess a molecular passport? Mechanistic insights into sperm selection in the female reproductive tract. Mol. Hum. Reprod. 21, 491–501. doi:10.1093/molehr/gav012

Hussain, Y.H., Guasto, J.S., Zimmer, R.K., Stocker, R., Riffell, J.A., 2016. Sperm chemotaxis promotes individual fertilization success in sea urchins. J. Exp. Biol. 1458–1466. doi:10.1242/jeb.134924

Jammalamadaka, S.R., Gupta, A. Sen, 2001. Topics in Circular Statistics. World Scientific Publishing Co, River Edge, NJ.

Johnson, D.W., Monro, K., Marshall, D.J., 2013. The maintenance of sperm variability: context-dependent selection on sperm morphology in a broadcast spawning invertebrate. Evolution (N. Y). 67, 1383–1395. doi:10.1111/evo.12022

Kashikar, N.D., Alvarez, L., Seifert, R., Gregor, I., Jäckle, O., Beyermann, M., Krause, E., Benjamin Kaupp, U., Kaupp, U.B., 2012. Temporal sampling, resetting, and adaptation orchestrate gradient sensing in sperm. J. Cell Biol. 198, 1075–91. doi:10.1083/jcb.201204024

Kaupp, U.B., Hildebrand, E., Weyand, I., 2006. Sperm chemotaxis in marine invertebrates — molecules and

mechanisms. J. Cell. Physiol. 208, 487–494. doi:10.1002/jcp

Kaupp, U.B., Kashikar, N.D., Weyand, I., 2008. Mechanisms of Sperm Chemotaxis. Annu. Rev. Physiol. 70, 93–117.

Kaupp, U.B., Solzin, J., Hildebrand, E., Brown, J.E., Helbig, A., Hagen, V., Beyermann, M., Pampaloni, F., Weyand, I., 2003. The signal flow and motor response controling chemotaxis of sea urchin sperm. Nat. Cell Biol. 5, 109–117.

Kinoh, H., Shimizu, T., Fujimoto, H., Suzuki, N., 1994. Expression of a putative precursor mRNA for sperm-activating peptide I in accessory cells of the ovary in the sea urchin Hemicentrotus pulcherrimus. Roux's Arch. Dev. Biol. 381–388.

Kirkman-Brown, J.C., Sutton, K.A., Florman, H.M., 2003. How to attract a sperm. Nat. Cell Biol. 5, 93–6. doi:10.1038/ncb0203-93

Kopf, G.S., Tubb, D.J., Garbers, D.L., 1979. Activation of sperm respiration by a low molecular weight egg factor and 8-bromoguanosine 3'5'-monophosphate. J. Biol. Chem. 254, 8554–8560.

Kosman, E.T., Levitan, D.R., 2014. Sperm competition and the evolution of gametic compatibility in externally fertilizing taxa. Mol. Hum. Reprod. 20, 1190–1197. doi:10.1093/molehr/gau069

Kregting, L.T., Thomas, F.I.M., Bass, A.L., Yund, P.O., 2014. Relative Effects of Gamete Compatibility and Hydrodynamics on Fertilization in the Green Sea Urchin Strongylocentrotus droebachiensis. Biol. Bull. 227, 33–39.

Krug, P.J., Riffell, J.A., Zimmer, R.K., 2009. Endogenous signaling pathways and chemical communication between sperm and egg. J. Exp. Biol. 212, 1092–1100. doi:10.1242/jeb.027029

Lazova, M.D., Ahmed, T., Bellomo, D., Stocker, R., Shimizu, T.S., 2011. Response rescaling in bacterial chemotaxis. Proc. Natl. Acad. Sci. 108, 13870–13875. doi:10.1073/pnas.1108608108

Lessios, H.A., Lockhart, S., Collin, R., Sotil, G., Sanchez-Jerez, P., Zigler, K.S., Perez, A.F., Garrido, M.J., Geyer, L.B., Bernardi, G., Vacquier, V.D., Haroun, R., Kessing, B.D., 2012. Phylogeography and bindin evolution in Arbacia, a sea urchin genus with an unusual distribution. Mol. Ecol. 21, 130–144. doi:10.1111/j.1365-294X.2011.05303.x

Levitan, D.R., 2012. Contemporary evolution of sea urchin gamete-recognition proteins: experimental evidence of density-dependent gamete performance predicts shifts in allele frequencies over time. Evolution (N. Y). 66, 1722–1736. doi:10.5061/dryad.0k2469h8

Levitan, D.R., 2006. The relationship between egg size and fertilization success in broadcast-spawning marine invertebrates. Integr. Comp. Biol. 46, 298–311. doi:10.1093/icb/icj025

Levitan, D.R., 2004. Density-dependent sexual selection in external fertilizers: variances in male and female fertilization success along the continuum from sperm limitation to sexual conflict in the sea urchin Strongylocentrotus franciscanus. Am. Nat. 164, 298–309. doi:10.1086/423150

Levitan, D.R., 2002. Density-Dependent Selection on Gamete Traits in Three Congeneric Sea Urchins. Ecology 83, 464–479.

Levitan, D.R., 2000. Sperm velocity and longevity trade off each other and influence fertilization in the sea urchin Lytechinus variegatus. Proc. R. Soc. 267, 531–534. doi:10.1098/rspb.2000.1032

Levitan, D.R., 1996. Effects of gamete traits on fertilization in the sea and the evolution of sexual dimorphism. Nature 382, 153–155.

Levitan, D.R., Terhorst, C.P., Fogarty, N.D., 2007. The risk of polyspermy in three congeneric sea urchins and its implications for gametic incompatibility and reproductive isolation. Evolution (N. Y). 61, 2007–14. doi:10.1111/j.1558-5646.2007.00150.x

Lillie, F.R., 1915. Studies of fertilization: VII. analysis of variations in the fertilizing power of sperm suspensions of Arbacia. Biol. Bull. 28, 229–251.

Lillie, F.R., 1912. The production of sperm iso-agglutinins by ova. Science (80-.). 36, 527–530. doi:10.1126/science.36.929.527

Lishko, P. V., Botchkina, I.L., Kirichok, Y., 2011. Progesterone activates the principal Ca2+ channel of human sperm. Nature 471, 387–391.

Lund, U., Agostinelli, C., 2002. CircStats: Circular Statistics, from "Topics in Circular Statistics" (2001).

Lüpold, S., Pitnick, S., Berben, K.S., Blengini, C.S., Belote, J.M., Manier, M.K., 2013. Female mediation of competitive fertilization success in Drosophila melanogaster. Proc. Natl. Acad. Sci. 110. doi:10.1073/pnas.1300954110

Manier, M.K., Belote, J.M., Berben, K.S., Novikov, D., Stuart, W.T., Pitnick, S., 2010. Resolving mechanisms of competitive fertilization success in Drosophila melanogaster. Science (80-.). 328, 354–357. doi:10.1126/science.1187096

Metz, E.C., Gómez-Gutiérrez, G., Vacquier, V.D., 1998. Mitochondrial DNA and bindin gene sequence evolution among allopatric species of the sea urchin genus Arbacia. Mol. Biol. Evol. 15, 185–195.

Miller, R.L., 1997. Specificity of sperm chemotaxis among Great Barrier Reef shallow-water Holothurians and Ophiuroids. J. Exp. Zool. 279, 189–200. doi:10.1002/(SICI)1097-010X(19971001)279:2<189::AID-JEZ10>3.0.CO;2-B

Miller, R.L., 1985. Sperm chemo-orientation in the Metazoa, in: Metz, C. (Ed.), Biology of Fertilization, v.2: Biology of the Sperm. Elsevier Science, pp. 275–331.

Morita, M., Nishikawa, A., Nakajima, A., Iguchi, A., Sakai, K., Takemura, A., Okuno, M., 2006. Eggs regulate sperm flagellar motility initiation, chemotaxis and inhibition in the coral Acropora digitifera, A. gemmifera and A. tenuis. J. Exp. Biol. 209, 4574–9. doi:10.1242/jeb.02500

Narayanan, A.S., Anwar, R.A., 1969. The specificity of purified porcine pancreatic elastase. Biochem. J. 114, 11–17.

Nozawa, Y., Isomura, N., Fukami, H., 2015. Influence of sperm dilution and gamete contact time on the fertilization rate of scleractinian corals. Coral Reefs. doi:10.1007/s00338-015-1338-3

Oliver, M., Evans, J.P., 2014. Chemically moderated gamete preferences predict offspring fitness in a broadcast spawning invertebrate. Proc. R. Soc. 281, 20140148.

Palumbi, S.R., 1999. All males are not created equal: fertility differences depend on gamete recognition polymorphisms in sea urchins. Proc. Natl. Acad. Sci. 96, 12632–12637.

Pennington, J.T., 1985. The ecology of fertilization of echinoid eggs: the consequences of sperm dilution, adult aggregation, and synchronous spawning. Biol. Bull. 169, 417–430.

Pfeffer, W., 1903. The Physiology of Plants, 2, Volume ed. Clarendon Press.

Pichlo, M., Bungert-Plümke, S., Weyand, I., Seifert, R., Bönigk, W., Strünker, T., Kashikar, N.D., Goodwin, N., Müller, A., Pelzer, P., Van, Q., Enderlein, J., Klemm, C., Krause, E., Trötschel, C., Poetsch, A., Kremmer, E., Kaupp, U.B., 2014. High density and ligand affinity confer ultrasensitive signal detection by a guanylyl cyclase chemoreceptor. J. Cell Biol. 206, 541–57. doi:10.1083/jcb.201402027

Podolsky, R.D., 2001. Evolution of egg target size: an analysis of selection on correlated characters. Evolution (N. Y). 55, 2470–2478.

Qasaimeh, M.A., Gervais, T., Juncker, D., 2011. Microfluidic quadrupole and floating concentration gradient. Nat. Commun. 2.

R Core Team, 2013. R: A language and environment for statistical computing.

Ralt, D., Goldenberg, M., Fetterolf, P., Thompson, D., Dor, J., Mashiach, S., Garbers, D.L., Eisenbach, M., 1991. Sperm attraction to a follicular factor(s) correlates with human egg fertilizability. Proc. Natl. Acad. Sci. 88, 2840–2844.

Ramarao, C.S., Burks, D.J., Garbers, D.L., 1990. A single mRNA encodes multiple copies of the egg peptide speract. Biochemistry 29, 3383–3388.

Riffell, J.A., Krug, P.J., Zimmer, R.K., 2004. The ecological and evolutionary consequences of sperm chemoattraction. Proc. Natl. Acad. Sci. 101, 4501–4506.

Riffell, J.A., Krug, P.J., Zimmer, R.K., 2002. Fertilization in the sea: the chemical identity of an abalone sperm attractant. J. Exp. Biol. 205, 1439–1450.

Rosen, W.G., 1962. Cellular Chemotropism and Chemotaxis. Q. Rev. Biol. 37, 242–259.

Rosman, J.H., Koseff, J.R., Monismith, S.G., Grover, J., 2007. A field investigation into the effects of a kelp forest (Macrocystis pyrifera) on coastal hydrodynamics and transport. J. Geophys. Res. 112, 1–16. doi:10.1029/2005JC003430

Rothschild, Lord, 1956. Fertilization. John Wiley & Sons, Inc, New York.

Sawada, H., Inoue, N., Iwano, M. (Eds.), 2014. Sexual Reproduction in Animals and Plants, Sexual Reproduction in Animals and Plants. Springer Japan, Tokyo. doi:10.1007/978-4-431-54589-7

Schmell, E.L.I., Earles, B.J., Breaux, C., Lennarz, W.J., William, J., Lennarz, W.J., 1977. Identification of a sperm receptor on the surface of the eggs of the sea urchin Arbacia punctulata. J. Cell Biol. 72, 35–46. doi:10.1083/jcb.72.1.35

Seltman, H.J., 2015. Experimental Design and Analysis. Carnegie Mellon University, Pittsburgh, PA.

Shiba, K., Baba, S.A., Inoue, T., Yoshida, M., 2008. Ca 2+ bursts occur around a local minimal concentration of attractant and trigger sperm chemotactic response. Proc. Natl. Acad. Sci. 105, 19312–19317.

Shimomura, H., Dangott, L.J., Garbers, D.L., 1986a. Covalent Coupling of a Resact Analogue to Guanylate Cyclase *. J. Biol. Chem. 261, 15778–15782.

Shimomura, H., Suzuki, N., Garbers, D.L., 1986b. Derivatives of speract are associated with the eggs of Lytechinus pictus sea urchins. Peptides 7, 491–495.

Simmons, L.W., Fitzpatrick, J.L., 2012. Sperm wars and the evolution of male fertility. Reproduction 144, 519–534. doi:10.1530/REP-12-0285

Simpson, J.L., Humphries, S., Evans, J.P., Simmons, L.W., Fitzpatrick, J.L., 2014. Relationships between sperm length and speed differ among three internally and three externally fertilizing species. Evolution (N. Y). 68, 92–104. doi:10.1111/evo.12199.This

Snook, R.R., 2005. Sperm in competition: not playing by the numbers. Trends Ecol. Evol. 20, 46–53. doi:10.1016/j.tree.2004.10.011

Spehr, M., Gisselmann, G., Poplawski, A., Riffell, J.A., Wetzel, C.H., Zimmer, R.K., Hatt, H., 2003. Identification of a testicular odorant receptor mediating human sperm chemotaxis. Science (80-.). 299, 2054–2058. doi:10.1126/science.1080376

Starkweather, J., 2010. Linear Mixed Effects Modeling using R. Univ. North Texas.

Strathmann, M.F., 1987. Reproduction and Development of Marine Invertebrates of the Northern Pacific Coast. University of Washington Press, Seattle, WA.

Strünker, T., Alvarez, L., Kaupp, U.B., 2015. At the physical limit — chemosensation in sperm. Curr. Opin. Neurobiol. 110–116. doi:10.1016/j.conb.2015.02.007

Suarez, S.S., Pacey, A.A., 2006. Sperm transport in the female reproductive tract. Hum. Reprod. Updat. 12, 23–37.

Suzuki, N., 1995. Structure, Function, and Biosynthesis of Sperm-Activating Peptides and Fucose Sulfate Glycoconjugate in the Extracellular Coat of Sea Urchin Eggs. Zoolog. Sci. 12, 13–27.

Suzuki, N., Garbers, D.L., 1984. Stimulation of sperm respiration rates by speract and resact at alkaline extracellular pH. Biol. Reprod. 30, 1167–74.

Suzuki, N., Shimomura, H., Radany, E.W., Ramarao, C.S., Ward, G.E., Bentley, J.K., Garbers, D.L., 1984. A peptide associated with eggs causes a mobility shift in a major plasma membrane protein of spermatozoa. J. Biol. Chem. 259, 14874–14879.

Swanson, W.J., Nielsen, R., Yang, Q., 2003. Pervasive adaptive evolution in mammalian fertilization proteins. Mol. Biol. Evol. 20, 18–20.

Swanson, W.J., Vacquier, V.D., 2002. The rapid evolution of reproductive proteins. Nat. Rev. Genet. 3, 137–144. doi:10.1038/nrg/733

Swanson, W.J., Yang, Z., Wolfner, M.F., Aquadro, C.F., 2001. Positive Darwinian selection drives the evolution of several female reproductive proteins in mammals. Proc. Natl. Acad. Sci. 98, 2509–2514.

Thomas, F.I.M., 1994. Physical Properties of Gametes in Three Sea Urchin Species. J. Exp. Mar. Bio. Ecol. 194, 263–84.

Thomas, F.I.M., Kregting, L.T., Badgley, B.D., Donahue, M.J., Yund, P.O., 2013. Fertilization in a sea urchin is not only a water column process: effects of water flow on fertilization near a spawing female. Mar. Ecol. Prog. Ser. 494, 231–240. doi:10.3354/meps10601

Tvedt, H.B., Benfey, T.J., Martin-Robichaud, D.J., Power, J., 2001. The relationship between sperm density, spermatocrit, sperm motility and fertilization success in Atlantic halibut, Hippoglossus hippoglossus. Aquaculture 194, 191–200. doi:10.1016/S0044-8486(00)00516-0

Vacquier, V.D., 1998. Evolution of Gamete Recognition Proteins. Science (80-.). 281, 1995–1998. doi:10.1126/science.281.5385.1995

Vacquier, V.D., Moy, G.W., 1977. Isolation of bindin: the protein responsible for adhesion of sperm to sea urchin eggs. Proc. Natl. Acad. Sci. 74, 2456–2460.

van der Horst, G., Maree, L., 2013. Sperm form and function in the absence of sperm competition. Mol. Reprod. Dev. 81, 204–216. doi:10.1002/mrd.22277

Veitinger, T., Riffell, J.A., Veitinger, S., Nascimento, J.M., Triller, A., Chandsawangbhuwana, C., Schwane, K., Geerts, A., Wunder, F., Berns, M.W., Neuhaus, E.M., Zimmer, R.K., Spehr, M., Hatt, H., 2011. Chemosensory Ca2+ Dynamics Correlate with Diverse Behavioral Phenotypes in Human Sperm. J. Biol. Chem. 286, 17311–17325.

Vinauger, C., Lutz, E.K., Riffell, J. a, 2014. Olfactory learning and memory in the disease vector mosquito, Aedes aegypti. J. Exp. Biol. 217, 2321–2330. doi:10.1242/jeb.101279

Ward, G.E., Brokaw, C.J., Garbers, D.L., Vacquier, V.D., 1985. Chemotaxis of Arbacia punctulata spermatozoa to resact, a peptide from the egg jelly layer. J. Cell Biol. 101, 2324–2329.

Watkins, H.D., Kopf, G.S., Garbers, D.L., 1978. Activation of sperm adenylate cyclase by factors associated with eggs. Biol. Reprod. 19, 890–894.

Wilburn, D.B., Swanson, W.J., 2016. From molecules to mating: Rapid evolution and biochemical studies of reproductive proteins. J. Proteomics 135, 12–25. doi:10.1016/j.jprot.2015.06.007

Wood, C.D., Darszon, A., Whitaker, M., 2003. Speract induces calcium oscillations in the sperm tail. J. Cell Biol.

161, 89–101.

Xiang, X., Kittelson, A., Olson, J., Bieber, A., Chandler, D., 2005. Allurin, a 21 kD sperm chemoattractant, is rapidly released from the outermost jelly layer of the Xenopus egg by diffusion and medium convection. Mol. Reprod. Dev. 70, 344–60. doi:10.1002/mrd.20201

Yanagimachi, R., Cherr, G., Matsubara, T., Andoh, T., Harumi, T., Vines, C., Pillai, M., Griffin, F., Matsubara, H., Weatherby, T., Kaneshiro, K., 2013. Sperm attractant in the micropyle region of fish and insect eggs. Biol. Reprod. 88, 47. doi:10.1095/biolreprod.112.105072

Yeates, S.E., Diamond, S.E., Einum, S., Emerson, B.C., Holt, W. V., Gage, M.J.G., 2013. Cryptic choice of conspecific sperm controlled by the impact of ovarian fluid on sperm swimming behavior. Evolution (N. Y). 67, 3523–3536. doi:10.1111/evo.12208

Yoshida, M., Hiradate, Y., Sensui, N., Cosson, J., Morisawa, M., 2013. Species-specificity of sperm motility activation and chemotaxis: a study on ascidian species. Biol. Bull. 224, 156–165.

Yoshida, M., Kawano, N., Yoshida, K., 2008. Control of sperm motility and fertility: diverse factors and common mechanisms. Cell. Mol. Life Sci. 65, 3446–3457. doi:10.1007/s00018-008-8230-z

Yoshida, M., Yoshida, K., 2011. Sperm chemotaxis and regulation of flagellar movement by Ca2+. Mol. Hum. Reprod. 17, 457–465.

Yoshino, K., Takao, T., Shimonishi, Y., Suzuki, N., 1991. Determination of the amino acid sequence of an intramolecular disulfide linkage-containing sperm-activating peptide by tandem mass spectrometry. FEBS Lett. 294, 179–82.

Zigler, K.S., McCartney, M.A., Levitan, D.R., Lessios, H.A., 2005. Sea urchin bindin divergence predicts gamete compatibility. Evolution (N. Y). 59, 2399–2404.

Zimmer, R.K., Riffell, J.A., 2011. Sperm Chemotaxis, Fluid Shear, and the Evolution of Sexual Reproduction. Proc. Natl. Acad. Sci. 108, 13200–13205.

Zuur, A.F., Ieno, E.N., Walker, N.J., Saveliev, A.A., Smith, G.M., 2009. Mixed Effects Models and Extensions in Ecology with R, Statistics for Biology and Health. Springer New York, New York, NY. doi:10.1007/978-0-387-87458-6

Chapter II: Individual female differences in chemoattractant production change the scale of sea urchin gamete interactions

Females change male fertilization success through sperm selection which, particularly in broadcast-spawning organisms, often occurs before sperm reach the egg. Waterborne sperm chemoattractants are one mechanism by which eggs selectively influence conspecific sperm behavior, but it has not been determined whether the eggs from different females produce different amounts of sperm chemoattractant. Here, we quantify the differences in attractant production between females of the sea urchin species *Lytechinus pictus* and use computational models and sperm chemotaxis assays to determine how differences in chemoattractant production between females affects their ability to attract sperm. Our study demonstrates that there is significant individual female variation in egg chemoattractant production, and that this variation changes the scope and strength of sperm attraction. These results provide evidence for the importance of individual female variability in differential sperm attraction.

INTRODUCTION

Sperm selection is common among animal taxa and can occur at multiple prezygotic stages. Females from organisms across the tree of life exhibit behavioral, physiological, and morphological traits with which they select sperm from certain males by various mechanisms. For example, female fruit flies select sperm from males with particular traits by ejecting sperm from non-preferred males (Lüpold et al., 2013), and mammals such as rodents and humans exhibit cryptic female choice within the reproductive tract (Fitzpatrick and Lüpold, 2014; Holt and Fazeli, 2015; Suarez and Pacey, 2006). Females from internally-fertilizing birds to

externally-fertilizing frogs to birds have reproductive traits that favor sperm with particular characteristics (Snook, 2005), and this selection activity can take place at the gametic level prior to sperm-egg contact, such as when female fish use chemoattractants in their externally-released ovarian fluid to preferentially attract conspecific sperm (Yeates et al., 2013).

Sperm selection in internal fertilizers can be mediated by a variety of mechanisms, including behavioral (Lüpold et al., 2013; Manier et al., 2010), variation in sperm-egg binding proteins (Swanson et al., 2001; Wilburn and Swanson, 2016), and morphological adaptations (e.g. complex structures as the female reproductive tract). However, the eggs of broadcast-spawning animals are limited to a smaller range of mechanisms (Evans and Sherman, 2013). For broadcast spawning animals, gamete recognition proteins have been shown to contribute to prezygotic sperm selection once gametes come into contact (Kosman and Levitan, 2014; Palumbi, 1999; Swanson and Vacquier, 2002), and upstream of these recognition proteins, eggs from ascidians (Aguirre et al., 2016) and mussels (Evans et al., 2012; Oliver and Evans, 2014) select compatible sperm, potentially through waterborne chemoattractants as in abalone (Riffell et al., 2004, 2002). In variable fertilization environments, the eggs of broadcast spawners are under selective pressure to increase conspecific gamete encounters, while either minimizing sperm contact to prevent polyspermy (Franke et al., 2002; Rothschild, 1956) or maximizing gamete interactions to counteract the effects of sperm dilution (Levitan, 2004; Nozawa et al., 2015).

One mechanism by which eggs can influence the rate of sperm-egg contacts is via production of waterborne sperm chemoattractants. Sea urchin sperm have been known to respond behaviorally and physiologically to egg-conditioned seawater for over a century (Lillie, 1912), and are a well-

43

studied and excellent model of sperm chemoattraction. Sperm attractant peptides have now been

identified for several urchin species (Suzuki, 1995), including the 10-amino-acid speract peptide

(Garbers et al., 1982; Hansbrough and Garbers, 1981; Kopf et al., 1979) in *Strongylocentrotus*

purpuratus eggs, as well as multiple similar sequences in the transcriptome (Ramarao et al.,

1990). Two speract analogues have been identified in *Lytechinus pictus* eggs (Shimomura et al.,

1986b) and resact, a 14-amino-acid peptide, has been isolated from *Arbacia punctulata* eggs

(Suzuki et al., 1984; Ward et al., 1985; Yoshino et al., 1991). While urchin sperm-attracting

peptides are considered to be species-specific (Suzuki et al., 1984; Ward et al., 1985), there is

some overlap in sperm physiological response to attractant peptides: for example, *L. pictus*

sperm respond to *S. purpuratus* speract (Guerrero et al., 2010; Hansbrough and Garbers, 1981),

which may be due to homologies in the peptide sequence (Shimomura et al., 1986b).

Previous studies of sperm chemotaxis have largely focused on species-specific differences in egg

chemoattractants and sperm behavior, and many have postulated that these population-level

differences could play a role in the evolution of gamete traits (Evans and Sherman, 2013; Riffell

et al., 2004; Yoshida et al., 2013). But it remains an open question whether individual differences

in either chemoattractant production by eggs or sperm sensitivity to attractants could also play an

evolutionary role. In our previous work, we found that individual sea urchin males differ in their

sperm chemotactic abilities, which correlates with differences in fertilization success (Hussain et

al., 2016). Although how individual variation in egg attractant production influences gamete-

interactions remains unclear, previous work examining other egg traits has shown that variability

plays an important role in fertilization. For instance, variation in egg size (Crean and Marshall,

2015; Levitan, 2006, 1996) and jelly coat volume (Farley and Levitan, 2001; Podolsky, 2001)

influence fertilization success, and a study in mussels points to differential attractive abilities of eggs (Evans et al., 2012). Previous studies have estimated attractant production by *A. punctulata* eggs using sperm behavior as a proxy (Kashikar et al., 2012), and sperm behavior has also been used to measure changes in sperm chemoattractant from groups of *Haliotis rufescens* abalone and *S. purpuratus* urchin eggs (Garbers and Hardman, 1976; Riffell et al., 2002). However, *A. punctulata* sperm can respond to a wide range of chemoattractant concentrations (Kaupp et al., 2008; Strünker et al., 2015) and the gradient conditions that sea urchin sperm experience are affected by the amount of chemoattractant produced by eggs as well as flow conditions which can be affected by egg location and clustering (Bell and Crimaldi, 2015; Kregting et al., 2014; Thomas et al., 2013). It remains unknown whether the eggs from individual females produce different amounts of chemoattractant, potentially influencing gamete interactions and fertilization success.

To determine whether there are differences in egg chemoattractant production between individual females, we characterized chemoattractant production by an average *Lytechinus pictus* egg using high-performance liquid chromatography and mass spectrometry. We then modeled the corresponding chemoattractant gradient around an individual egg, recreated the gradient conditions in a microfluidic device, and measured sperm responses with video microscopy and tracking. Our results show that individual females differ in their production levels of sperm chemoattractants, which may have important implications for gamete interactions and sexual selection.

METHODS

Sample preparation

Female sea urchins of the species *L. pictus* (South Coast Bio-Marine, San Pedro, CA) were housed in 75 L tanks at 8-10ºC under 12/12 light/dark conditions and supplied with *Macrocystis spp.* kelp (South Coast Bio-Marine). Urchins were spawned by injection with 0.5 mL of 0.5 M KCl into the coelomic cavity through the mouth and inverted over a glass petri dish containing 15 mL of artificial seawater consisting of 423 mM NaCl, 25.5 mM $MgSO_4$, 10 mM HEPES, 22.94 mM $MgCl_2$, 9.27 mM $CaCl_2$, 9 mM KCl, and 0.1 mM EDTA, adjusted to pH 7.8 using NaOH (ASW; (Alvarez et al., 2012)). Seawater was slightly acidified to prevent premature acrosome reaction of sperm, used later in the study. Females were allowed to spawn for 10 minutes and the eggs and seawater were moved into a 50 mL Falcon tube (BD Biosciences, San Jose, CA) for each female. ASW was added to each tube to a total volume of 40 mL and split into 9 4-mL aliquots. The egg concentration (eggs/mL) was calculated using counts from 6-8 aliquots on a hemocytometer (Marienfield, Germany). An analysis of 9 of 15 females established that urchin test diameter did not affect egg concentration ($R2 = -0.142$, $p = 0.948$). Three time points post-spawning were selected to balance the range of both egg and sperm viability (Levitan, 2000; Pennington, 1985; Riffell et al., 2004); we sampled 5 females at 20, 40, and 60 minutes, 9 females at 10, 30, and 50 minutes, and 1 female at 30, 60, and 90 minutes. Three aliquots from each time point were centrifuged at 1000×g for 5 minutes; the supernatant was retained and referred to as egg-conditioned seawater (ESW).

Egg-conditioned seawater (ESW) purification

Contaminants that affect High Performance Liquid Chromatography (HPLC) performance were removed by running ESW samples through a Sep Pak column (C18 Plus Light cartridge, Waters Corporation, Milford, MA). To control for recovery of the attractant peptide through the Sep-Pak column, several known-attractant standards in ASW were subjected to the same cleaning process as ESW samples (average recovery was 48%). Solutions were injected into the column using a syringe pump (Becton Dickinson and Co., Franklin Lakes, NJ). The column was cleaned with 3 mL of 50% acetonitrile (ACN) in Milli-Q water and equilibrated in 3 mL of Milli-Q water at a flow rate of 1 mL/min. 3 mL of each ESW sample was loaded onto the column at 0.3 mL/min. The column was washed with 1.2 mL of Milli-Q water and the attractant peptides were eluted at 0.3 mL/min with 1 mL of 25% ACN 1% acetic acid (AA) solution in Milli-Q water. Eluted samples were collected into 2 mL Eppendorf vials and frozen overnight at -80˚C. All samples were freeze-dried in a lyophilizer (VirTis 6K Benchtop Lyophilizer) for 8 hours and stored at -80˚C until analysis with High-Performance Liquid Chromatography with Mass Spectrometry (HPLC-MS).

High-Performance Liquid Chromatography with Mass Spectrometry (HPLC-MS)

Purified, lyophilized ESW samples were reconstituted in 100 μL Milli-Q water and analyzed using HPLC-MS (Hewlett Packard 1100 Liquid Chromatograph, Hewlett Packard Co. Palo Alto, California; Bruker Esquire Ion Trap Mass Spectrometer, Bruker Daltonics, Billerica, Massachusetts). Samples were separated on a C-18 narrow bore (2.1×100 mm) column (Zorbax Stable-Bond; Agilent Technologies, Santa Clara, CA) at 0.2 mL/min using a linear gradient starting at 100% of Solvent A (5% ACN 1% AA) and 0% of Solvent B (ACN with 1% AA),

reversing to 0% Solvent A and 100% Solvent B over 10 minutes, followed by 100% solvent B for 5 minutes. A full calibration curve of synthesized speract in Milli-Q water (Phoenix Pharmaceuticals, Burlingame, CA) was run in parallel to the ESW samples.

The base peak chromatogram (BPC) as determined by Bruker DataAnalysis software (Bruker Daltonics, Version 3.0) was used to find key peaks and target the corresponding mass fragments of putative attractants. *Lytechinus pictus* ESW samples contained several reproducible peaks, the most prominent containing mass/charge (m/z) units of 806.8, 887.8, 950.6, 890.9, and 891.8 (Figure 1). The peak for 893.0, an expected ion, was targeted but not consistently found in samples. Fragments of interest were isolated by extracted ion chromatograms with a width of 1 m/z and peak areas were obtained by manual integration.

High-resolution tandem mass spectrometric data was obtained by combining ESW samples from five different females and analyzing the mixture on an Orbitrap Fusion Tribrid mass spectrometer (Thermo Scientific, Waltham, MA). Samples were run on a custom-made 3 cm × 75 μm trap column followed by a 35 cm × 75 μm analytical column at 0.3 μL/min of ReproSil-Pur C-18 AQ 5 μm / 120A° beads (Dr. Maisch High Performance LC GmbH, Ammerbuch-Entringen, Germany). The 90-minute gradient started at 98% of Solvent A (0.1% formic acid in water; Optima LC/MS Solvent Blend, Fisher Chemical Waltham, MA) and 2% of Solvent B (0.1% formic acid in acetonitrile; Optima LC/MS Solvent Blend, Fisher Chemical, Waltham, MA), dropping to 70% Solvent A over 60 minutes, then reversing to 20% A for 10 minutes. A full scan over the 380-1500 m/z mass range was acquired at 120,000 resolution and the data-dependent MS/MS scans at 30,000 resolution included precursor charge states from +1 to +6.

The MS/MS data was analyzed by identifying major chromatogram peaks that also appeared in low-resolution HPLC-MS and performing de novo peptide sequencing to obtain amino acid sequence candidates that fit the tandem mass spectra.

Peptide Identification and Synthesis

Shimomura et al (Shimomura et al., 1986b) identified two speract analogues in *L. pictus* and tested them for sperm stimulation using respiration and cyclic nucleotide concentration assays: GFDLTGGGVQ, which corresponds to the 950.6 ion in ESW samples, and FDLTGGGVQ, an expected ion of mass 893.0 which was not found consistently in samples. We synthesized these peptides for use as HPLC-MS standards and in sperm behavior assays. Peptide synthesis of each speract analogue (GFDLTGGGVQ, FDLTGGGVQ) was carried out on a Liberty Blue solid-phase peptide synthesizer (CEM Corporation, Matthews, NC) using standard Fmoc synthesis on a 0.1 mmol scale. Briefly, amino acid solutions were suspended 0.2 mol/L in dimethylformamide (DMF) with DIC coupling reagent and Oxyma in DMF, over rink amide resin. The resin was washed with dichloromethane (DCM) after synthesis and cleaved with a solution of trifluoroacetic acid (TFA; 95%), triisopropylsilane (TIPS; 2.5%), and nanopure water (2.5%) for 1.5 hours under constant inversion. The resin was filtered out and peptide was precipitated out of solution by addition of cold diethyl ether and centrifugation, repeated 3 times. The peptide was dried overnight and stored dry at -80°C until dilution and use in calibration curves and sperm behavior tests. Synthesized sea urchin sperm attractant peptides have the same attractant properties as ESW and peptides isolated from ESW (Suzuki et al., 1984; Ward et al., 1985). A calibration curve of each speract analogue was run alongside a calibration curve of the speract standard to account for differences in ionization efficiency.

Chemoattractant Data Analysis

The concentration of speract analogues in each sample was calculated from the peak area of extracted ion chromatograms using the calibration curve of standards. Calibration curves of speract were generated for each HPLC-MS run using a linear regression. The difference between a calibration curve of speract and its analogues was used to adjust the calculated attractant concentration of corresponding extracted ions. Fraction recovery of ESW samples run through the Sep-Pak cleaning process was determined by standards run through the cleaning process alongside the ESW samples (fraction recovery = moles recovered / moles injected). Samples were divided by the fraction recovery for each experiment date to account for variability in solutions.

To determine the average amount of attractant produced per egg, the moles of peptide calculated from the calibration of extracted ion chromatograms was adjusted to account for the volume of injection, the ratio of volumes cleaned and centrifuged, and then divided by the egg count per female. Flux, the change in the amount of attractant over time, was calculated from a linear regression of moles of attractant produced over time.

Comparing the amount of each chemoattractant produced by eggs of different females required a model which was compatible with data that is not entirely independent, as observations from the same female at different timepoints are dependent. We therefore used a random-slopes random-intercepts mixed effects (Zuur et al., 2009) with individual females as a random effect, time as the independent variable, and log moles of attractant as the dependent variable. This type of

model investigates the differences between individual females in both the starting amount and rate of change of chemoattractant. 95% confidence intervals for the standard deviations were obtained using a bootstrap procedure, which allowed us to obtain the distribution of statistics through random resampling of the data set. Standard deviation of the female random effect intercept was compared to that of the residuals (Seltman, 2015), and the variance of the female random effect intercept was considered as a percentage of total random effect variance (Starkweather, 2010). The linear mixed effect model was computed in R (Bates et al., 2014; R Core Team, 2013); code and raw data are provided in the online material.

Model of Chemoattractant Gradient:

Using results from Chemoattractant Data Analysis, the peptide attractant production from a single egg (mol $\times$ min^{-1}) from data analysis was averaged and converted to flux of attractant over the surface of the egg (mol $\times$ m^{-2}s^{-1}) for use as a parameter in a model of attractant dispersal. Attractant dispersal was modeled using Advection-Diffusion and Navier-Stokes equations, which were solved numerically using COMSOL (Version 5.2a; COMSOL Inc., Burlington, MA). Parameters for the model were: average egg diameter of *L. pictus* sea urchins (111 μm), diffusion coefficient of speract (3×10^{-10} m^2 s^{-1} (Guerrero et al., 2013)), and a constant flux from eggs determined experimentally (described above) (mol $\times$ m^{-2}s^{-1}). Concentration of attractant was considered within 1.11 mm of the egg, and the gradient was monitored for 60 minutes -- full model details are provided in the supplementary material. The chemoattractant gradient surrounding one or a cluster of 100 eggs, with and without unidirectional 0.001 m $\times$ s^{-1} flow (Crimaldi and Zimmer, 2014; Rosman et al., 2007), was calculated in COMSOL. Comparisons between these advection-diffusion numerical solutions were performed using data exported from

a cut line at 60 seconds originating at the center of the surface of the egg and following the

vertical axis downstream of the egg. Due to differences in mesh geometry between models,

numerical comparisons of models were performed using spline fits in R. The gradient conditions

in the microfluidic device (detailed below) were scaled to the gradient conditions from the

model.

Microfluidic Sperm Chemotaxis Assays:

Male sea urchins of the species *L. pictus* were spawned by injection with 0.5 mL of 0.5 M KCl

into the coelomic cavity through the mouth and the gametes were collected dry and kept at 21°C

until use within 2 hours.

Microfluidic devices were produced as described in Hussain et al 2016. Briefly,

polydimethylsiloxane (PDMS; Dow Corning, Midland, MI) channels with three input branch

channels that met in a single 'test' channel 4 cm long, 99 μm deep, and 1.02 mm wide were

patterned onto a silicon wafer by exposure of negative photoresist to ultraviolet light. PDMS was

molded against the silicon master and attached to a glass slide.

The concentration of attractant c with diffusion coefficient D can be described as a function of

position x and time t inside the microfluidic channel of width L by solving the advection

diffusion equation

$\frac{\partial c}{\partial t} = D^2 \frac{\partial^2 c}{\partial x^2}$ with boundary conditions $\frac{\partial c}{\partial x}(0, t) = \frac{\partial c}{\partial x}(L, t) = 0$ and initial conditions $c(x, 0) =$

c_0 within the attractant source and $c(x, 0) = 0$ outside the attractant source, where the location

of the attractant layer within the channel is α. The analytical solution derived from this equation

using a Fourier transform is

$C(x,t) = (1 - \alpha) + \sum_{i=1}^{\infty} (\frac{-2}{i\pi}) sin(i\pi\alpha) cos(i\pi x) exp(-i^2\pi^2 t)$, where i is the summation

index (Ahmed et al., 2010a; Asmar, 2004).

Sperm diluted 1000x in ASW (~ 10^7 sperm/mL), ASW, and the relevant peptide attractant

(speract, Phoenix Pharmaceuticals; speract analogues, synthesized as detailed above) diluted to

concentrations derived from the gradient model as well as 10x higher and 10x lower were

contained in gastight syringes (Hamilton Company, Reno, NV) and attached to polyethylene

tubing (BD Intramedic[TM], Franklin Lakes, New Jersey) that was inserted into input channels. In

order to make a gradient with appropriate steepness to approximate the COMSOL model, sperm

were injected on one side using a 0.5 mL syringe, ASW into the middle using a 1 mL syringe,

and the predetermined speract or analogue into the opposite side using a 0.5 mL syringe.

Sperm were imaged as in Hussain et al 2016. Briefly, a flow rate of 10 μL min^{-1} was applied

using a syringe pump (Harvard Apparatus, Holliston, MA) for 60 seconds before it was stopped

to allow diffusion to form the attractant gradient. Sperm in the microfluidic device was imaged

for 60 seconds starting from stoppage of flow, using a 10× Nikon Plan Fluor objective (Nikon

Instruments, Melville, NY) on an inverted microscope (Nikon TE 2000) and saved to video using

a 512 × 512-pixel (8.2 × 8.2 mm field of view) CCD camera (iXon Ultra 897; Andor

Technology, Belfast, UK). Videos were blinded prior to analysis for sperm behavior with Nikon-

NIS Elements image analysis software.

Chemotaxis Data Analysis:

In each treatment, the first and last points of the trajectories of 85-115 sperm (pooled from 5 males, 723 sperm total) were used to determine the orientation of the full trajectory, calculated as $\theta = tan^{-1}(\Delta y/\Delta x)$, using original scripts in Matlab (Mathworks, Natick, MA). The orientation of all sperm tracks in each treatment was reflected about the x-axis to yield a range of 0-180° and used to calculate the mean orientation for each treatment; R (R Core Team, 2013) and the WindRose function (Clifton, 2015) were used to display orientation data. Sperm orientation between treatments was compared with a one-way ANOVA coupled with a post-hoc Tukey test for comparisons of multiple means. Sperm vector length was calculated as $\sqrt{(\Delta x)^2 + (\Delta y)^2}$.

RESULTS

Peptide production rates from females

To determine individual female variability in chemoattractant peptide production, we collected egg-conditioned seawater from individual females and compared the relative per-egg concentrations obtained by HPLC-MS. We were able to identify ion fragments from sperm chemoattractant peptides characterized in previous studies of *L. pictus* (Shimomura et al., 1986b) as well as several other peaks in the base peak chromatogram which have similar retention times to the known peptides and mass spectra that suggest peptide structure (Figure 1). We obtained putative sequences of two of these novel peptides: the putative sequence of the peptide eluting at 41.5 minutes, corresponding to the extracted ion with mass/charge 806.8 (in Orbitrap, singly and doubly charged ions at 806.4 and 403.7, respectively) is PSGGVSFVG and the putative sequence of the extracted ion with mass/charge 893.8 (in Orbitrap, 893.4) is NGTFDLVQ (Figure 2). Due to differences in ionization efficiency between peptide structures, we are unable to quantify all of

the six present peptides. However, we are able to compare the relative quantities of each

extracted ion between females and find that, for all six peptides, there are statistically significant

differences between females (Figure 3, Figure 4). A random-slopes, random-intercepts mixed

effects model was used to investigate the differences in both rate of change and starting

concentration of peptide. Between-female variation ranges from 0.87 to 0.94, with an average

standard deviation of the variance of 0.92 (Table 1). The between-female variation is on average

8.7× (range 5.3× - 10.0×) the magnitude of the within-female variation and accounts for on

average 98.5% (range 96.6% - 99.1%) of the random effect variance (Table 1). The model with a

random female effect has a lower AIC than the model that excludes the random effect (e.g., for

the peptide with mass/charge 950.6, AIC with random effect is -69.47 and AIC without random

effect is 250.69), indicating that random effect results in a better fit. The random effect of slope

is consistently statistically significant according to its confidence intervals (Table 1, Figure 3b)

but contributes little to the overall differences between females.

Using the peptide GFDLTGGGVQ (EIC 950.6, Shimomura et al., 1986) for which we have an

exact calibration curve, we obtained a range of attractant production from eggs of 4×10^{-15} to

5×10^{-15} mol $\times$ min^{-1} with a mean of 1.35×10^{-15} mol $\times$ min^{-1} (Table 2). From this range, we

calculated the flux of attractant over the surface of the egg (mol/m^2/s) and used it as a parameter

in a model of the spatiotemporal dynamics of realistic egg gradient conditions. The range of flux

was 8.04×10^{-11} to 2.21×10^{-9} mol $\times$ m^{-2}s^{-1} with a mean of 7.74×10^{-10} mol $\times$ m^{-2}s^{-1}.

Within this range and over the course of 60 minutes, there are differences between individual

females. The eggs from Female 4 have the highest flux of 2.21×10^{-9} mol $\times$ m^{-2}s^{-1}, which is two

orders of magnitude higher than those assayed from Female 10 with 8.04×10^{-11} mol $\times$ m^{-2}s^{-1}, but also starts at a lower concentration than eggs from Female 10 (6.81×10^{-13} moles and 1.03×10^{-12} moles, respectively). There is a ten-fold difference in the attractant production between Female 1 (1.62×10^{-9} mol $\times$ m^{-2}s^{-1}) and Female 14 (1.62×10^{-10} mol $\times$ m^{-2}s^{-1}) but only a two-fold difference in the starting concentration (3.63×10^{-13} moles and 1.84×10^{-13} moles, respectively). All females have a flux within 10$\times$ of 10^{-10} mol $\times$ m^{-2}s^{-1} except for Female 11, which has a negative flux. Our results show significant differences between females in egg chemoattractant production, and the flux information is used as a parameter in the computational model of egg chemoattractant dispersal.

Numerical models of attractant dispersal

In order to determine the effects of individual female chemoattractant production differences on the attractant gradients that sperm experience, we modeled the dispersal of chemoattractant from eggs under several conditions. The results of the advection-diffusion numerical solution, with and without flow, are shown in Figure 5a-d. Time lapse videos of the advection-diffusion numerical model for an average single egg without flow and with flow are compared in Video 1 and Video 2, and the model for a cluster of 100 eggs is shown in Video 3. All comparisons are reported at 60 seconds, which is the length of time for which sperm behavior videos were recorded.

In no-flow conditions, a single egg with the maximum attractant flux yields a steeper gradient than both the minimum flux and the mean flux (at 0.1 mm from the egg surface, 27.5$\times$ higher and 2.83$\times$ higher, respectively) due to the higher concentration of attractant at the surface of the

egg (Figure 5a). Higher egg fluxes also result in higher absolute concentrations; for example, sperm experience the minimum attractant concentration to which they can respond (10^{-12} mol/L = 10^{-9} mol/m^3, (Guerrero et al., 2010)) as far as 1.1 mm from the surface of an egg with maximum egg attractant flux, while sperm at mean flux experience that concentration within 1 mm of an egg with mean attractant flux and only within 0.79 mm of an egg with the minimum flux (Figure 5a). The 0.1 mm difference between mean and maximum is equivalent to a 10% increase in detection distance by the sperm, and the 0.31 mm difference between minimum and maximum yields a 39% increase in detection distance between minimum and maximum attractant flux.

Under no-flow conditions, the concentration of attractant surrounding a single egg and a cluster of eggs is the same at 0.05 mm from the surface of the egg, but diverges linearly, with 3.1× the concentration of attractant 0.55 mm from a cluster of 100 eggs than a single egg (Figure 5b). When 0.001 m × s^{-1} unidirectional flow is applied, a cluster of 100 eggs sustains an average of 7.2× the attractant concentration of a single egg (standard deviation 1.5) (Figure 5c). Individual female variation in egg chemoattractant production leads to differences in attractant gradient formation and sperm detection distance in a variety of conditions.

Sperm behavior in chemoattractant gradients

In order to describe the effect of differential attractant gradients on sperm chemotaxis, we assayed sperm behavior in microfluidic-device-created gradients designed to emulate the results of our advection-diffusion model. The computational model shows that a single egg in no-flow conditions creates a concentration gradient of chemoattractant that increases in absolute

concentration over time (Figure 5d). We recreated the concentration gradient from an egg at 60 seconds, the length of time that we selected record sperm behavior in the microfluidic device, by scaling the starting concentration of attractant in the microfluidic device. A starting concentration of 100 nM of chemoattractant (speract or GFDLTGGGVQ) yields an equivalent gradient; for example dc/dx in the microfluidic channel was 2.3×10^{-4} mol $\times$ m^{-4} at 0.03 mm from the attractant source, which matches the gradient in the advection-diffusion numerical model at 0.16 mm from the surface of the egg (denoted by asterisks in Figure 5d, 5e)

The orientation of sperm to gradients formed with this starting concentration of attractant at 100 nM, as well as 10 nM and 1000 nM and an artificial seawater control, is shown in Figure 6. The results of an ANOVA and Tukey post-hoc test for comparison of multiple means indicate that there is a significant effect of treatment on sperm orientation ($p < 0.001$) (Table 3) and vector length ($p < 0.001$). Sperm orientation in the ASW control was $78.3 \pm 3.3°$, and all attractant (GFDLTGGGVQ and speract) treatments except for 10 nM and 100 nM GFDLTGGGVQ yielded sperm tracks that were closer to 0° (the direction of the attractant source) than the control (Tukey test; all $p < 0.05$) (Figure 6, Figure 7a). Sperm oriented towards the attractant most strongly when the starting concentration was 100 nM speract ($46.9 \pm 2.9°$) and 1000 nM speract ($51.2 \pm 2.7°$), which were not statistically different from each other ($p = 0.97$); sperm in the 10 nM speract treatment were less strongly-oriented ($59.1 \pm 3.5°$). Only the highest concentration of GFDLTGGGVQ, 1000 nM, resulted in sperm orientation different from the ASW control ($56.6 \pm 3.39°$, $p < 0.05$). Sperm traveled the greatest distance in the 100 nM speract and 1000 nM speract treatments (0.589 ± 0.022 mm and 0.570 ± 0.021 mm respectively), and all mean sperm vector lengths for attractant treatments significantly differed from the ASW control ($0.364 \pm$

0.023 mm) except for 10 nM and 100 nM GFDLTGGGVQ ($p < 0.01$) (Figure 7b). Our results show that sperm have stronger chemotactic responses to higher concentrations of chemoattractant.

DISCUSSION

In this study, we investigated individual variation in egg chemoattractant production and its effect on the gradients that attract sperm. We used high-performance liquid chromatography and mass spectrometry to measure attractant production from the eggs of individual *L. pictus* females over time. We then numerically modeled the chemoattractant gradient formed by attractant flux from eggs and measured sperm responses to the average chemoattractant gradient. We found that for all peptides present in *L. pictus* egg-conditioned seawater, including novel peptides, eggs of individual females exhibit differences in chemoattractant production. Models of the chemoattractant gradient originating from an egg show that differences in flux between eggs of individual females can substantially change the distance from which sperm perceive eggs. We also found that sperm respond behaviorally to chemoattractant gradients corresponding to a wide range of starting peptide concentrations, including the gradient formed by a single egg, but that their responses were strongest to higher starting concentrations of attractant.

Individual female differences in chemoattractant production

The eggs of individual females vary widely in their starting levels of chemoattractant and rates of attractant production, with starting concentrations spanning an order of magnitude and female effects in a linear mixed-effects model accounting for an average of 98.5% of the random effect variance. The physiological processes underlying individual female differences in egg attractant

production have yet to be studied, but modulation of transcription of attractant-encoding genes or translation of precursor mRNA in the ovary (Kinoh et al., 1994) and potential posttranslational cleavage (Ramarao et al., 1990) could explain the variation we observe. In addition to previously-described attractant peptides in *L. pictus* egg-conditioned seawater, our study finds six peptides with similar masses and we suggest two putative sequences (PSGGVSFVG and NGTFDLVQ) for these peptides. The question remains as to how these peptides interact to attract sperm and whether individual females modulate production of particular peptides to create a signature signal that attracts sperm from particular males. Future work will be required to understand the interaction of these newly-uncovered peptides and their effects on sperm chemoattraction.

Individual female variation in egg chemoattractant production could compound with other egg-level differences that affect gamete interactions. For instance, egg-level differences in gamete recognition proteins can influence sperm binding and female and male fitness (Kosman and Levitan, 2014; Palumbi, 1999; Swanson and Vacquier, 2002). In another example, individual sand dollar females were found to have eggs with different ovum and jelly coat sizes, influencing sperm-egg encounters by either directly increasing the physical target size of the egg or indirectly increasing the attractant around the egg that serves to attract sperm (Podolsky, 2001). Egg size has also been demonstrated to be a plastic trait in broadcast-spawning ascidians, affected by adult population density (Crean and Marshall, 2008). Ascidians are sessile as adults and are therefore subject to different life-history pressures than urchins, but populations of sea urchins also have different densities and distributions that can change gamete interaction dynamics (Levitan, 2012, 2002).

Effects of female differences on sperm responses

A critical component of gamete interactions is the spatial scale at which sperm can detect and move towards eggs. The range of positive flux from individual eggs varied by two orders of magnitude, with a range of 8.04×10^{-11} to 2.21×10^{-9} mol $\times$ m^{-2}s^{-1}. This range of flux substantially changes the distance to which the attractant disperses and subsequently the distance of detection by sperm. The maximum distance at which sperm can perceive and move towards eggs at the lowest attractant flux is 0.31 mm closer than at the highest attractant flux, which is large portion of the estimated 1 mm from the oocyte from which chemotaxis is expected to influence gamete interactions (Crimaldi and Zimmer, 2014; Guerrero et al., 2010; Miller, 1985).

Hydrodynamic conditions interact with chemoattractant plumes to change gamete encounters, with intermediate flow increasing the dispersal of attractant and subsequently fertilization success in abalone (Bell and Crimaldi, 2015; Zimmer and Riffell, 2011). *Lytechinus pictus* aggregate in relatively sheltered conditions (Rosman et al., 2007) where shear is low compared to urchins on wave-swept shores. In unidirectional flow, urchin eggs tend to cluster on the aboral surface of the female (Thomas, 1994), where they encounter higher overall fertilization success (Thomas et al., 2013) and allow greater selection on gamete compatibility to occur (Kregting et al., 2014) than in the water column. The observed increase in fertilization success may be due to greater sperm attraction capability from the higher level of attractant around these eggs, but as seen in our model, the increase in attractant due to egg clustering does not scale linearly as egg clusters have a lower surface area to volume ratio over which attractant can flux. Both flux and

61

flow affect the chemoattractant gradient and therefore the spatiotemporal dynamics and magnitude of sperm chemosensory responses.

We find that sperm orient to low concentrations of attractant, including that formed by a single egg, but that sperm orient preferentially to higher concentrations of chemoattractant, corresponding to $10\times$ the gradient formed by a single egg. This indicates a lack of tuning of sperm responsiveness to specific attractant concentrations, and instead corroborates previous findings that sea urchin sperm can respond to extremely small attractant concentrations – femtomolar in *Arbacia punctulata* (Kashikar et al., 2012; Kaupp et al., 2003) and picomolar in *Lytechinus pictus* (Guerrero et al., 2010) – but have stronger responses to higher concentrations. Given the variation in attractant dispersal due to differences in attractant flux from the egg and the wide range in fluxes between females, we would expect sperm to orient more directly towards the eggs of females with higher chemoattractant fluxes. It is also plausible that sperm response is dependent not only on the concentration of attractant but also the mixture of multiple attractant peptides, which appears to differ between females. It remains to be determined whether individual female differences in attractant production correlate to relative differences in fertilization success.

Individual differences and sexual selection

In our previous work, we found that sperm from individual males had different levels of behavioral response to egg-derived chemoattractants, affecting their relative fertilization success (Hussain et al., 2016). Here, we find that individual females have eggs that production different amounts of chemoattractant, suggesting that female investment in sperm chemoattraction differs

and may affect sperm behavior to change fertilization success. The question then arises: are individual sea urchin males and females operating under joint or opposing selective pressure? Reproductive protein evolution in many broadcast spawners (Clark et al., 2009; Evans and Sherman, 2013; Hellberg et al., 2012; Vacquier, 1998) and internal fertilizers (Clark et al., 2006; Swanson et al., 2003, 2001) is under positive, divergent selection, indicating male-female antagonism. The type of selective pressure on broadcast-spawning females also depends on whether conditions lead to sperm limitation or sperm overabundance with the threat of polyspermy (Crean and Marshall, 2015; Franke et al., 2002; Levitan, 2012; Levitan et al., 2007; Zimmer and Riffell, 2011). Fertilization success is dependent on a breadth of variables, one of which is the interplay between egg investment in chemoattractant production and sperm chemoreceptivity in relation to fertilization.

Summary

Using high-performance liquid chromatography with mass spectrometry, numerical and analytical models of attractant dispersal, and microfluidic sperm orientation assays, we show that individual *L. pictus* females have eggs with differing amounts of chemoattractant production that can dramatically affect sperm chemoattractive behavior. Our study is the first to quantify differences in egg attractant production between females and provides a basis for investigating the effects of varying levels of female investment in sperm chemoattraction on fertilization success.

FIGURES

Figure 1:

Identification of primary peptides in chromatograms and mass spectra of egg-conditioned seawater **(A)** Comparison of raw base peak chromatograms (BPCs) of egg-conditioned seawater from eggs of two representative females, illustrating the differences between females and the multiple peaks indicating multiple potential peptides. Samples from all females (n = 15) produced BPCs similar to these. Peaks are labeled with their respective primary masses (m/z). Chromatogram and mass spectrum intensity are given in arbitrary units (AU). **(B)** The total ion chromatogram (TIC) of a representative egg-conditioned seawater sample subtracted to the baseline. Each extracted ion chromatogram (EIC) was based off the most common masses in the TIC. The peak in the TIC at 8.7 minutes is the common contaminant polyethylene glycol (212.1); the peak in the TIC at 7.3 minutes has a mass of 659.9; we focused on masses similar to already-identified peptide attractants. **(C)** Mass spectra of peaks from (B), in order of retention time.
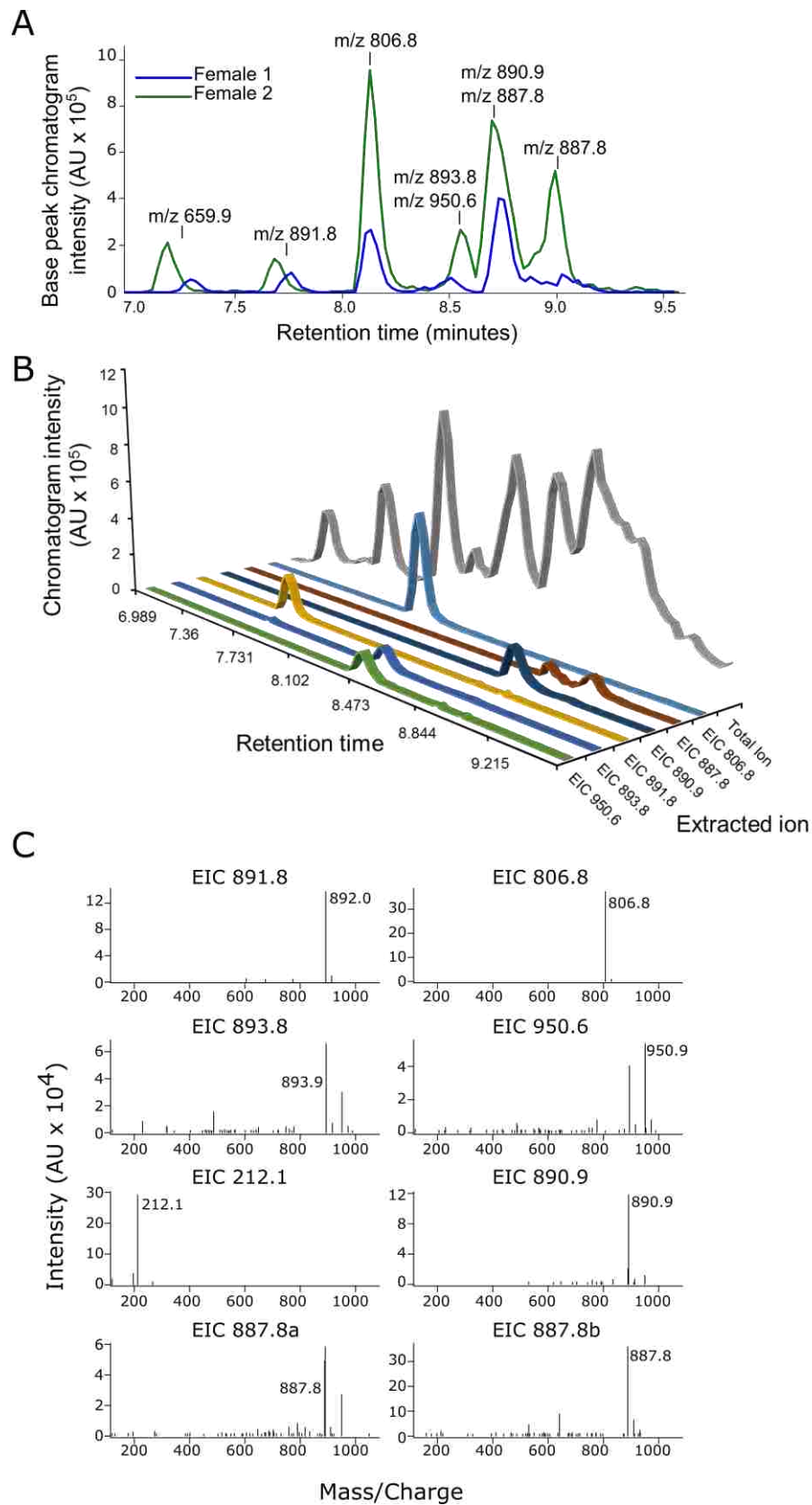
Figure 2 -

High-resolution tandem mass spectrometry for peptide sequence derivation. (**A**) Total ion chromatogram of ESW samples on a high-resolution hybrid mass spectrometer (Orbitrap Fusion) for full mass spectrometric scan, with highlighted peaks corresponding to base peaks observed on the low-resolution HPLC-MS system. (**B**) MS/MS spectrum for precursor ion 806.4, with major masses highlighted. (**C**) MS/MS spectrum for precursor ion 893.4, with major masses highlighted. The tandem mass spectra for singly and doubly charged precursors were nearly identical.
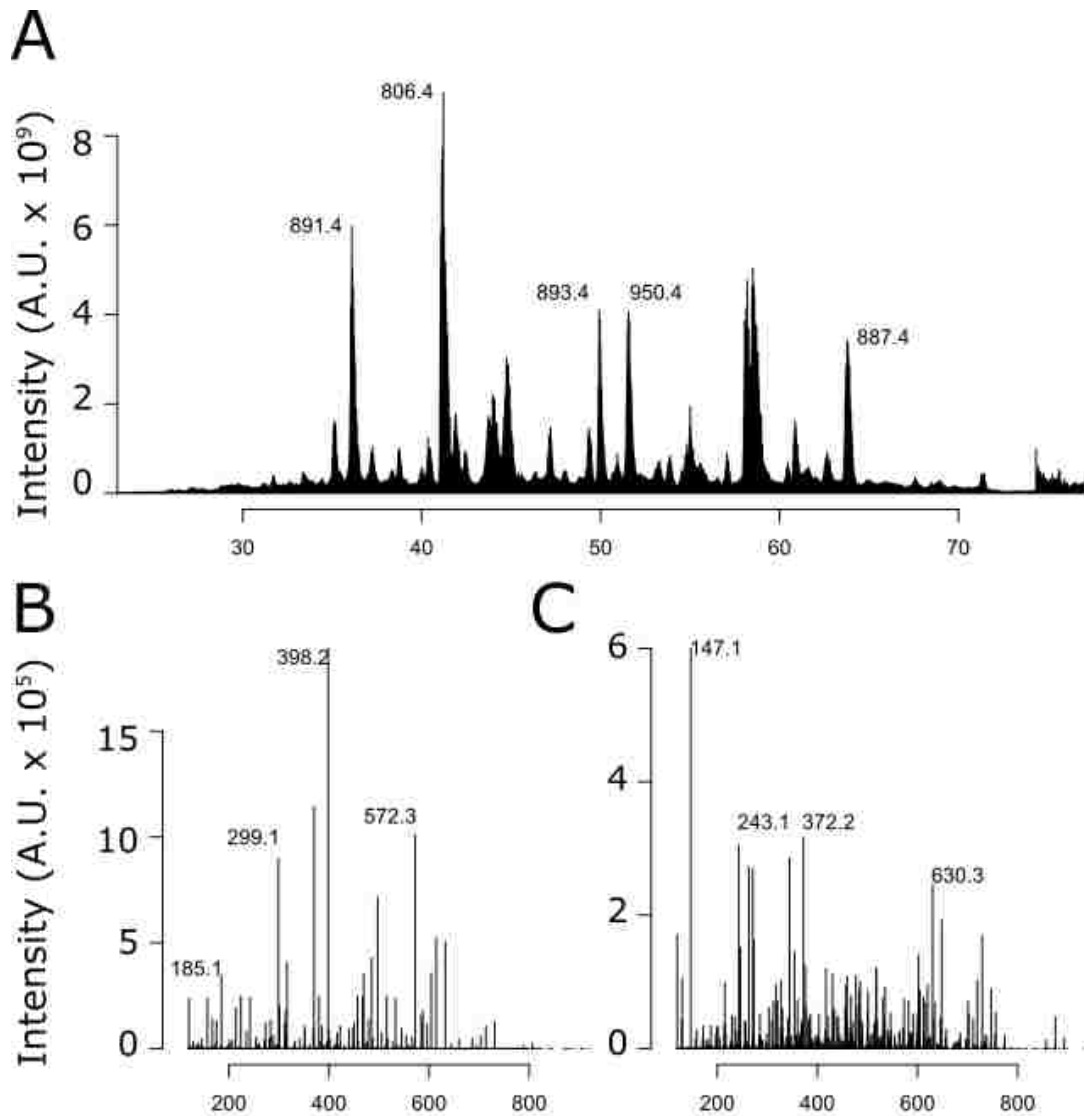
Figure 3 -

Individual females (n = 15) have eggs with different starting concentrations and production of the peptide attractant GFDLTGGGVQ, corresponding to the mass/charge of 950.6 **(A)** Moles of attractant per egg, with each color representing eggs from a different female. Between-female variation is 8.4× the magnitude of the within-female variation and accounts for 98.6% of the random effect variance. Error bars denote s.e.m. (many standard errors are smaller than point size) **(B)** Moles of attractant per egg, normalized to the maximum attractant concentration for each female to illustrate differences in attractant production rate. Normalizing to the maximum value for each female qualitatively shows the differences in relative attractant production, and 95% confidence intervals indicate that the random effect of slope is statistically significant. Although the differences in attractant production rate between individual females are statistically significant, they explain a small portion of total differences between females.
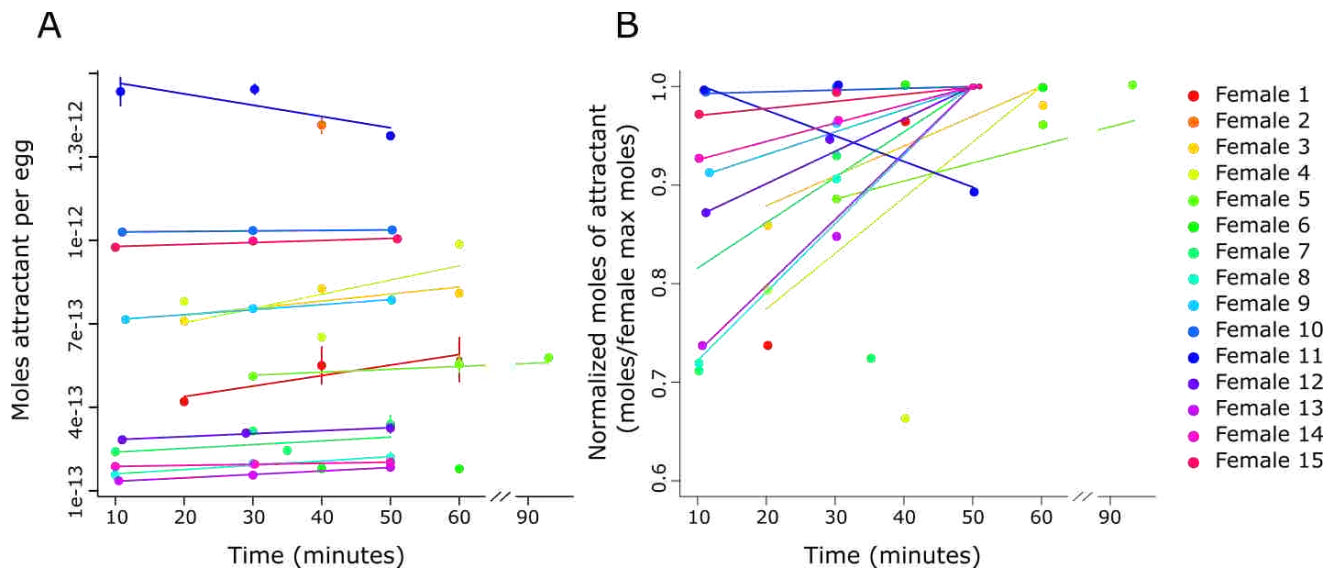
Figure 4 -

Individual females (n=15) have eggs with different starting concentrations and production of six speract analogue peptides. Between-female variation is on average 8.7× the magnitude of the within-female variation and accounts for on average 98.5% of the random effect variance. Error bars indicate s.e.m. (many standard errors are smaller than point size). (**A**) Peptide with mass/charge of 806.8 (**B**) Peptide with mass/charge of 887.8 (**C**) Peptide with mass/charge of 890.9 (**D**) Peptide with mass/charge of 891.8 (**E**) Peptide with mass/charge of 893.8
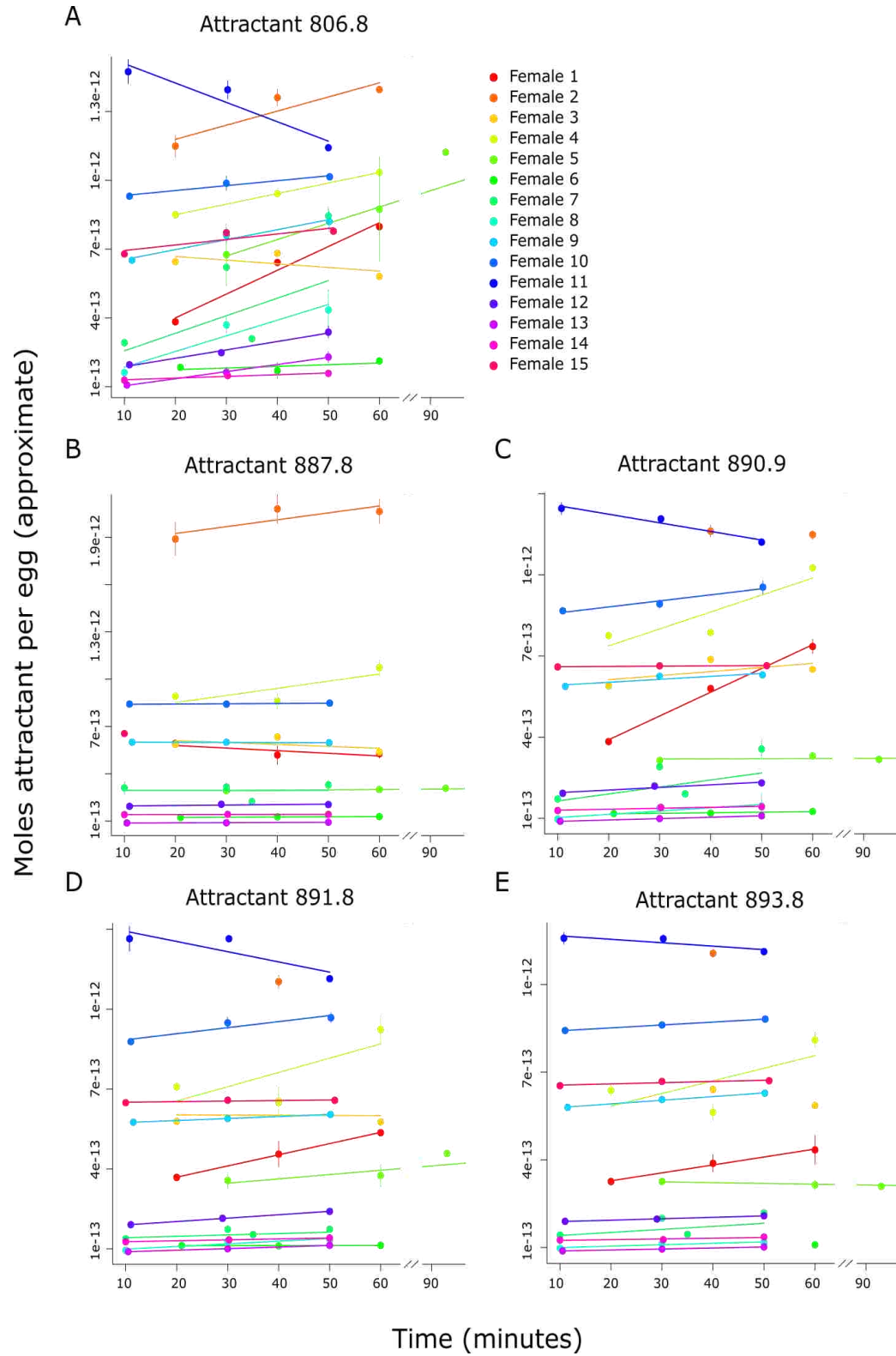
Table 1 -

Results of a random-slopes random-intercepts mixed effects model with individual female as the random effect, time as the independent variable, and log moles of attractant as the dependent variable (95% confidence intervals obtained by a bootstrap procedure). Average standard deviation of the variance, corresponding to between-female variation, is on average 0.92, or 8.7× the magnitude of average within-female variation. Confidence intervals indicate that both the random effect of intercept and slope are statistically significant.

Attractant	Random Effect	Variance	Standard deviation	Confidence interval lower bound	Confidence interval upper bound	Intercept/ Residual	Female intercept % of random effect
EIC 806.8	female intercept	8.13E-01	0.9014	0.8312	0.9499	5.30	96.5
	female slope	7.50E-05	0.0086	0.0060	0.0098		
	residual	2.89E-02	0.1700	0.11122	0.1864		
EIC 887.8	female intercept	8.05E-01	0.8974	0.8668	0.9339	10.00	99.1
	female slope	2.34E-08	0.0001	0.00002	0.0014		
	residual	8.05E-03	0.0897	0.0691	0.1006		
EIC 890.9	female intercept	8.82E-01	0.9389	0.8954	0.9837	8.62	98.7
	female slope	2.66E-05	0.0051	0.0033	0.0060		
	residual	1.19E-02	0.1089	0.0621	0.1269		
EIC 891.8	female intercept	8.92E-01	0.9445	0.9095	0.9854	10.27	99.1
	female slope	8.40E-06	0.0028	0.0012	0.0035		
	residual	8.46E-03	0.0919	0.0660	0.1011		
EIC 893.8	female intercept	8.83E-01	0.9393	0.8909	0.9846	9.65	98.9
	female slope	6.67E-06	0.0025	0.0006	0.0032		
	residual	9.47E-03	0.0973	0.0703	0.1052		
EIC 950.6	female intercept	7.60E-01	0.8715	0.8258	0.9294	8.44	98.6
	female slope	7.23E-06	0.0026	0.0014	0.0039		
	residual	1.07E-02	0.1032	0.0765	0.1090		

Table 2 -

Rate of production of the peptide attractant GFDLTGGGVQ (mass/charge 950.6) from a single

egg. Mean positive attractant production of this peptide is 1.80×10^{-15} mol $\times$ min^{-1}, translating to a

mean flux of 7.74×10^{-10} mol $\times$ m^{-2}s^{-1}.

Female	Intercept (mol)	Slope (mol/min)	Flux (mol/m²/s)
LP1	3.63E-13	3.77E-15	1.62E-9
LP3	6.81E-13	2.52E-15	1.08E-9
LP4	6.01E-13	5.13E-15	2.21E-9
LP5	4.84E-13	1.06E-15	4.55E-10
LP7	2.17E-13	2.16E-15	9.29E-10
LP8	1.45E-13	1.55E-15	6.66E-10
LP9	6.97E-13	1.80E-15	7.75E-10
LP10	1.03E-12	1.87E-16	8.04E-11
LP11	1.61E-12	-4.07E-15	(negative)
LP12	2.73E-13	1.08E-15	4.63E-10
LP13	1.22E-13	1.24E-15	5.33E-10
LP14	1.84E-13	3.77E-16	1.62E-10
LP15	9.71E-13	7.25E-16	3.12E-10

Figure 5 -

Models of gradients of the peptide attractant GFDLTGGGVQ (mass/charge 950.6) (**A**) Results

of the 2-D advection-diffusion numerical solution at 60 seconds for a single egg with the

maximum (red), minimum (blue), and mean (purple) attractant flux. (**B**) Model results at 60

seconds for a cluster of 100 eggs (blue) and a single egg (red), using the mean flux of 7.74×10^{-10}

mol $\times$ m^{-2}s^{-1}. (**C**) Model results at 60 seconds under no-flow and unidirectional flow (0.001 m $\times$

s^{-1}) conditions for 100 eggs (blue) and a single egg (red). (**D)** Results from a cut line of an

advection-diffusion numerical solution at 60 second time steps over 60 minutes. The attractant

source is the surface of a spherical egg with the mean flux.   (**E**) Gradient in microfluidic device

that recreates conditions in the advection-diffusion numerical solution, where the attractant source is the plane of attractant in the channel. The gradient is created using a starting concentration of 100 nM speract. "*" demarcates a concentration gradient of 2.3×10^{-4} mol $\times$ m^{-4} at 60 seconds, which matches the concentration gradient at the same point in (E).
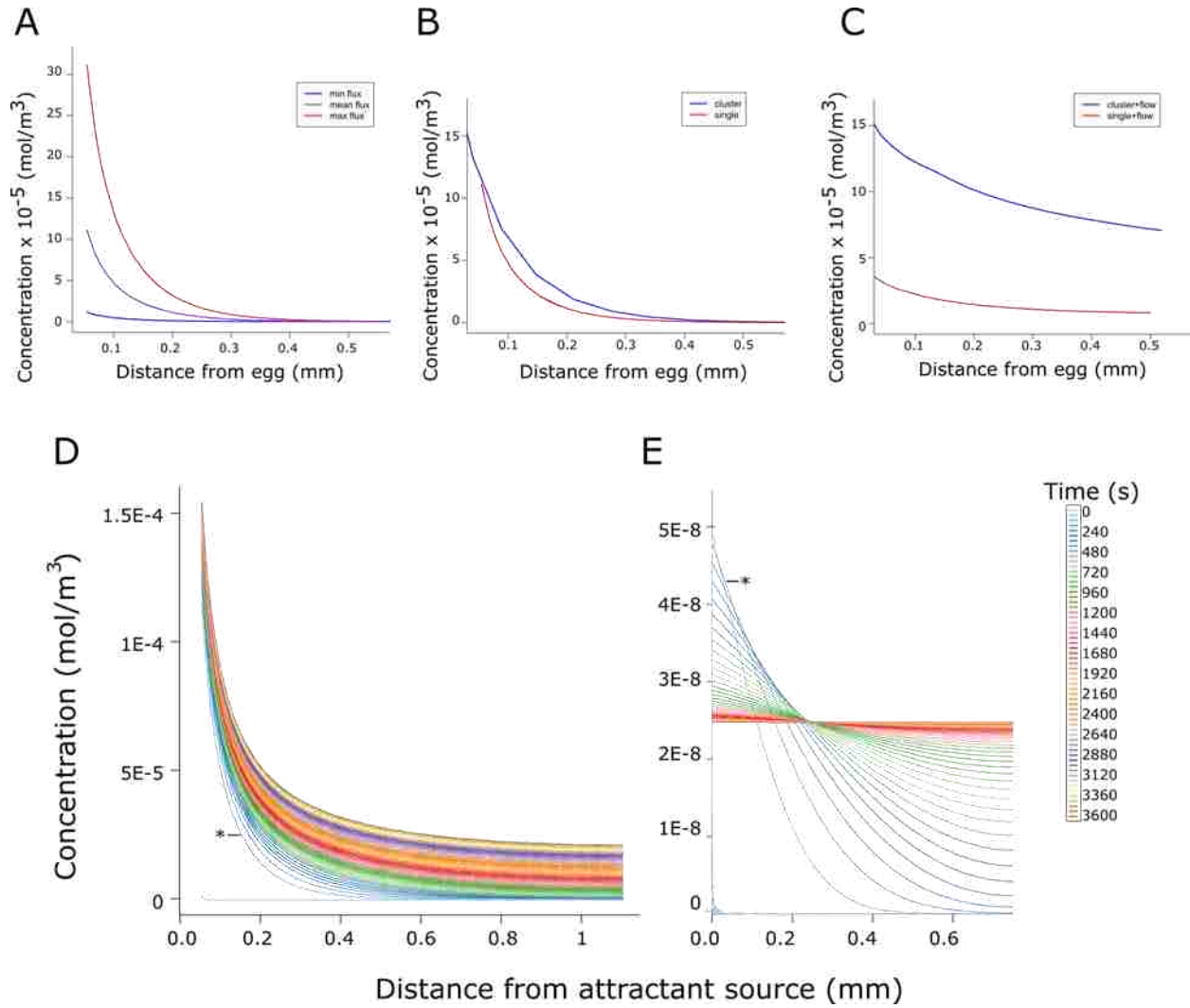
Figure 6 -

Orientation and path length of sperm to gradients replicating the predicted egg-produced gradient. Two attractant peptides (GFDLTGGGVQ and Speract) with starting concentrations of attractant at 100 nM, 10x higher, 10x lower, and an artificial seawater control were tested (723 sperm, 85-115 per treatment, pooled from 5 males). An ANOVA indicates a significant effect of treatment condition on sperm orientation (p < 0.001). Mean orientations determined to be statistically the same by a Tukey post-hoc test are denoted with the same lowercase letter. **(A)** Control **(B)** GFDLTGGGVQ 10 nM **(C)** GFDLTGGGVQ 100 nM **(D)** GFDLTGGGVQ 1000 nM **(E)** Speract 10 nM **(F)** Speract 100 nM **(G)** Speract 1000 nM

72
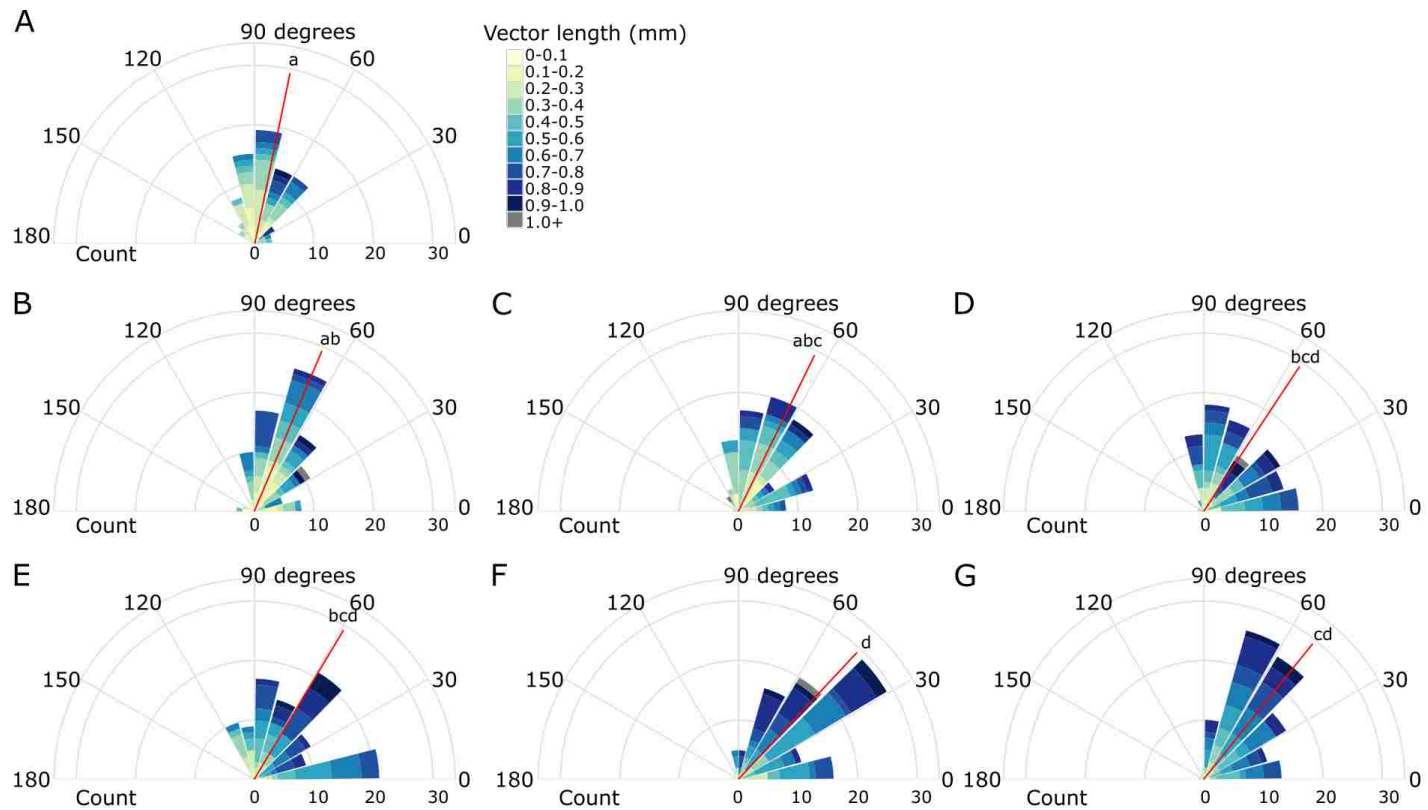
Figure 7 -

Summary of orientation (A) and path length (B) of sperm to gradients replicating the predicted

egg-produced gradient (723 sperm, 85-115 per treatment, pooled from 5 males). Two attractants

with starting concentrations of attractant at 100 nM, 10x higher, 10x lower, and an artificial

seawater control were tested. An ANOVA indicates a significant effect of treatment condition on

sperm orientation

($p < 0.001$) and

vector length ($p <$

0.001). Mean

orientations

determined to be

statistically the

same by a Tukey

post-hoc test are

denoted with the

same lowercase

letter
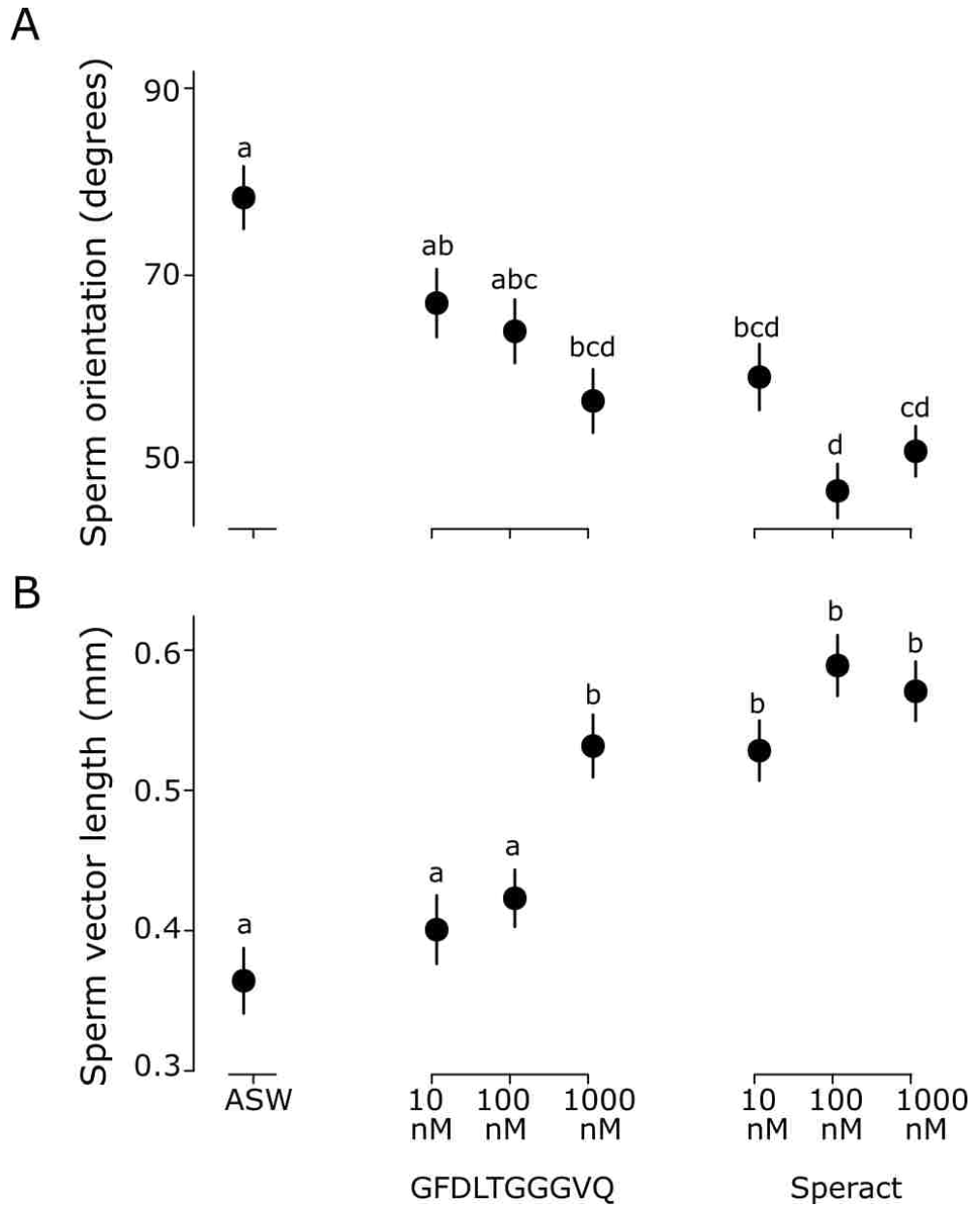
Table 3 -

Results of ANOVA of sperm orientation with respect to treatment (723 sperm total, 85-115 per

treatment, pooled from 5 males), followed by a Tukey post-hoc test. * indicates significance with

$\alpha = 0.05$

ANOVA	Degrees of freedom	Sum of Squares	F value	p
treatment	6	62695	9.344	6.95e-10*
residuals	716	800673		
Tukey Test	Difference (degrees)	Confidence Interval Lower Bound (95%)	Confidence Interval Upper Bound (95%)	p (adjusted)
Long 10 nM - ASW	-11.28	-25.90	3.34	0.2542
Long 100 nM - ASW	-14.29	-28.72	0.13	0.0539
Long 1000 nM - ASW	-21.75	-36.09	-7.42	0.0002*
Speract 10 nM - ASW	-19.20	-33.34	-5.05	0.0013*
Speract 100 nM - ASW	-31.38	-45.77	-16.98	0.0000*
Speract 1000 nM - ASW	-27.13	-41.56	-12.70	0.0000*
Long 100 nM - Long 10 nM	-3.01	-16.87	10.84	0.9953
Long 1000 nM - Long 10 nM	-10.47	-24.23	3.29	0.2704
Speract 10 nM - Long 10 nM	-7.91	-21.47	5.64	0.5987
Speract 100 nM - Long 10 nM	-20.09	-33.91	-6.27	0.0039*
Speract 1000 nM - Long 10 nM	-15.85	-29.70	-2.00	0.0133*
Long 1000 nM - Long 100 nM	-7.45	-21.01	6.10	0.6652
Speract 10 nM - Long 100 nM	-4.90	-18.25	8.45	0.9324
Speract 100 nM - Long 100 nM	-17.08	-30.69	-3.47	0.0042*
Speract 1000 nM - Long 100 nM	-12.83	-26.48	0.81	0.0811
Speract 10 nM - Long 1000 nM	2.56	-10.69	15.80	0.9976
Speract 100 nM - Long 1000 nM	-9.63	-23.14	3.89	0.3510
Speract 1000 nM - Long 1000 nM	-5.38	-18.93	8.17	0.9040
Speract 100 nM - Speract 10 nM	-12.18	-25.49	1.13	0.0984
Speract 1000 nM - Speract 10 nM	-7.93	-21.28	5.41	0.5774
Speract 1000 nM - Speract 100 nM	4.25	-9.37	17.86	0.9689

Supplementary Material

Video 1 – One egg without flow

https://drive.google.com/open?id=0B4-mb1mjQlPDMndQUGlvOFZrUVU

Video 2 - One egg with flow

https://drive.google.com/open?id=0B4-mb1mjQlPDN0tfZENWY1BiT3c

Video 3 - Cluster of eggs with flow

https://drive.google.com/open?id=0B4-mb1mjQlPDT2p4b0k2WGlMVjg

REFERENCES

Aguirre, J.D., Blows, M.W., Marshall, D.J., 2016. Genetic Compatibility Underlies Benefits of Mate Choice in an External Fertilizer. Am. Nat. 187, 000–000. doi:10.1086/685892

Ahmed, T., Shimizu, T.S., Stocker, R., 2010a. Microfluidics for bacterial chemotaxis. Integr. Biol. 2, 604–629. doi:10.1039/c0ib00049c

Ahmed, T., Shimizu, T.S., Stocker, R., 2010b. Bacterial Chemotaxis in Linear and Nonlinear Steady Microfluidic Gradients. Nano Lett. 10, 3379–3385. doi:10.1021/nl101204e

Ahmed, T., Stocker, R., 2008. Experimental verification of the behavioral foundation of bacterial transport parameters using microfluidics. Biophys. J. 95, 4481–4493.

Alvarez, L., Dai, L., Friedrich, B.M., Kashikar, N.D., Gregor, I., Pascal, R., Kaupp, U.B., 2012. The rate of change in Ca 2+ concentration controls sperm chemotaxis. J. Cell Biol. 196, 653–663. doi:10.1083/jcb.201106096

Asmar, N.H., 2004. Partial Differential Equations, 2nd ed. Pearson.

Bates, D., Maechler, M., Bolker, B., Walker, S., 2014. lme4: Linear mixed-effects models using Eigen and S4.

Bell, A.F., Crimaldi, J.P., 2015. Effect of steady and unsteady flow on chemoattractant plume formation and sperm taxis. J. Mar. Syst. 148, 236–248. doi:10.1016/j.jmarsys.2015.03.008

Beltrán, C., Galindo, B.E., Rodríguez-Miranda, E., Sánchez, D., 2007. Signal transduction mechanisms regulating ion fluxes in the sea urchin sperm. Signal Transduct. 7, 103–117. doi:10.1002/sita.200600129

Bentley, J.K., Shimomura, H., Garbers, D.L., 1986. Retention of a Functional Resact Receptor in Isolated Sperm Plasma Membranes. Cell 45, 281–288.

Birkhead, T., Moller, A. (Eds.), 1998. External Fertilizers, in: Sperm Competition and Sexual Selection. Academic Press, San Diego, California, pp. 177–191.

Böhmer, M., Van, Q., Weyand, I., Hagen, V., Beyermann, M., Matsumoto, M., Hoshi, M., Hildebrand, E., Kaupp, U.B., 2005. Ca2+ spikes in the flagellum control chemotactic behavior of sperm. EMBO J. 24, 2741–52. doi:10.1038/sj.emboj.7600744

Brokaw, C.J., 1957. Chemotaxis of bracken spermatozoids. J. Exp. Biol. 35, 192–196.

Brown, D.A., Berg, H.C., 1974. Temporal stimulation of chemotaxis in Escherichia coli. Proc. Natl. Acad. Sci. 71, 1388–92.

Burnett, L.A., Anderson, D.M., Rawls, A., Bieber, A.L., Chandler, D.E., 2011. Mouse sperm exhibit chemotaxis to allurin, a truncated member of the cysteine-rich secretory protein family. Dev. Biol. 360, 318–328. doi:10.1016/j.ydbio.2011.09.028

Chang, H., Kim, B.J., Kim, Y.S., Suarez, S.S., Wu, M., 2013. Different migration patterns of sea urchin and mouse sperm revealed by a microfluidic chemotaxis device. PLoS One 8, e60587. doi:10.1371/journal.pone.0060587

Clark, N.L., Aagaard, J.E., Swanson, W.J., 2006. Evolution of reproductive proteins from animals and plants. Reproduction 131, 11–22. doi:10.1530/rep.1.00357

Clark, N.L., Gasper, J., Sekino, M., Springer, S.A., Aquadro, C.F., Swanson, W.J., 2009. Coevolution of interacting fertilization proteins. PLoS Genet. 5, e1000570. doi:10.1371/journal.pgen.1000570

Clifton, A., 2015. WindRose [WWW Document]. Stack Overflow. URL http://stackoverflow.com/questions/17266780/wind-rose-with-ggplot-r

Cook, S.P., Brokaw, C.J., Muller, C.H., Babcock, D.F., 1994. Sperm Chemotaxis: Egg Peptides Control Cytosolic Calcium to Regulate Flagellar Responses. Dev. Biol. 165, 10–19.

Crean, A.J., Marshall, D.J., 2015. Eggs with larger accessory structures are more likely to be fertilized in both low and high sperm concentrations in Styela plicata (Ascidiaceae). Mar. Biol. 162, 2251–2256. doi:10.1007/s00227-015-2755-0

Crean, A.J., Marshall, D.J., 2008. Gamete plasticity in a broadcast spawning marine invertebrate. Proc. Natl. Acad. Sci. U. S. A. 105, 13508–13513. doi:10.1073/pnas.0806590105

Crimaldi, J.P., Zimmer, R.K., 2014. The physics of broadcast spawning in benthic invertebrates. Ann. Rev. Mar. Sci. 6, 141–65. doi:10.1146/annurev-marine-010213-135119

Darszon, A., Guerrero, A., Galindo, B.E., Nishigaki, T., Wood, C.D., 2008. Sperm-activating peptides in the regulation of ion fluxes, signal transduction and motility. Int. J. Dev. Biol. 52, 595–606. doi:10.1387/ijdb.072550ad

De Lisa, E., Salzano, A.M., Moccia, F., Scaloni, A., Di Cosmo, A., 2013. Sperm-attractant peptide influences the spermatozoa swimming behavior in internal fertilization in Octopus vulgaris. J. Exp. Biol. 216, 2229–37. doi:10.1242/jeb.081885

Eisenbach, M., 1999. Sperm chemotaxis. Rev. Reprod. 4, 56–66.

Engqvist, L., 2013. A general description of additive and nonadditive elements of sperm competitiveness and their relation to male fertilization success. Evolution 67, 1396–1405. doi:10.1111/evo.12024

Evans, J.P., Garcia-Gonzalez, F., Almbro, M., Robinson, O., Fitzpatrick, J.L., 2012. Assessing the potential for egg chemoattractants to mediate sexual selection in a broadcast spawning marine invertebrate. Proc. R. Soc. 279, 2855–2861. doi:10.1098/rspb.2012.0181

Evans, J.P., Sherman, C.D.H., 2013. Sexual selection and the evolution of egg-sperm interactions in broadcast-spawning invertebrates. Biol. Bull. 224, 166–183.

Farley, G.S., Levitan, D.R., 2001. The role of jelly coats in sperm-egg encounters, fertilization success, and selection on egg size in broadcast spawners. Am. Nat. 157, 626–636. doi:10.1086/320619

Fitzpatrick, J.L., Lüpold, S., 2014. Sexual selection and the evolution of sperm quality. Mol. Hum. Reprod. 20, 1180–1189. doi:10.1093/molehr/gau067

Fitzpatrick, J.L., Simmons, L.W., Evans, J.P., 2012. Complex patterns of multivariate selection on the ejaculate of a broadcast spawning marine invertebrate. Evolution (N. Y). 66, 2451–2460. doi:10.5061/dryad.307c3n10

Foltz, K.R., Lennarz, W.J., 1990. Purification and characterization of an extracellular fragment of the sea urchin egg receptor for sperm. J. Cell Biol. 111, 2951–2959. doi:10.1083/jcb.111.6.2951

Franke, E.S., Babcock, R.C., Styan, C.A., 2002. Sexual conflict and polyspermy under sperm-limited conditions: in situ evidence from field simulations with the free-spawning marine echinoid Evechinus chloroticus. Am. Nat. 160, 485–96. doi:10.1086/342075

Friedrich, B.M., Julicher, F., 2007. Chemotaxis of sperm cells. Proc. Natl. Acad. Sci. 104, 13256–13261. doi:10.1073/pnas.0703530104

Gage, M.J.G., Macfarlane, C.P., Yeates, S., Ward, R.G., Searle, J.B., Parker, G. a., 2004. Spermatozoal traits and sperm competition in Atlantic salmon. Curr. Biol. 14, 44–47. doi:10.1016/j.cub.2003.12.028

Garbers, D.L., Hardman, J.G., 1976. Effects of egg factors on cyclic nucleotide metabolism in sea urchins. J. Cyclic Nucleotide Res. 2, 59–70.

Garbers, D.L., Watkins, H.D., Hansbrough, J.R., Smith, A., Misono, K.S., 1982. The amino acid sequence and chemical synthesis of speract and of speract analogues. J. Biol. Chem. 257, 2734–2737.

Gray, J., 1928. The Effect of Egg-Secretions on the Activity of Spermatozoa. BJEB 362–365.

Guerrero, A., Espinal, J.J., Wood, C.D., Rendon, J.M., Carneiro, J., Martínez-Mekler, G., Darszon, A., Rendón, J.M., Carneiro, J., Martínez-Mekler, G., Darszon, A., 2013. Niflumic acid disrupts marine spermatozoan chemotaxis without impairing the spatiotemporal detection of chemoattractant gradients. J. Cell Sci. 126, 1477–1487. doi:10.1242/jcs.121442

Guerrero, A., Nishigaki, T., Carneiro, J., Tatsu, Y., Wood, C.D., Darszon, A., 2010. Tuning sperm chemotaxis by calcium burst timing. Dev. Biol. 344, 52–65.

Hansbrough, J.R., Garbers, D.L., 1981. Speract: purification and characterization of a peptide associated with eggs that activates spermatozoa. J. Biol. Chem. 256, 1447–1452.

Harvey, E.B., 1956. The American Arbacia and Other Sea Urchins. Princeton University Press, Princeton, NJ.

Heck, D.E., Laskin, J.D., 2003. Ryanodine-Sensitive Calcium Flux Regulates Motility of Arbacia punctulata Sperm. Biol. Bull. 205, 185–186.

Hellberg, M.E., Dennis, A.B., Arbour-Reily, P., Aagaard, J.E., Swanson, W.J., 2012. the Tegula Tango: a Coevolutionary Dance of Interacting, Positively Selected Sperm and Egg Proteins. Evolution (N. Y). 66, 1681–94. doi:10.1111/j.1558-5646.2011.01530.x

Holt, W. V., Fazeli, a., 2015. Do sperm possess a molecular passport? Mechanistic insights into sperm selection in the female reproductive tract. Mol. Hum. Reprod. 21, 491–501. doi:10.1093/molehr/gav012

Hussain, Y.H., Guasto, J.S., Zimmer, R.K., Stocker, R., Riffell, J.A., 2016. Sperm chemotaxis promotes individual fertilization success in sea urchins. J. Exp. Biol. 1458–1466. doi:10.1242/jeb.134924

Jammalamadaka, S.R., Gupta, A. Sen, 2001. Topics in Circular Statistics. World Scientific Publishing Co, River Edge, NJ.

Johnson, D.W., Monro, K., Marshall, D.J., 2013. The maintenance of sperm variability: context-dependent selection on sperm morphology in a broadcast spawning invertebrate. Evolution (N. Y). 67, 1383–1395. doi:10.1111/evo.12022

Kashikar, N.D., Alvarez, L., Seifert, R., Gregor, I., Jäckle, O., Beyermann, M., Krause, E., Benjamin Kaupp, U., Kaupp, U.B., 2012. Temporal sampling, resetting, and adaptation orchestrate gradient sensing in sperm. J. Cell Biol. 198, 1075–91. doi:10.1083/jcb.201204024

Kaupp, U.B., Hildebrand, E., Weyand, I., 2006. Sperm chemotaxis in marine invertebrates — molecules and mechanisms. J. Cell. Physiol. 208, 487–494. doi:10.1002/jcp

Kaupp, U.B., Kashikar, N.D., Weyand, I., 2008. Mechanisms of Sperm Chemotaxis. Annu. Rev. Physiol. 70, 93–117.

Kaupp, U.B., Solzin, J., Hildebrand, E., Brown, J.E., Helbig, A., Hagen, V., Beyermann, M., Pampaloni, F., Weyand, I., 2003. The signal flow and motor response controling chemotaxis of sea urchin sperm. Nat. Cell Biol. 5, 109–117.

Kinoh, H., Shimizu, T., Fujimoto, H., Suzuki, N., 1994. Expression of a putative precursor mRNA for sperm-activating peptide I in accessory cells of the ovary in the sea urchin Hemicentrotus pulcherrimus. Roux's Arch. Dev. Biol. 381–388.

Kirkman-Brown, J.C., Sutton, K.A., Florman, H.M., 2003. How to attract a sperm. Nat. Cell Biol. 5, 93–6. doi:10.1038/ncb0203-93

Kopf, G.S., Tubb, D.J., Garbers, D.L., 1979. Activation of sperm respiration by a low molecular weight egg factor and 8-bromoguanosine 3'5'-monophosphate. J. Biol. Chem. 254, 8554–8560.

Kosman, E.T., Levitan, D.R., 2014. Sperm competition and the evolution of gametic compatibility in externally fertilizing taxa. Mol. Hum. Reprod. 20, 1190–1197. doi:10.1093/molehr/gau069

Kregting, L.T., Thomas, F.I.M., Bass, A.L., Yund, P.O., 2014. Relative Effects of Gamete Compatibility and Hydrodynamics on Fertilization in the Green Sea Urchin Strongylocentrotus droebachiensis. Biol. Bull. 227, 33–39.

Krug, P.J., Riffell, J.A., Zimmer, R.K., 2009. Endogenous signaling pathways and chemical communication between sperm and egg. J. Exp. Biol. 212, 1092–1100. doi:10.1242/jeb.027029

Lazova, M.D., Ahmed, T., Bellomo, D., Stocker, R., Shimizu, T.S., 2011. Response rescaling in bacterial chemotaxis. Proc. Natl. Acad. Sci. 108, 13870–13875. doi:10.1073/pnas.1108608108

Lessios, H.A., Lockhart, S., Collin, R., Sotil, G., Sanchez-Jerez, P., Zigler, K.S., Perez, A.F., Garrido, M.J., Geyer, L.B., Bernardi, G., Vacquier, V.D., Haroun, R., Kessing, B.D., 2012. Phylogeography and bindin evolution in Arbacia, a sea urchin genus with an unusual distribution. Mol. Ecol. 21, 130–144. doi:10.1111/j.1365-294X.2011.05303.x

Levitan, D.R., 2012. Contemporary evolution of sea urchin gamete-recognition proteins: experimental evidence of density-dependent gamete performance predicts shifts in allele frequencies over time. Evolution (N. Y). 66, 1722–1736. doi:10.5061/dryad.0k2469h8

Levitan, D.R., 2006. The relationship between egg size and fertilization success in broadcast-spawning marine invertebrates. Integr. Comp. Biol. 46, 298–311. doi:10.1093/icb/icj025

Levitan, D.R., 2004. Density-dependent sexual selection in external fertilizers: variances in male and female fertilization success along the continuum from sperm limitation to sexual conflict in the sea urchin Strongylocentrotus franciscanus. Am. Nat. 164, 298–309. doi:10.1086/423150

Levitan, D.R., 2002. Density-Dependent Selection on Gamete Traits in Three Congeneric Sea Urchins. Ecology 83, 464–479.

Levitan, D.R., 2000. Sperm velocity and longevity trade off each other and influence fertilization in the sea urchin Lytechinus variegatus. Proc. R. Soc. 267, 531–534. doi:10.1098/rspb.2000.1032

Levitan, D.R., 1996. Effects of gamete traits on fertilization in the sea and the evolution of sexual dimorphism. Nature 382, 153–155.

Levitan, D.R., Terhorst, C.P., Fogarty, N.D., 2007. The risk of polyspermy in three congeneric sea urchins and its implications for gametic incompatibility and reproductive isolation. Evolution (N. Y). 61, 2007–14. doi:10.1111/j.1558-5646.2007.00150.x

Lillie, F.R., 1915. Studies of fertilization: VII. analysis of variations in the fertilizing power of sperm suspensions of Arbacia. Biol. Bull. 28, 229–251.

Lillie, F.R., 1912. The production of sperm iso-agglutinins by ova. Science (80-.). 36, 527–530. doi:10.1126/science.36.929.527

Lishko, P. V., Botchkina, I.L., Kirichok, Y., 2011. Progesterone activates the principal Ca2+ channel of human sperm. Nature 471, 387–391.

Lund, U., Agostinelli, C., 2002. CircStats: Circular Statistics, from "Topics in Circular Statistics" (2001).

Lüpold, S., Pitnick, S., Berben, K.S., Blengini, C.S., Belote, J.M., Manier, M.K., 2013. Female mediation of competitive fertilization success in Drosophila melanogaster. Proc. Natl. Acad. Sci. 110. doi:10.1073/pnas.1300954110

Manier, M.K., Belote, J.M., Berben, K.S., Novikov, D., Stuart, W.T., Pitnick, S., 2010. Resolving mechanisms of competitive fertilization success in Drosophila melanogaster. Science (80-.). 328, 354–357. doi:10.1126/science.1187096

Metz, E.C., Gómez-Gutiérrez, G., Vacquier, V.D., 1998. Mitochondrial DNA and bindin gene sequence evolution among allopatric species of the sea urchin genus Arbacia. Mol. Biol. Evol. 15, 185–195.

Miller, R.L., 1997. Specificity of sperm chemotaxis among Great Barrier Reef shallow-water Holothurians and Ophiuroids. J. Exp. Zool. 279, 189–200. doi:10.1002/(SICI)1097-010X(19971001)279:2<189::AID-JEZ10>3.0.CO;2-B

Miller, R.L., 1985. Sperm chemo-orientation in the Metazoa, in: Metz, C. (Ed.), Biology of Fertilization, v.2: Biology of the Sperm. Elsevier Science, pp. 275–331.

Morita, M., Nishikawa, A., Nakajima, A., Iguchi, A., Sakai, K., Takemura, A., Okuno, M., 2006. Eggs regulate sperm flagellar motility initiation, chemotaxis and inhibition in the coral Acropora digitifera, A. gemmifera and A. tenuis. J. Exp. Biol. 209, 4574–9. doi:10.1242/jeb.02500

Narayanan, A.S., Anwar, R.A., 1969. The specificity of purified porcine pancreatic elastase. Biochem. J. 114, 11–17.

Nozawa, Y., Isomura, N., Fukami, H., 2015. Influence of sperm dilution and gamete contact time on the fertilization rate of scleractinian corals. Coral Reefs. doi:10.1007/s00338-015-1338-3

Oliver, M., Evans, J.P., 2014. Chemically moderated gamete preferences predict offspring fitness in a broadcast spawning invertebrate. Proc. R. Soc. 281, 20140148.

Palumbi, S.R., 1999. All males are not created equal: fertility differences depend on gamete recognition polymorphisms in sea urchins. Proc. Natl. Acad. Sci. 96, 12632–12637.

Pennington, J.T., 1985. The ecology of fertilization of echinoid eggs: the consequences of sperm dilution, adult aggregation, and synchronous spawning. Biol. Bull. 169, 417–430.

Pfeffer, W., 1903. The Physiology of Plants, 2, Volume ed. Clarendon Press.

Pichlo, M., Bungert-Plümke, S., Weyand, I., Seifert, R., Bönigk, W., Strünker, T., Kashikar, N.D., Goodwin, N., Müller, A., Pelzer, P., Van, Q., Enderlein, J., Klemm, C., Krause, E., Trötschel, C., Poetsch, A., Kremmer, E., Kaupp, U.B., 2014. High density and ligand affinity confer ultrasensitive signal detection by a guanylyl cyclase chemoreceptor. J. Cell Biol. 206, 541–57. doi:10.1083/jcb.201402027

Podolsky, R.D., 2001. Evolution of egg target size: an analysis of selection on correlated characters. Evolution (N. Y). 55, 2470–2478.

Qasaimeh, M.A., Gervais, T., Juncker, D., 2011. Microfluidic quadrupole and floating concentration gradient. Nat. Commun. 2.

R Core Team, 2013. R: A language and environment for statistical computing.

Ralt, D., Goldenberg, M., Fetterolf, P., Thompson, D., Dor, J., Mashiach, S., Garbers, D.L., Eisenbach, M., 1991. Sperm attraction to a follicular factor(s) correlates with human egg fertilizability. Proc. Natl. Acad. Sci. 88, 2840–2844.

Ramarao, C.S., Burks, D.J., Garbers, D.L., 1990. A single mRNA encodes multiple copies of the egg peptide speract. Biochemistry 29, 3383–3388.

Riffell, J.A., Krug, P.J., Zimmer, R.K., 2004. The ecological and evolutionary consequences of sperm chemoattraction. Proc. Natl. Acad. Sci. 101, 4501–4506.

Riffell, J.A., Krug, P.J., Zimmer, R.K., 2002. Fertilization in the sea: the chemical identity of an abalone sperm

attractant. J. Exp. Biol. 205, 1439–1450.

Rosen, W.G., 1962. Cellular Chemotropism and Chemotaxis. Q. Rev. Biol. 37, 242–259.

Rosman, J.H., Koseff, J.R., Monismith, S.G., Grover, J., 2007. A field investigation into the effects of a kelp forest (Macrocystis pyrifera) on coastal hydrodynamics and transport. J. Geophys. Res. 112, 1–16. doi:10.1029/2005JC003430

Rothschild, Lord, 1956. Fertilization. John Wiley & Sons, Inc, New York.

Sawada, H., Inoue, N., Iwano, M. (Eds.), 2014. Sexual Reproduction in Animals and Plants, Sexual Reproduction in Animals and Plants. Springer Japan, Tokyo. doi:10.1007/978-4-431-54589-7

Schmell, E.L.I., Earles, B.J., Breaux, C., Lennarz, W.J., William, J., Lennarz, W.J., 1977. Identification of a sperm receptor on the surface of the eggs of the sea urchin Arbacia punctulata. J. Cell Biol. 72, 35–46. doi:10.1083/jcb.72.1.35

Seltman, H.J., 2015. Experimental Design and Analysis. Carnegie Mellon University, Pittsburgh, PA.

Shiba, K., Baba, S.A., Inoue, T., Yoshida, M., 2008. Ca 2+ bursts occur around a local minimal concentration of attractant and trigger sperm chemotactic response. Proc. Natl. Acad. Sci. 105, 19312–19317.

Shimomura, H., Dangott, L.J., Garbers, D.L., 1986a. Covalent Coupling of a Resact Analogue to Guanylate Cyclase *. J. Biol. Chem. 261, 15778–15782.

Shimomura, H., Suzuki, N., Garbers, D.L., 1986b. Derivatives of speract are associated with the eggs of Lytechinus pictus sea urchins. Peptides 7, 491–495.

Simmons, L.W., Fitzpatrick, J.L., 2012. Sperm wars and the evolution of male fertility. Reproduction 144, 519–534. doi:10.1530/REP-12-0285

Simpson, J.L., Humphries, S., Evans, J.P., Simmons, L.W., Fitzpatrick, J.L., 2014. Relationships between sperm length and speed differ among three internally and three externally fertilizing species. Evolution (N. Y). 68, 92–104. doi:10.1111/evo.12199.This

Snook, R.R., 2005. Sperm in competition: not playing by the numbers. Trends Ecol. Evol. 20, 46–53. doi:10.1016/j.tree.2004.10.011

Spehr, M., Gisselmann, G., Poplawski, A., Riffell, J.A., Wetzel, C.H., Zimmer, R.K., Hatt, H., 2003. Identification of a testicular odorant receptor mediating human sperm chemotaxis. Science (80-.). 299, 2054–2058. doi:10.1126/science.1080376

Starkweather, J., 2010. Linear Mixed Effects Modeling using R. Univ. North Texas.

Strathmann, M.F., 1987. Reproduction and Development of Marine Invertebrates of the Northern Pacific Coast. University of Washington Press, Seattle, WA.

Strünker, T., Alvarez, L., Kaupp, U.B., 2015. At the physical limit — chemosensation in sperm. Curr. Opin. Neurobiol. 110–116. doi:10.1016/j.conb.2015.02.007

Suarez, S.S., Pacey, A.A., 2006. Sperm transport in the female reproductive tract. Hum. Reprod. Updat. 12, 23–37.

Suzuki, N., 1995. Structure, Function, and Biosynthesis of Sperm-Activating Peptides and Fucose Sulfate Glycoconjugate in the Extracellular Coat of Sea Urchin Eggs. Zoolog. Sci. 12, 13–27.

Suzuki, N., Garbers, D.L., 1984. Stimulation of sperm respiration rates by speract and resact at alkaline extracellular pH. Biol. Reprod. 30, 1167–74.

Suzuki, N., Shimomura, H., Radany, E.W., Ramarao, C.S., Ward, G.E., Bentley, J.K., Garbers, D.L., 1984. A peptide associated with eggs causes a mobility shift in a major plasma membrane protein of spermatozoa. J. Biol. Chem. 259, 14874–14879.

Swanson, W.J., Nielsen, R., Yang, Q., 2003. Pervasive adaptive evolution in mammalian fertilization proteins. Mol. Biol. Evol. 20, 18–20.

Swanson, W.J., Vacquier, V.D., 2002. The rapid evolution of reproductive proteins. Nat. Rev. Genet. 3, 137–144. doi:10.1038/nrg/733

Swanson, W.J., Yang, Z., Wolfner, M.F., Aquadro, C.F., 2001. Positive Darwinian selection drives the evolution of several female reproductive proteins in mammals. Proc. Natl. Acad. Sci. 98, 2509–2514.

Thomas, F.I.M., 1994. Physical Properties of Gametes in Three Sea Urchin Species. J. Exp. Mar. Bio. Ecol. 194, 263–84.

Thomas, F.I.M., Kregting, L.T., Badgley, B.D., Donahue, M.J., Yund, P.O., 2013. Fertilization in a sea urchin is not only a water column process: effects of water flow on fertilization near a spawing female. Mar. Ecol. Prog. Ser. 494, 231–240. doi:10.3354/meps10601

Tvedt, H.B., Benfey, T.J., Martin-Robichaud, D.J., Power, J., 2001. The relationship between sperm density, spermatocrit, sperm motility and fertilization success in Atlantic halibut, Hippoglossus hippoglossus. Aquaculture 194, 191–200. doi:10.1016/S0044-8486(00)00516-0

Vacquier, V.D., 1998. Evolution of Gamete Recognition Proteins. Science (80-.). 281, 1995–1998.

doi:10.1126/science.281.5385.1995

Vacquier, V.D., Moy, G.W., 1977. Isolation of bindin: the protein responsible for adhesion of sperm to sea urchin eggs. Proc. Natl. Acad. Sci. 74, 2456–2460.

van der Horst, G., Maree, L., 2013. Sperm form and function in the absence of sperm competition. Mol. Reprod. Dev. 81, 204–216. doi:10.1002/mrd.22277

Veitinger, T., Riffell, J.A., Veitinger, S., Nascimento, J.M., Triller, A., Chandsawangbhuwana, C., Schwane, K., Geerts, A., Wunder, F., Berns, M.W., Neuhaus, E.M., Zimmer, R.K., Spehr, M., Hatt, H., 2011. Chemosensory Ca2+ Dynamics Correlate with Diverse Behavioral Phenotypes in Human Sperm. J. Biol. Chem. 286, 17311–17325.

Vinauger, C., Lutz, E.K., Riffell, J. a, 2014. Olfactory learning and memory in the disease vector mosquito, Aedes aegypti. J. Exp. Biol. 217, 2321–2330. doi:10.1242/jeb.101279

Ward, G.E., Brokaw, C.J., Garbers, D.L., Vacquier, V.D., 1985. Chemotaxis of Arbacia punctulata spermatozoa to resact, a peptide from the egg jelly layer. J. Cell Biol. 101, 2324–2329.

Watkins, H.D., Kopf, G.S., Garbers, D.L., 1978. Activation of sperm adenylate cyclase by factors associated with eggs. Biol. Reprod. 19, 890–894.

Wilburn, D.B., Swanson, W.J., 2016. From molecules to mating: Rapid evolution and biochemical studies of reproductive proteins. J. Proteomics 135, 12–25. doi:10.1016/j.jprot.2015.06.007

Wood, C.D., Darszon, A., Whitaker, M., 2003. Speract induces calcium oscillations in the sperm tail. J. Cell Biol. 161, 89–101.

Xiang, X., Kittelson, A., Olson, J., Bieber, A., Chandler, D., 2005. Allurin, a 21 kD sperm chemoattractant, is rapidly released from the outermost jelly layer of the Xenopus egg by diffusion and medium convection. Mol. Reprod. Dev. 70, 344–60. doi:10.1002/mrd.20201

Yanagimachi, R., Cherr, G., Matsubara, T., Andoh, T., Harumi, T., Vines, C., Pillai, M., Griffin, F., Matsubara, H., Weatherby, T., Kaneshiro, K., 2013. Sperm attractant in the micropyle region of fish and insect eggs. Biol. Reprod. 88, 47. doi:10.1095/biolreprod.112.105072

Yeates, S.E., Diamond, S.E., Einum, S., Emerson, B.C., Holt, W. V., Gage, M.J.G., 2013. Cryptic choice of conspecific sperm controlled by the impact of ovarian fluid on sperm swimming behavior. Evolution (N. Y). 67, 3523–3536. doi:10.1111/evo.12208

Yoshida, M., Hiradate, Y., Sensui, N., Cosson, J., Morisawa, M., 2013. Species-specificity of sperm motility activation and chemotaxis: a study on ascidian species. Biol. Bull. 224, 156–165.

Yoshida, M., Kawano, N., Yoshida, K., 2008. Control of sperm motility and fertility: diverse factors and common mechanisms. Cell. Mol. Life Sci. 65, 3446–3457. doi:10.1007/s00018-008-8230-z

Yoshida, M., Yoshida, K., 2011. Sperm chemotaxis and regulation of flagellar movement by Ca2+. Mol. Hum. Reprod. 17, 457–465.

Yoshino, K., Takao, T., Shimonishi, Y., Suzuki, N., 1991. Determination of the amino acid sequence of an intramolecular disulfide linkage-containing sperm-activating peptide by tandem mass spectrometry. FEBS Lett. 294, 179–82.

Zigler, K.S., McCartney, M.A., Levitan, D.R., Lessios, H.A., 2005. Sea urchin bindin divergence predicts gamete compatibility. Evolution (N. Y). 59, 2399–2404.

Zimmer, R.K., Riffell, J.A., 2011. Sperm Chemotaxis, Fluid Shear, and the Evolution of Sexual Reproduction. Proc. Natl. Acad. Sci. 108, 13200–13205.

Zuur, A.F., Ieno, E.N., Walker, N.J., Saveliev, A.A., Smith, G.M., 2009. Mixed Effects Models and Extensions in Ecology with R, Statistics for Biology and Health. Springer New York, New York, NY. doi:10.1007/978-0-387-87458-6

Chapter III: Sea urchin sperm respond to extremely low concentrations of chemoattractant but are non-uniform in behavior and physiology

ABSTRACT

The molecular mechanisms controlling sea urchin sperm chemotaxis are well-known and indicate that sperm can respond to a wide range of chemoattractant concentrations. However, it is not known what minimum concentration sperm respond to in a gradient. Here, we capture the point at which sperm of the sea urchin *Arbacia punctulata* respond to a gradient of the peptide attractant resact by creating finely tuned chemoattractant gradients in a microfluidic device and using calcium imaging and high-speed video microscopy to capture physiological and behavioral parameters, respectively. We find that sperm 'run' responses, characterized by progressive linear motility, occur at a resact concentration of 8.5×10^{-16} M and sperm density evidence indicates that it takes over 30 seconds for 10% of sperm respond chemotactically to resact gradients formed by both 1 nM and 10 nM starting concentrations. A decision tree clustering algorithm trained on sperm behavioral and physiological parameters was able to correctly classify 74.1% of sperm by their chemotactic status. We investigated the variability in sperm behavior and found that the majority of sperm swim in stationary or shifting circles, with very few engaging in the linear run behavior often used to characterize chemotaxis. Sperm calcium flux measured by fluo-4 intensity in the sperm head did not correlate with path curvature, but calcium intensity did associate with sperm behavior. Our study shows that *A. punctulata* sperm run responses occur at a low threshold concentration of resact and indicates that progressive circling behaviors may effectively result in productive sperm chemotaxis.

INTRODUCTION

Chemotaxis, the "movement of entire motile cells or organisms toward or away from specific materials" (Rosen, 1962), is a phenomenon ubiquitous to cells of all types, from leukocytes searching for infection vectors (Rosen, 1962) to bacteria seeking out nutrient patches (Ahmed et al., 2010b). In 1883, the sperm of bracken ferns were found to accumulate at the mouth of a capillary containing particular substances in the first recorded evidence of sperm chemotaxis (Pfeffer, 1903). Now, sperm chemotaxis has been identified across the span of eukaryotes, from internal fertilizers such as mice (Burnett et al., 2011) and humans (Lishko et al., 2011; Spehr et al., 2003; Veitinger et al., 2011) to external-fertilizing vertebrates such as fish (Yanagimachi et al., 2013), frogs (Xiang et al., 2005), and octopuses (De Lisa et al., 2013), to marine invertebrates such as ascidians (Yoshida et al., 2013), corals (Morita et al., 2006), and abalone (Riffell et al., 2002). Sea urchins are a particularly prolific model of sperm chemotaxis which have been well-studied since the first indication that egg-conditioned media increased sperm oxygen consumption (Gray, 1928).

Arbacia punctulata sea urchins have been an important model of developmental biology for over a century (Harvey, 1956), including studies of the molecular mechanisms of sperm chemotaxis. The 14-amino-acid peptide resact has been isolated from *A. punctulata* egg jelly (Suzuki et al., 1984; Ward et al., 1985; Yoshino et al., 1991) and elicits species-specific sperm physiological responses (Ward et al., 1985), including increases in sperm respiration and intracellular cGMP (Suzuki and Garbers, 1984) and calcium (Böhmer et al., 2005). Sperm responses through this cyclic peptide, mediated by a guanylate cyclase receptor (Bentley et al., 1986; Pichlo et al., 2014;

Shimomura et al., 1986a; Yoshino et al., 1991), may be dependent on extracellular (Ward et al.,

1985) and intracellular (Heck and Laskin, 2003) stores of calcium.

Resact binding to receptors leads to an intracellular increase in cGMP followed by a calcium

response on the order of 500 ms (Kashikar et al., 2012; Kaupp et al., 2003). Intracellular calcium

increases modulate flagellar beat asymmetry (Cook et al., 1994) and the time derivative of

calcium changes path curvature (Alvarez et al., 2012); calcium intensity peaks occur when *A.*

punctulata sperm make chemotactic turns towards the source of a chemoattractant. The

molecular mechanisms mediating sea urchin sperm chemotaxis are thoroughly reviewed in

several articles (Beltrán et al., 2007; Darszon et al., 2008; Kaupp et al., 2006; Kirkman-Brown et

al., 2003; Yoshida and Yoshida, 2011).

While the molecular mechanisms of sea urchin sperm chemotaxis are well-studied, the

intricacies of chemoattractant gradients stimulating these responses are not. Research in bacterial

chemotaxis has led to an understanding of the *E. coli* signaling molecules and the dependence of

the chemoattractant concentration and exposure time required for chemotactic response (Brown

and Berg, 1974; Lazova et al., 2011). For urchin sperm chemotaxis, signaling cascades have

been identified and, while it is clear that sperm chemotaxis can occur at a wide range of

chemoattractant concentrations (Friedrich and Julicher, 2007; Kaupp et al., 2008, 2003), it is

unknown what absolute and relative concentrations of resact initiate the sperm response, ensure

that sperm response continues, and re-recruit sperm that have adapted to chemoattractant

conditions. In this study, we use laminar-flow microfluidic channels to create specifically

defined chemoattractant gradients and investigate the gradient conditions under which sperm

recruitment and adaptation occur. We couple this tool with calcium imaging to record sperm

physiological changes and form a more complete picture of spatiotemporal changes in sperm

behavior and physiology in a chemoattractant gradient.

METHODS

Sample preparation

Male sea urchins of the species *Arbacia punctulata* (Marine Biological Laboratories, Woods

Hole, MA) were spawned by injection of 0.5 mL of 0.5M KCl into the coelomic cavity through

the mouth. Sperm was collected dry and stored on ice for up to two hours. Artificial seawater

was prepared as in Alvarez 2012 (Alvarez et al., 2012), by adding 9 mM KCl (Sigma Aldrich),

423 mM NaCl (Fisher Scientific), 9.27 mM $CaCl_2$ (Acros Organics), 22.94 mM $MgCl_2$ (Sigma

Aldrich), 25.5 mM $MgSO_4$ (Sigma Aldrich), 0.1 mM EDTA (Sigma Aldrich), and 10 mM Hepes

(Sigma Aldrich) to Milli-Q water and adjusting to pH 7.8 with NaOH (Mallinckrodt Chemicals).

Fluo-4 calcium dye was prepared by adding 100 μL of dimethylsulfoxide (DMSO; Sigma

Aldrich, St. Louis, MO) to a 50 μg vial of fluo-4 (Invitrogen, Carlsbad, CA) and keeping the

mixture on ice and in the dark until use. Calcium dye was loaded into sperm as in Alvarez 2012

(Alvarez et al., 2012): 3.95 μL of the dye mixture was added to 10 μL of sperm and 60 μL ASW

with 0.5% pluronic F-127 (Sigma-Aldrich, St. Louis, MO) for a final dye concentration of 30

μM and the mixture was incubated in the dark at 21°C for 60 minutes. Previous work with

calcium indicators has suggested no change in sperm behavior as a result of their presence

(Guerrero 2010, Kaupp 2003). After incubation, 600 μL of ASW was added to the sperm mixture

and the solution was centrifuged at 1000×g for 10 minutes. The supernatant was discarded and

pelleted sperm were stored in the dark at 21°C until use. Calcium-dyed sperm were diluted in ASW (prepared as above) and non-calcium-dyed sperm were diluted into filtered seawater with 0.2% bovine serum albumin to prevent cell adherence to surfaces.

Microfluidic sperm chemotaxis assays and calcium imaging

As previously described (Ahmed and Stocker, 2008; Hussain et al., 2016), microfluidic devices with 3 inputs leading to a test channel 4 cm long, 99 μm deep, and 1020 mm wide were created by molding polydimethylsiloxane (PDMS; Dow Corning, Midland, MI) against a patterned silicon wafer and attaching the cured PDMS to a glass slide.

The chemoattractant gradient was established by connecting one 1 mL and two 0.5 mL gastight syringes (Hamilton Company, Reno, NV) via non-toxic polyethylene tubing (BD Intramedic, Franklin Lakes, New Jersey) to the three inlets (middle and each side, respectively) on the microfluidic channel. The rightmost inlet was connected to a syringe filled with 0.5 mL of resact (Phoenix Pharmaceuticals, Burlingame, CA) diluted to concentrations ranging from 0.1 nM to 100 nM in ASW. In control experiments, this syringe was filled with ASW. The leftmost inlet was connected to a syringe filled with 0.5 mL of fluo-4-dyed sperm diluted 1000× in ASW. The center inlet was connected to a syringe filled with 1 mL of ASW. The diffusion of chemoattractant in the channel was modeled using a COMSOL computational fluid dynamics model (see Chapter 2 for details); the numerical solution accounts for diffusion occurring both before and after flow is stopped (Figure 1).

A syringe pump (Harvard Apparatus, Holliston, MA) was used to set a flow rate of 10 µL/min, which was maintained for 60 seconds before being stopped to allow the attractant gradient to develop. Video recording began simultaneously with the cessation of flow. A microscope (Nikon TE2000; Nikon Instruments, Melville, NY) equipped with a 10× Nikon Plan Fluor objective was used to view the channel. The camera used to capture all calcium-dyed sperm videos was a 512 × 512-pixel (field of view: 8.2 × 8.2 mm) CCD (iXon Ultra 897; Andor Technology, Belfast, UK), a 1920 × 1080 pixel CCD (sCMOS, Andor) for all non-fluorescing sperm in chemoattractant gradients, and a 1920 × 1080 pixel CCD (Neo SCC-01263, Andor) for non-fluorescing sperm in no-attractant conditions. Videos were recorded at 32 frames per second, mid-depth in the channel, 5 mm from the inlet, for 60-120 seconds. ASW was used to flush the channel between each experimental condition.

Video analysis

Sperm tracks were obtained from recorded calcium-fluorescence videos using NIS Elements (Nikon Instruments, Melville, NY). The researcher was blind to the experimental treatment of sperm in each video before monitoring and identifying all motile cells. A random number generator was used to choose five sperm to track from each date and experimental condition. Sperm were tracked for the entire time the sperm head was motile, in focus, and visible in the field of view. Although calcium fluctuations in chemotaxing sperm cells originate in the flagellum, the bulk changes are reflected in the sperm head (Wood et al., 2003). Maximum fluorescence and position in time of each sperm head were exported for use in custom scripts in Matlab (MathWorks, Natick, MA), and sperm tracks were manually scored for progressive and circling behavior.

Custom scripts in Matlab calculated 23 sperm parameters: calcium fluorescence intensity

(normalized to the minimum fluorescence by subtraction and division, to the maximum by

division, and to a unit scale by the equation $\frac{F-F_{min}}{F_{max}-F_{min}}$), change in fluorescence intensity (with

and without a Gaussian filter), track velocity, velocity x and y components, track acceleration

(overall and in the x direction), angle of movement, change in x and y, track curvature (with and

without a Gaussian filter), and angular velocity at every point in the track. The change in resact

gradient for sperm, dc/dx and dc/dt, were calculated, as well as the temporal gradient

experienced by sperm at every point in time and space, given by $\frac{dc}{dt} + vel_x * \frac{dc}{dx}$, and the

response parameter for bacterial chemotaxis $\frac{1}{c} * \frac{dc}{dx}$ (Brown and Berg, 1974). Tracks were

manually scored for behavior, and these data were exported along with 3 parameters from the

raw track (time, x position, y position). 75 full sperm tracks with calcium activity were recorded

from 17 videos of sperm from 17 males in the 1 nM resact gradient condition, and 49 tracks were

recorded from 11 videos of sperm from 11 males in the ASW control condition.

For non-fluorescence videos, custom Matlab scripts were written to track all sperm heads in each

video and post-process the resulting tracks to remove those of nonmotile sperm and link together

sperm that were tracked separately. 1,350 sperm tracks were obtained from 6 videos of 2 males'

sperm in the ASW control, 172,979 sperm tracks from 45 videos of 14 males' sperm in the 1 nM

resact gradient, and 172,979 sperm tracks from 49 videos of 15 males' sperm in the 10 nM resact

gradient.

Data analysis

Raw data for all 26 sperm parameters was normalized to the mean and mapped to determine

which parameters were correlated; 18 parameters were determined to be non-redundant and

selected for comparison. Because sperm tracks varied in length, tracks were considered in 60-

frame intervals to compare behavioral (e.g. directionality) and physiological (e.g. calcium

intensity) parameters across sperm. Intervals were iteratively shifted and layered in order to

capture the full spatiotemporal range of activity, allowing us to align and study time-dependent

parameters.

A singular value decomposition (SVD) was performed on these sperm-parameter combinations

(43,812 in the control condition, 72,846 in the 1 nM gradient condition) and kept the first eight

modes. We then performed supervised machine learning on these mode structures using four

classification methods: Support Vector Machine (SVM), Naïve Bayes (NB), and Decision Tree

(DT). In each case, the classifier was trained to 1000 randomly-selected singular vectors from the

SVD of sperm from the control condition and 1000 randomly-selected singular vectors from the

SVD of sperm from the 1 nM gradient condition, and tested the classifier on a separate

randomly-selected set of the same size.

RESULTS

Aggregate sperm behavior

We investigated *A. punctulata* sperm chemotactic responses to gradients of the chemoattractant

resact threshold using a tri-input microfluidic device to develop gradients with 1 nM and 10 nM

starting concentrations of resact diffusing over 90 seconds (Figure 1). Sperm were video-

recorded and tracks analyzed with special attention given to movement in the cross-channel

direction, along the gradient. To understand overall sperm behavioral dynamics in chemoattractant gradients, we investigated track behavior of the entire sperm population in three conditions (Figure 2). Sperm were video recorded over a 90-second test period in a microfluidic device with no gradient in an ASW control (n = 1,350 sperm) or chemoattractant gradients formed by starting concentrations of 1 nM resact (n = 172,979 sperm) or 10 nM resact (n = 395,334 sperm). It took 10.01 seconds for 1% of the sperm in the 1 nM gradient to move into the right quarter of the channel (where the attractant source is located) and 31.56 seconds for 10% of sperm to respond under the same conditions. The 10 nM gradient yields similar results, with 1% of sperm responding in 11.88 seconds and 10% of sperm responding in 34.16 seconds. The highest concentration of resact in the sperm inlet within these time periods was 5.04×10^{-12}, 1.28×10^{-11} (1 nM: 1%, 10%), 8.28×10^{-11}, and 1.55×10^{-10} (10 nM: 1%, 10%), respectively. In contrast, it took 31.25 seconds for 1% of sperm to move into the right quarter of the control (ASW) channel and 46.59 seconds for 10% of sperm to move into the same area.

It is important to note that aggregate sperm response over the entirety of video recording was dependent on attractant gradient conditions. In no-attractant control conditions, 0.02% of tracked sperm have some portion of their track in the right quarter of the channel, whereas 0.69% of sperm in the 1 nM gradient and 1.03% of sperm in the 10 nM gradient show the same response. The maximum proportion of sperm in the right quarter of the channel was 6.2% in the ASW control (at 68 seconds), 38.2% in the 1 nM gradient (at 88 seconds), 58.8% in the 10 nM gradient (at 89 seconds). Many more sperm were motile and responsive in the chemoattractant gradient than in a seawater control, with strength of response greater in the gradient formed with a

starting concentration of 10 nM than 1 nM. These data describing aggregate sperm behavior led to an examination of how individual sperm respond to a chemoattractant gradient.

Threshold of sperm response to chemoattractant

We determined the threshold resact concentration at which sperm chemotactically respond by filtering the 729,141 *A. punctulata* sperm tracks recorded from three gradient conditions to study those that had a visible "run," defined as a sequence of positive Δx values that spanned 5% of the channel width, starting within 30 seconds of the flow being stopped (n = 551 sperm, representative tracks shown in Figure 3 and 4).

Using these criteria, we found that the threshold non-zero resact concentration that elicited a run was 8.5×10^{-16} M (n = 338 sperm, Figure 5). The threshold non-zero resact concentration eliciting a run for sperm in the 1 nM gradient was also 8.5×10^{-16} M (n = 135 sperm). For sperm in the 10 nM gradient, the threshold non-zero resact concentration that elicited a run was 2.0×10^{-15} M (n = 203 sperm). For 32 of the 338 sperm (7 in 1 nM gradient, 25 in 10 nM gradient), a run response occurred at a resact concentration less than the model's computational lower limit of 1×10^{-46} M.

Relating sperm physiology and behavior

We also investigated whether the threshold of sperm response to attractant is detectable using sperm physiological changes, measured by loading sperm with the calcium-indicating dye fluo-4 and recording calcium fluorescence intensity, a proxy for intracellular physiological changes. Investigation of these complex behaviors was limited to a comparison of sperm in the seawater

control to sperm in the gradient formed by a starting concentration of 1 nM resact. Using a

dataset with 75 full sperm tracks in 1 nM resact and 49 tracks in an ASW control with calcium

flux information, we first replicated previous work which indicated that, for *A. punctulata* sperm

in resact gradients formed by flash photolysis of 1 µM caged resact, the change in fluorescence

intensity in time is correlated with sperm path curvature (Alvarez et al., 2012). However, our

data do not yield the same positive correlation that was found in previous studies, with a mean

Pearson correlation coefficient of -0.028 and a mean p-value of 0.33 (Figure 6, 7A). All of the

five sperm cells with reasonably strong correlations between dF/dt and curvature ($\rho > 0.5$) had

tracks with only linear and curving paths and no circling behavior (Figure 7 B, C).

This finding led directly into the question of whether physiological responses associate with the

behavior types found earlier (linear, curving, circling), using this calcium-imaged sperm dataset

(Figure 8). We first investigated changes in calcium intensity in response to changes in resact

concentration for all sperm and found no clear difference in calcium intensity over the span of

concentrations found in the channel (Figure 8). However, calcium fluorescence intensity does

differ between sperm behaviors in the same chemoattractant gradient, with sperm engaged in

circling behavior having the highest calcium fluorescence intensity and linearly-swimming

sperm having the lowest calcium fluorescence intensity (Kruskall-Wallis test with Bonferroni

correction for multiple comparisons of medians, $p < 0.001$; Figure 8).

Identifying chemotaxis by clustering and machine learning

To further explore which parameters explain the differences between chemotaxing and non-

chemotaxing sperm, we used clustering and machine learning algorithms. A singular value

decomposition (SVD) on 18 parameters performed separately on each gradient condition (49 sperm in ASW control and 75 sperm in 1 nM resact) yielded several primary modes (Figure 9). Supervised machine learning based on the first eight modes of the singular value decomposition yielded mixed results (Table 1), with Support Vector Machine and Naïve Bayes algorithms failing to surpass a 50% correct classification on the test data set, while Decision Tree (DT) and Boosted Decision Tree algorithms accomplished nearly 70% correct classification.

We also tested clustering and classification on data reduced by three mechanisms: filtering the data for sperm located outside the inlet stream, reducing the effect of long sperm tracks (over 180 frames) by randomly selecting time iterations to the length of 180 frames (the 3rd quartile of track length), or focusing only on calcium parameters. The most successful clustering was on sperm that were located outside the inlet stream, with the reduction of long sperm tracks (74.11 ± 1.18% correctly classified by DT; 12,186 control sperm-parameter combinations, 27,630 in attractant). The decision tree for this classifier had 308 nodes, 56 based on the second mode of the singular value decomposition, 42 based on the third mode, 50 from the fourth mode, 30 on the fifth mode, 40 on the sixth mode, 34 on the seventh mode, and 56 on the eighth mode. The sixth, eighth, and second modes determined the first three levels of decision in the tree and were therefore the most impactful in the classification algorithm. This same dataset with only calcium parameters clustered less successfully (using DT, 69.98 ± 1.22% correct with only calcium data).

Sperm behavior in response to chemoattractant

In the process of attempting to determine what parameters define sperm chemotaxis, we found that sperm behavior was more diverse than expected. Five randomly-selected 100-sperm samples

were drawn from each gradient condition, from the subset of sperm that begin their track within 30 seconds of video recording, have at least 2 seconds of recorded behavior, and move more than 50 microns (ASW control n = 45, 1 nM resact n = 5,973, 10 nM resact n = 14,864 sperm tracks). From this subset of sperm, we identified three types of swimming behavior: a straight path ("run"), circling in place ("static circle"), and circling while moving progressively ("moving circle"). Some sperm tracks had behavior that did not fit any of these qualitative classifiers, and some sperm had tracks that were combinations of 2-3 of these behaviors (Figure 10).

Sperm behavior varied between conditions, with the largest differences between sperm in the ASW control and in resact gradients (Table 2). Behavior in the 1 nM and 10 nM gradients appeared similar overall. The majority of sperm in the ASW control exhibited static circling behavior (61.4%, n = 45 sperm) and fewer swimming in moving circles (38.6%). In contrast, sperm in the gradient formed by starting concentrations of 1 nM of resact and 10 nM of resact are primarily found in moving circle behavior (respectively, 73.0% and 76.4%, n = 500 sperm randomly sampled from 5,973 and 14,864 total tracks) and fewer swimming in static circles (24.7% and 22.4%, respectively). 'Run' behaviors were uncommon, with fewer than 6% of sperm tracks showing any run behavior in any gradient condition. Given the scarcity of linear run behavior, we investigated the cross-channel displacement of sperm swimming in moving circles and found that the average displacement of these sperm is 66.39 µm in the 1 nM resact gradient and 56.18 µm in the 10 nM resact gradient, both positive displacements towards the chemoattractant source, in contrast to -8.42 µm in the ASW control, which indicates that these sperm on average move away from the opposite channel wall. While linear motility was

uncommon across all conditions, most sperm in the seawater control swam in static circles and most sperm in the chemoattractant gradients moved in a progressive circular motion.

DISCUSSION

In this study, we investigated the concentration of resact chemoattractant which stimulates *A. punctulata* sea urchin sperm chemotactic response. Using gradients generated in a microfluidic device along with calcium imaging and high-speed video microscopy of sperm, we tracked individual and aggregate sperm behavior in multiple gradient conditions, classified sperm behavior manually and with a decision tree classifying algorithm, and linked sperm behavior with calcium-indicated intracellular physiology.

Analysis of the behavioral dynamics of 172,979 sperm in a 1 nM resact gradient, 395,334 sperm in a 10 nM resact gradient, and 1,350 sperm in a seawater control indicates that sperm in attractant gradients are far more motile than sperm in control conditions, and that they cross the entire microfluidic channel in greater numbers and more quickly. It is, however, notable that it takes over 30 seconds for 10% of sperm in attractant gradients to behaviorally respond by swimming to the source of chemoattractant, as previous work has reported sperm intracellular signaling cascade responses within 1 second of resact binding (Kashikar et al., 2012).

The concentration of resact that stimulated linear run responses from sperm was 8.5×10^{-16} M. This low threshold concentration is certainly within the realm of *A. punctulata* sperm's ability to detect the resact peptide (Strünker et al., 2015), based on receptor density and sensitivity. Each sperm flagellum contains an extraordinary ~300,000 guanylate cyclase resact receptors (Pichlo et

al., 2014), providing the potential for high detection sensitivity as just one resact molecule binding can trigger a physiological response through an intracellular signaling cascade (Kaupp et al., 2008).

Using sperm behavior and calcium behavior from 75 sperm in a 1 nM resact gradient and 49 sperm in a seawater control, we found that calcium flux did not correlate with sperm path curvature, unlike previous studies of *A. punctulata* sperm chemotaxis (Alvarez et al., 2012; Kashikar et al., 2012). However, intracellular calcium differs between sperm linear, curving, and circling behavioral patterns, even within the same chemoattractant gradient. This contrasting evidence indicates that including and distinguishing sperm behavior could be critical to separating chemotaxing sperm from those which are not responding. It is also possible that the microfluidic device used in this study may generate a different gradient than the chamber with flash-photolysis-released attractant used in previous studies, resulting in different sperm responses than observed previously.

A decision tree algorithm applied to sperm tracks with both behavior and calcium data achieved $74.11 \pm 1.18\%$ correct clustering of sperm from chemoattractant and control treatments. These classification results showed that we can distinguish chemotaxing from non-chemotaxing sperm with statistically significant accuracy, indicating that chemotaxing sperm have unique behavioral and physiological signatures that interact to form a nearly-complete picture of chemotaxis under these conditions. Calcium parameters alone yielded lower classification accuracy ($69.98 \pm 1.22\%$), suggesting that physiology alone may be able to distinguish chemotaxing and nonchemotaxing sperm, but that behavior interacts to more clearly delineate the groups.

Analysis of sperm behavior types reveals that sperm in chemoattractant gradients spend the majority of their time swimming in moving circles (73.0% and 76.4% in 1 nM and 10 nM resact gradients) and most of the remainder in static circles (24.7% and 22.4%), a pattern reversed in sperm in the ASW control. These data highlight the rarity of 'run-tumble-run' and linear sperm tracks. It is possible that our sperm-tracking algorithm is not adept at following sperm engaging in progressive linear runs. This would suggest that the behaviors tabulated in this study may reflect the proportion of time that sperm spend engaged in any particular behavior rather than the proportion of individual sperm that behave in a particular way. Another caveat is that this work studied sperm behavior over a short distance, and sperm may engage in different behaviors over longer distances from a chemoattractant source. Nonetheless, the evidence suggests that future work regarding sperm responses to chemoattractant gradients would benefit from encompassing the breadth of sperm behaviors.

Summary

Our investigation of *A. punctulata* sperm behavior and physiology in well-defined chemoattractant gradients shows that sperm respond to the exquisitely low resact concentration of 8.5×10^{-16} M. Our aggregate sperm density behavior suggests a narrow window between sperm response and gradient adaptation, raising the possibility that some sperm take longer to respond to the gradient. We were able to train a decision tree machine-learning algorithm to correctly classify nearly 75% of sperm tracks by chemotactic parameters. However, it became clear that not all sperm swim in stereotyped run-and-tumble patterns, and our data show that most sperm swim in static or moving circles, with very few engaging in linear run behavior. This

study provides evidence of high sperm sensitivity to a species-specific chemoattractant as well as

a template for investigating the diversity of sperm behavioral and physiological responses to

chemoattractant gradients.

FIGURES

Figure 1: Resact gradient in microfluidic channel. *(solid lines)* Analytical solution of

concentration assuming no diffusion prior to flow being stopped. *(dotted lines)* Numerical

solution accounting for steady-state gradient forming during flow in channel.
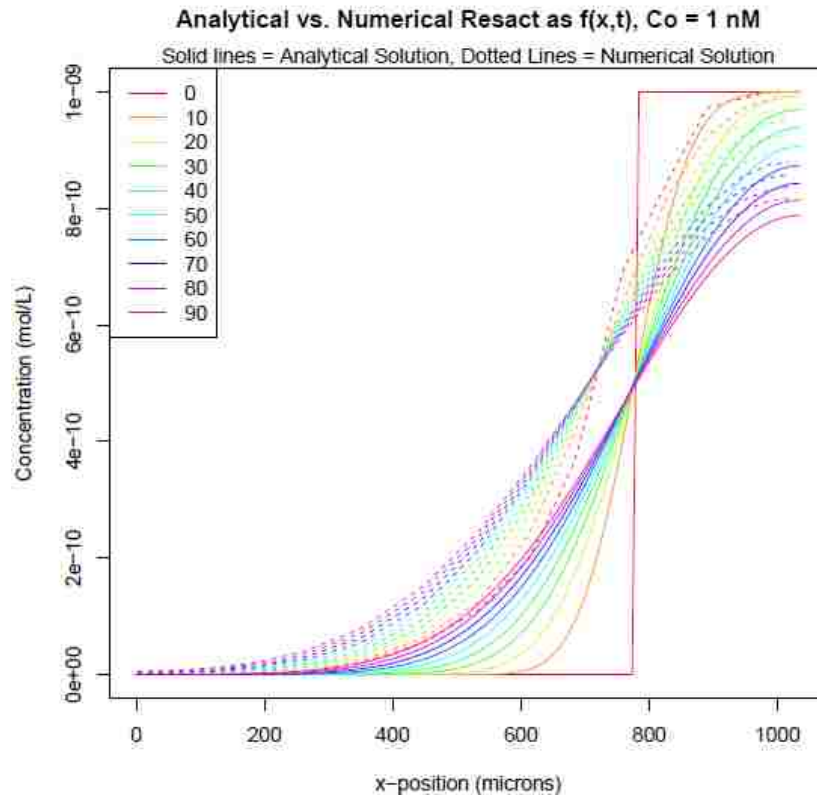
Figure 2: Visualization of sperm population dynamics in resact gradients. (**A-C**) Point x

locations of tracked sperm over time, average count per video, for no-resact ASW control (**A**,

1,350 total sperm tracks), 1 nM resact gradient (**B**, 172,979 total sperm tracks) and 10 nM resact

gradient (**C**, 395,334 total sperm tracks). The color white indicates no sperm (**D-F**) Difference

between the proportion of sperm in the sperm source (left side of the channel) and the attractant

source (right side of the channel) over time for (**D**) no-resact ASW control, (**E**) 1 nM resact

gradient, and (**F**) 10 nM resact gradient. Positive values indicate more sperm in the source

location than the attractant location.
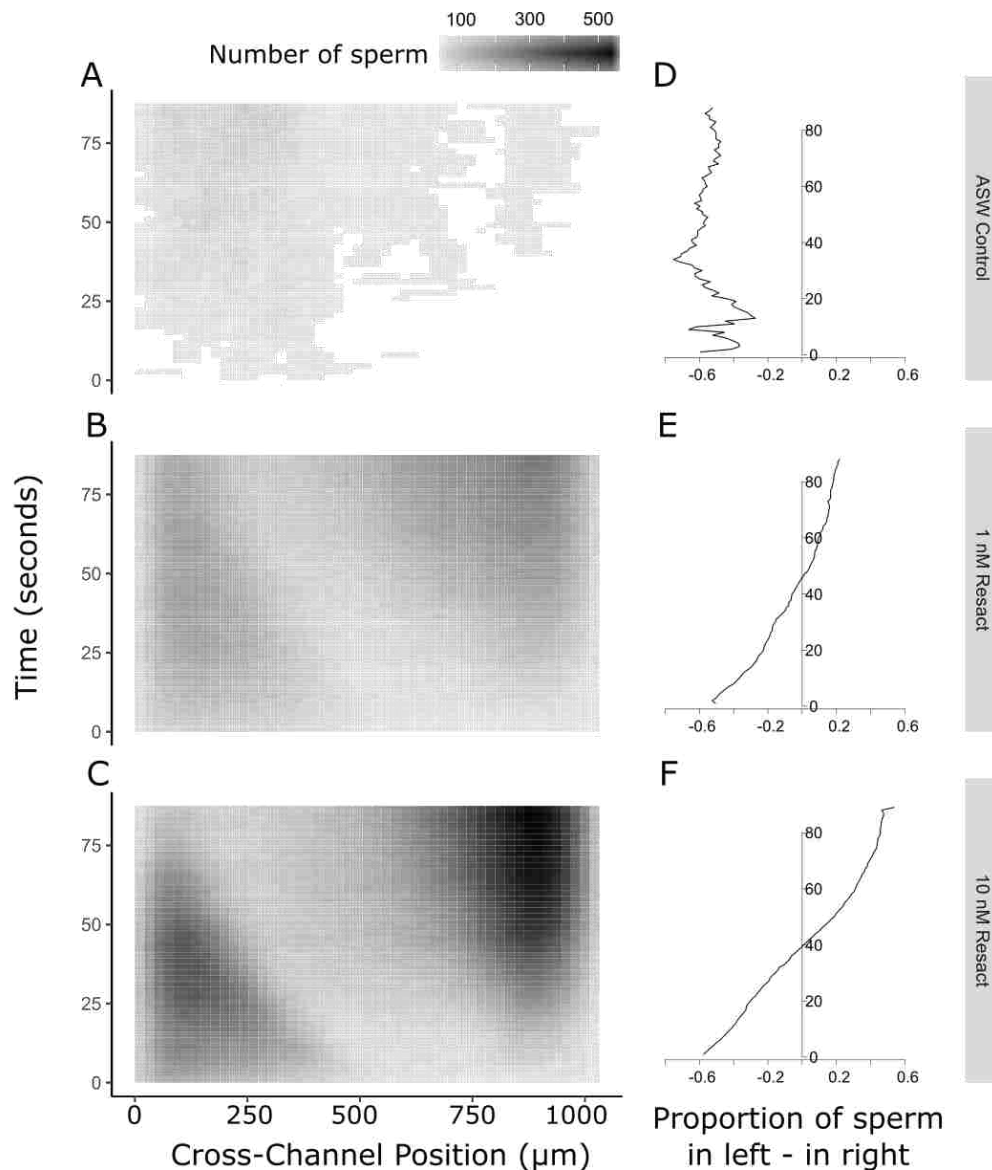
Figure 3: Representative sperm track in 1 nM resact gradient *(left)* Full sperm track, x and y position; time after flow is stopped is denoted by track color. *(bottom left)* Sperm x position in time, showing sperm cell moving towards the source of the attractant. *(bottom middle)* Log resact concentration along sperm track in time. (*bottom right*) Sperm x position as resact concentration changes.
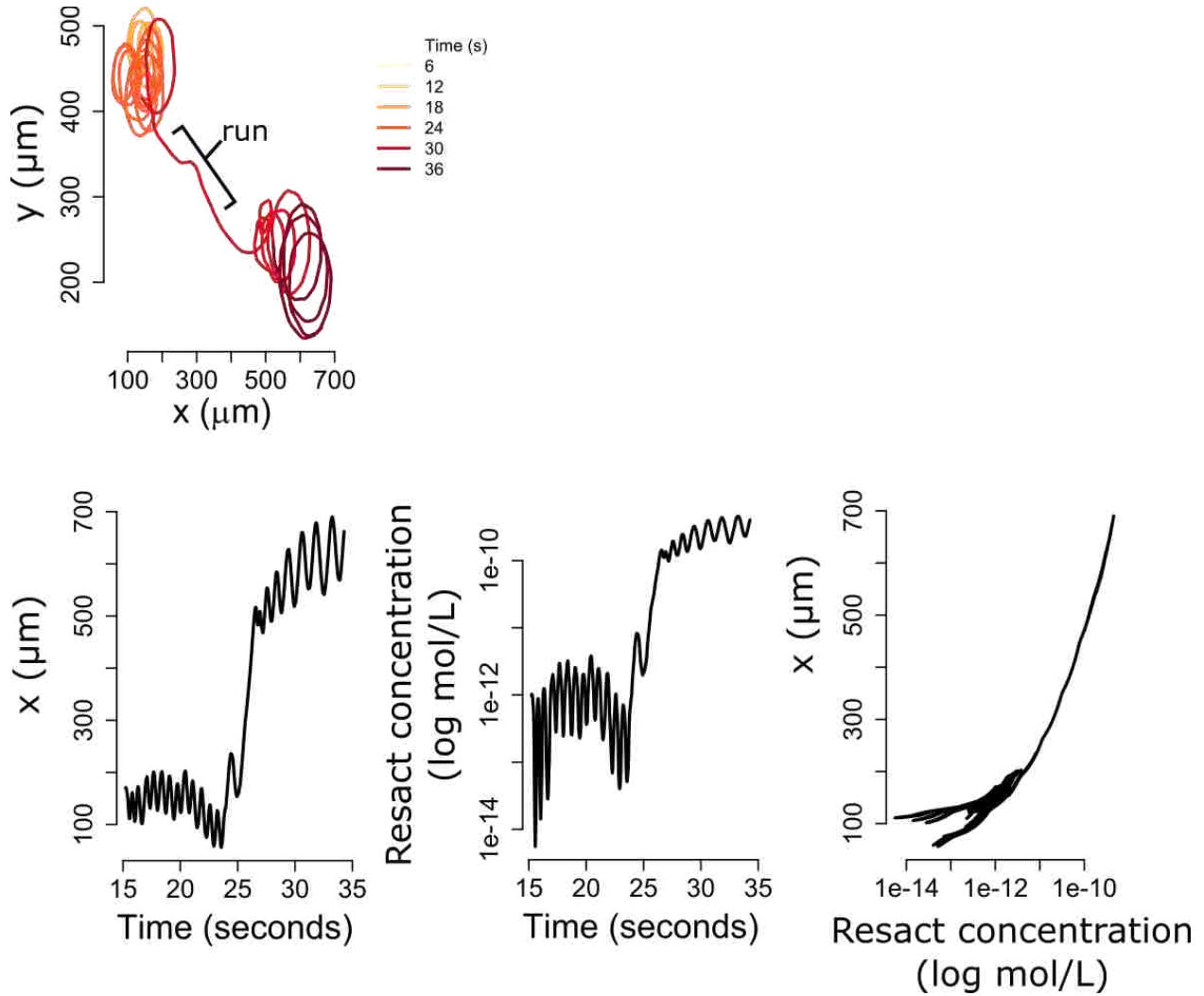
Figure 4: Movement towards the attractant source of sperm (positive x direction) conducting run behavior within 30 seconds of gradient development. (*left*) Starting concentration of resact is 1×10^{-9} M (46 tracks). (*right*) Starting concentration of resact is 1×10^{-8} M (90 tracks)
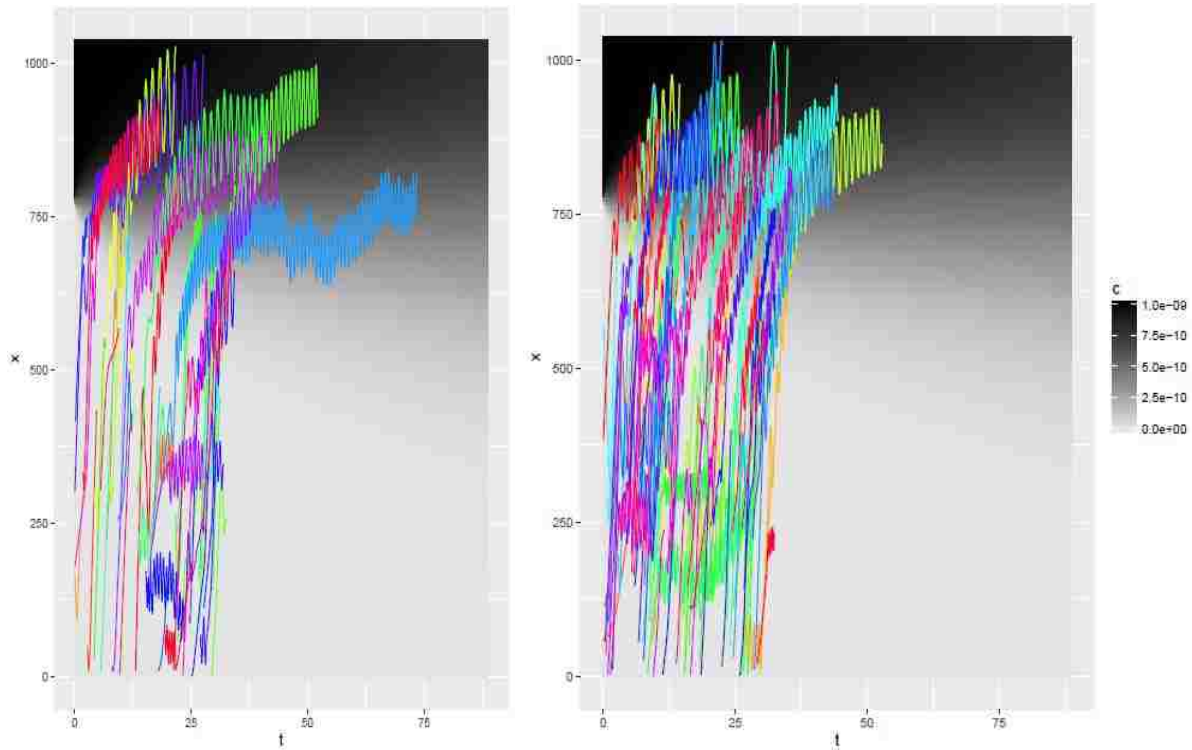
Figure 5: Log resact concentration at which run behavior is initiated and ended for (**A**) sperm in

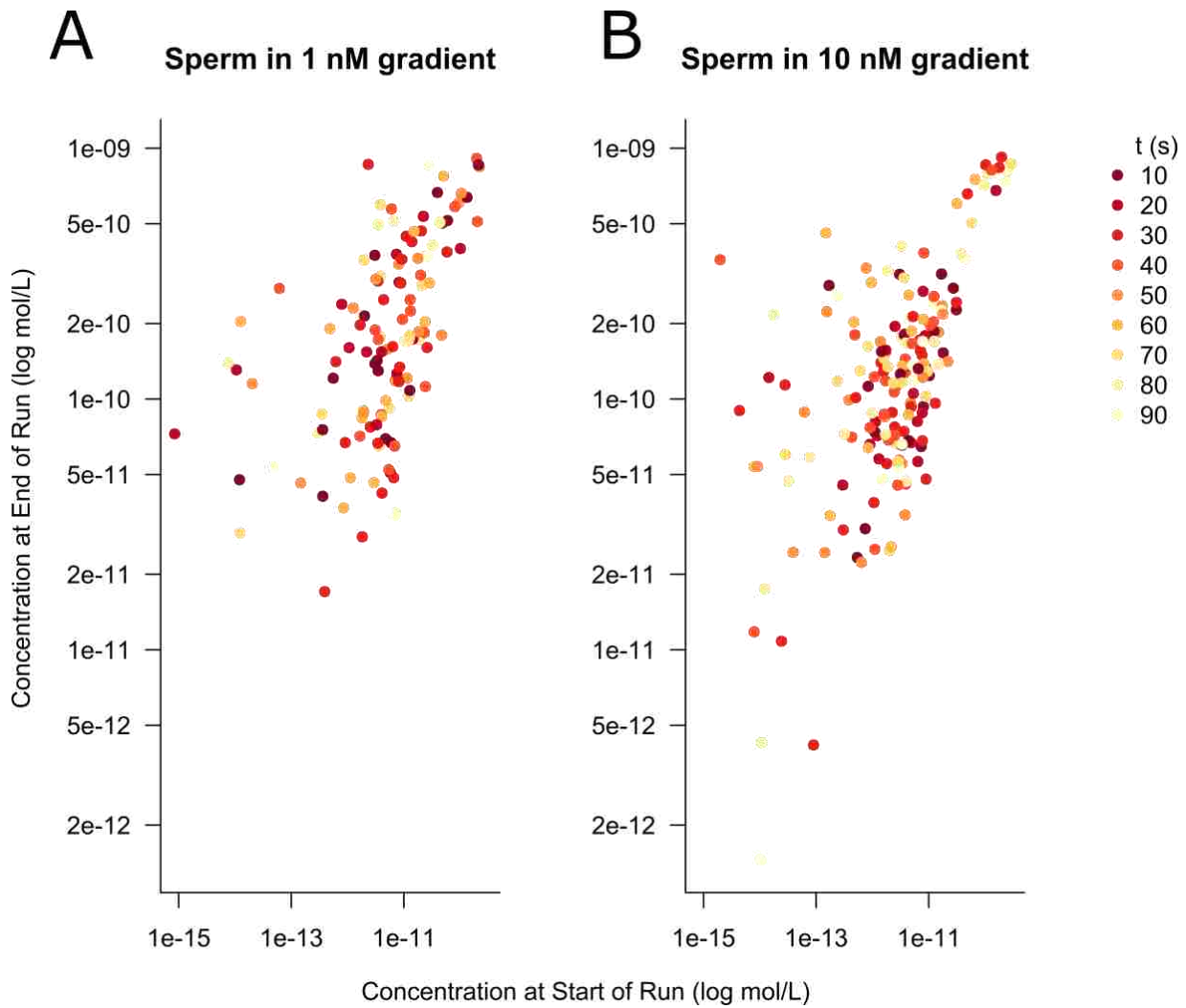1 nM gradient (n = 135) and (**B**) sperm in 10 nM gradient (n = 203)

Figure 6: Representative tracks and calcium fluorescence of sperm in a 1nM resact gradient (**A, B**) Sperm track for which dF/dt and curvature are correlated (ρ = 0.83, p < 0.001). (**C, D**) Sperm track for which dF/dt and curvature are not correlated (ρ = -0.01, p = 0.86).
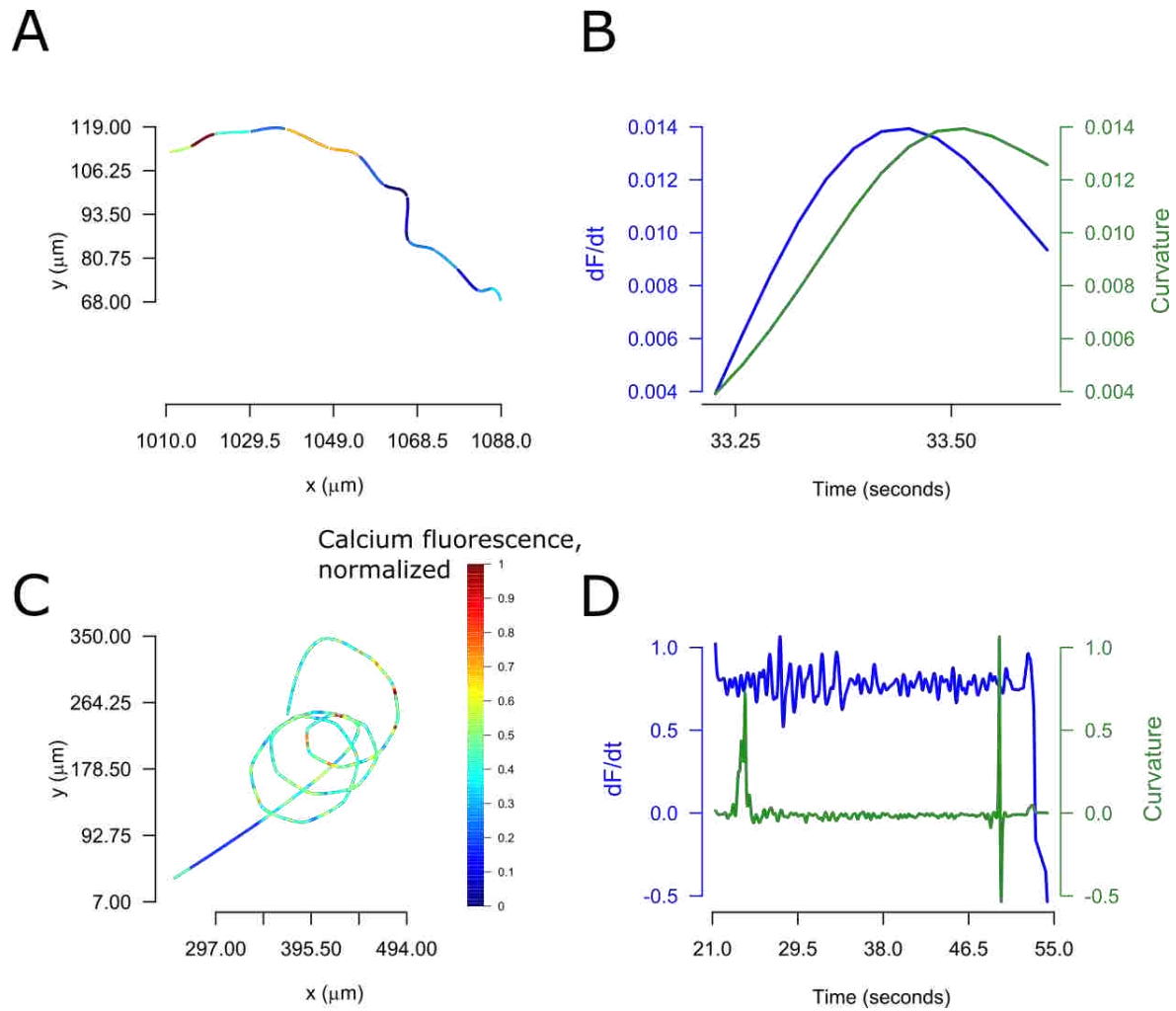
Figure 7: Sperm in a 1 nM resact gradient do not consistently show correlations between change in calcium fluorescence intensity and path curvature. (**A**, *left panel*) Pearson correlation between path curvature and dF/dt, mean marked in red (n = 75 sperm). Positive correlations (correlation coefficient > 0.5) are circled in red. (**A**, *right panel*) p-values of Pearson correlations between path curvature and dF/dt, mean marked in red (n = 75 sperm). Values corresponding with the five positive correlations are plotted in red. (**B**) Swimming paths for five sperm with positive correlations, with color corresponding to normalized calcium fluorescence. (**C**) Normalized calcium fluorescence and track behavior over time for five sperm with correlations between path curvature and dF/dt.
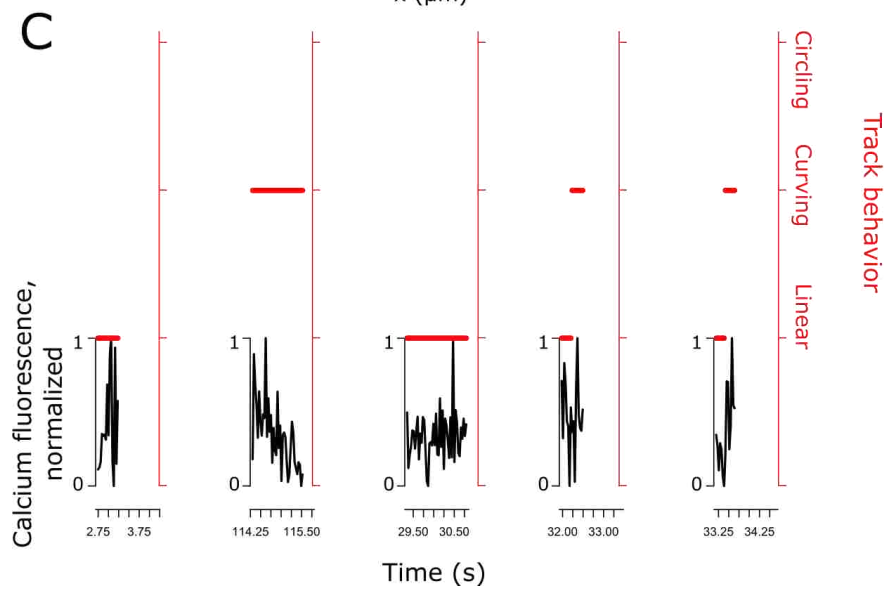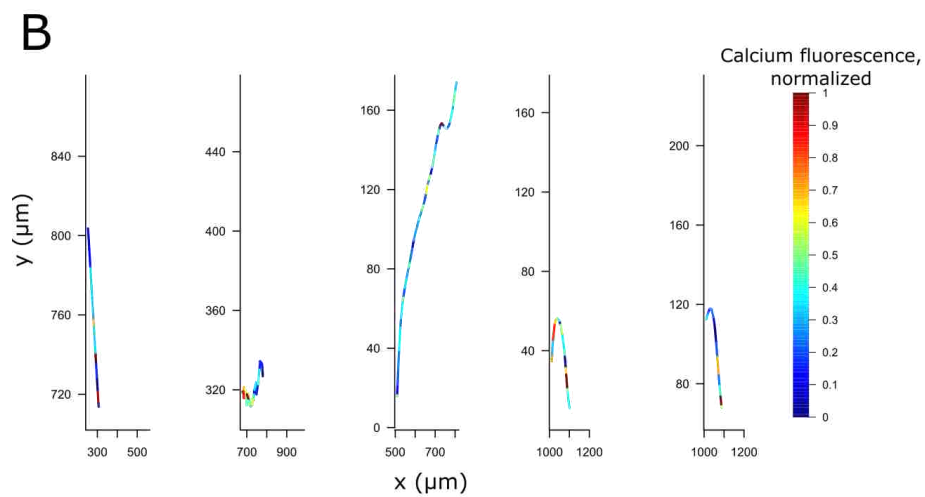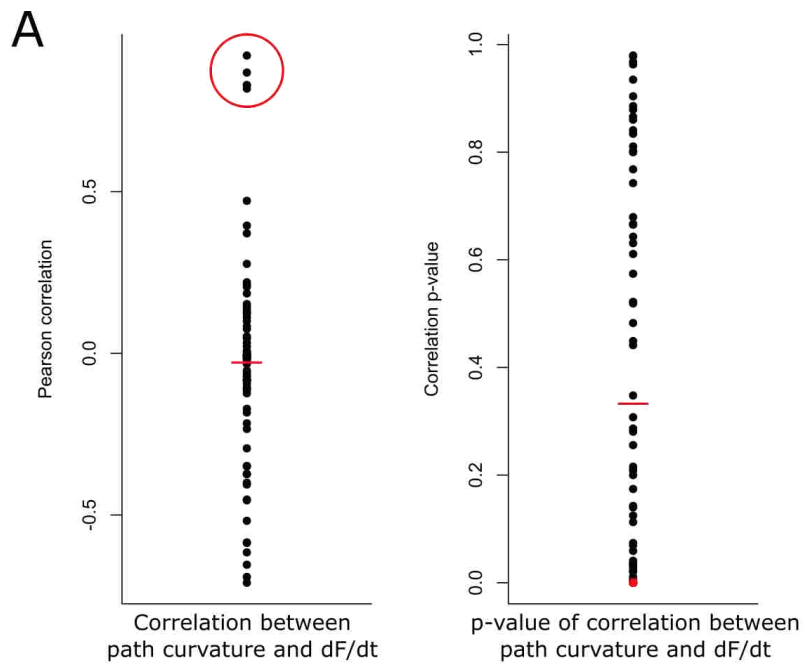
Figure 8: Calcium fluorescence intensity as related to chemoattractant concentration and sperm track behavior (n = 11,841 data points from 75 sperm) (*top*) dF/dt over resact concentration. *(bottom)* Calcium fluorescence intensity in linear, curved, and circling sperm behaviors, with median marked in red, in seawater control (*left*) and 1 nM resact gradient *(right)* conditions.
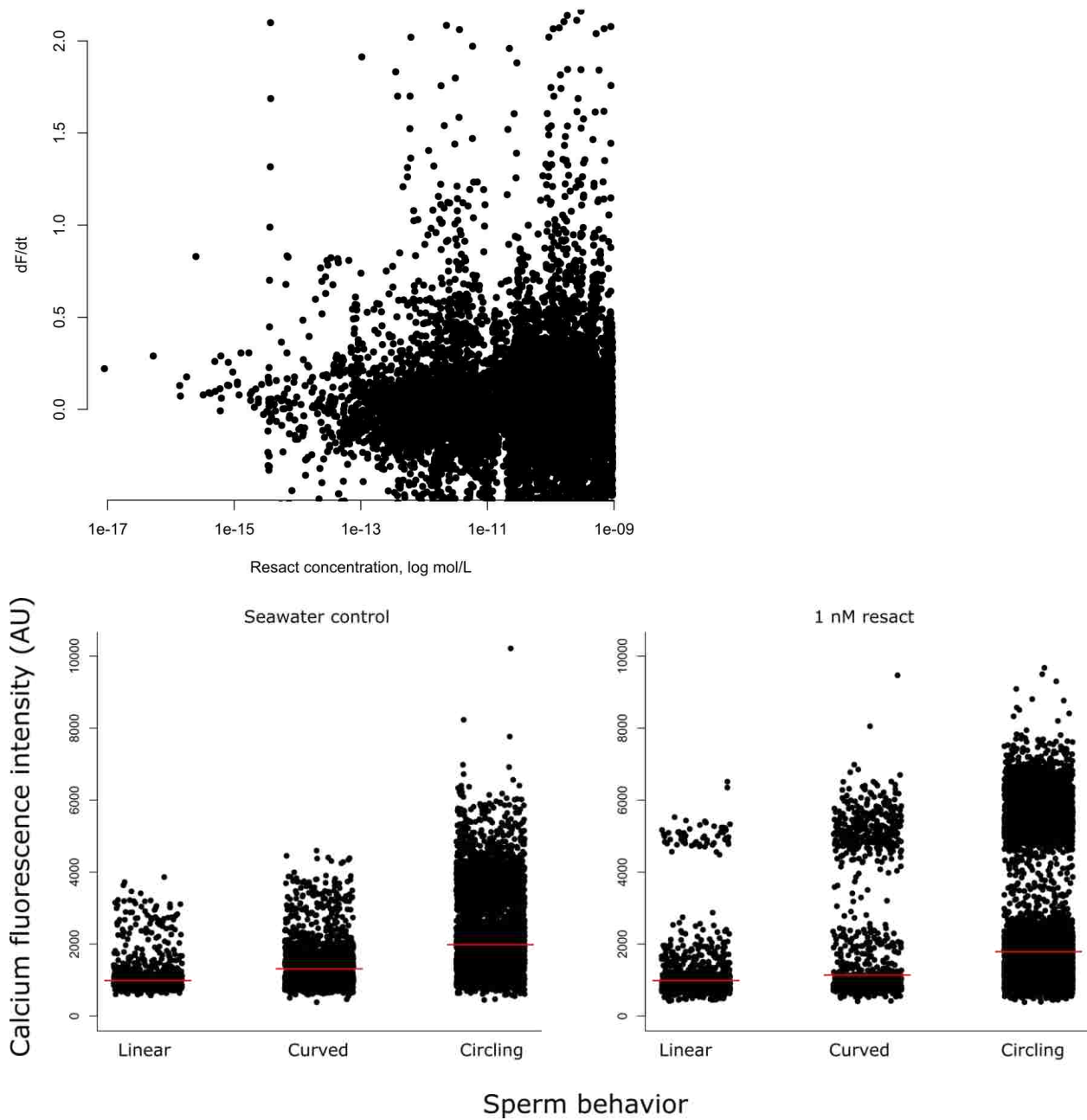
Figure 9: SVD modes from sperm-parameter combinations from (*top*) sperm in control conditions (43812 data points) and (*bottom*) sperm in a 1 nM gradient (72486 data points).
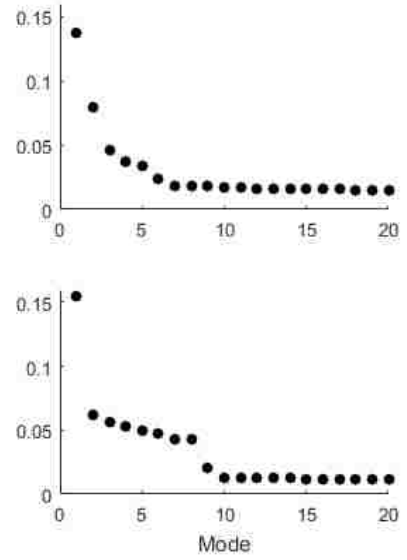

Table 1: Classification methods and their effectiveness at separating parameters of sperm in chemoattractant from sperm in an ASW control.

Classification Method	Data Set (# data points from ASW control, # data points from 1 nM resact)	Classification Score (% correct)	Classification Standard Deviation
Support Vector Machine	All sperm (43812, 72846)	49.71	1.29
Naive Bayes	All sperm (43812, 72846)	49.80	1.19
Decision Tree	All sperm (43812, 72846)	69.12	1.29
Decision Tree	Sperm outside the inlet (12186, 27630)	74.11	1.18

Figure 10: Sperm behavior types shown by representative tracks' x,y position. Color of track indicates time elapsed since flow was stopped. *(top left)* Moving circle behavior *(top right)* Static circle behavior *(bottom left)* "Other" behavior *(bottom right)* Combined behavior: static circle, run, moving circle. The majority of sperm in the ASW control are found in static circling behavior (61.4%, n = 45 sperm) and fewer swimming in moving circles (38.6%). In contrast,

sperm in the gradient formed by starting concentrations of 1 nM of resact and 10 nM of resact are primarily found in moving circle behavior (respectively, 73.0% and 76.4%, n = 500 sperm randomly sampled from 5973 and 14,864 total tracks) and fewer swimming in static circles (24.7% and 22.4%, respectively).
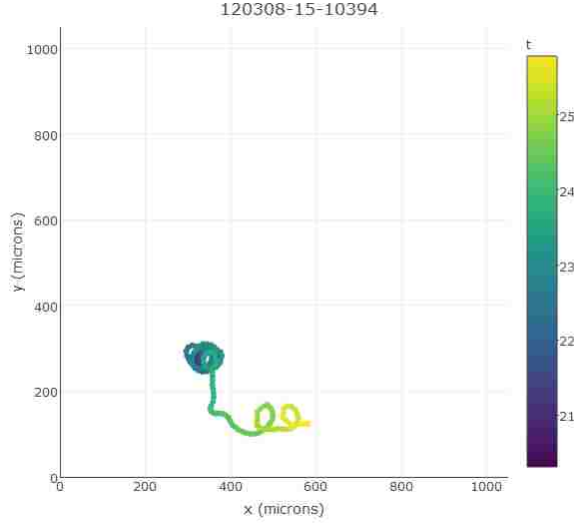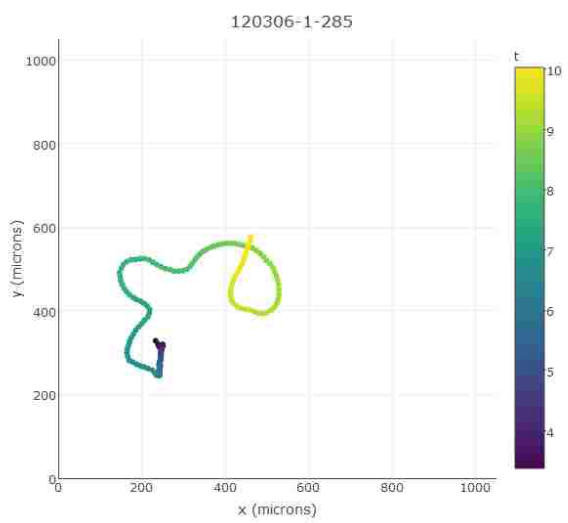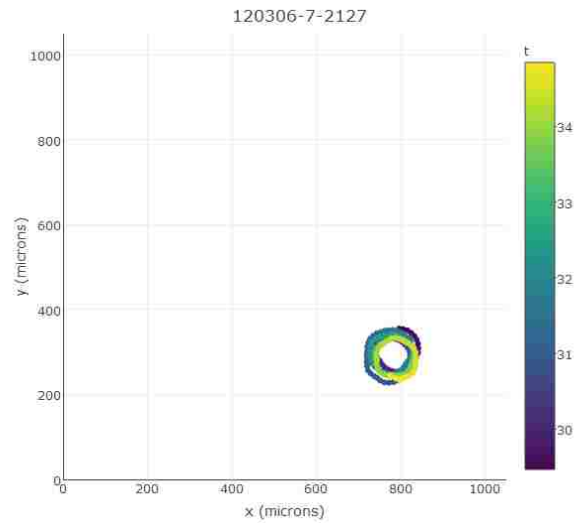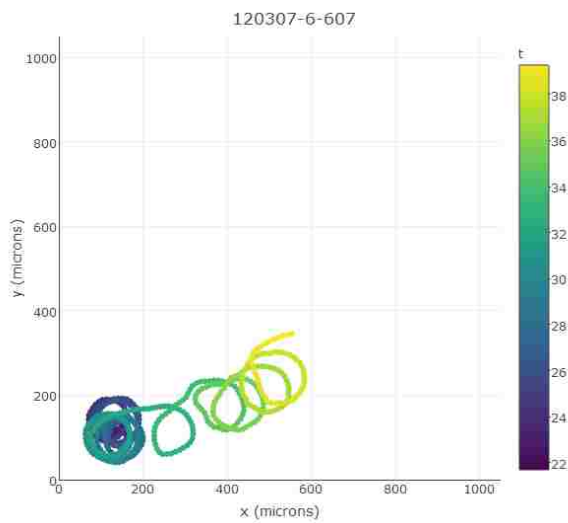
Table 2: Behavioral classification of sperm tracks by gradient condition, for 5 random samples

of 100 tracks from each gradient condition (45 total from control)

Gradient condition / Behavior	Control (ASW) n = 45	1 nM resact n = 500, N = 5,973	10 nM resact n = 500, N = 14,684
Static circle	61.4%	21.2%	18.6%
+ Run	-	2.4%	1.7%
+ Other	-	0.8%	1.9%
Moving circle	38.6%	68.2%	73.3%
+ Run	-	3.1%	2.1%
+ Other	-	1.7%	1.0%
Run	-	0.4%	0.2%
Other	-	1.5%	0.8%
Combination of 3+	-	0.2%	0.2%

REFERENCES

Aguirre, J.D., Blows, M.W., Marshall, D.J., 2016. Genetic Compatibility Underlies Benefits of Mate Choice in an External Fertilizer. Am. Nat. 187, 000–000. doi:10.1086/685892

Ahmed, T., Shimizu, T.S., Stocker, R., 2010a. Microfluidics for bacterial chemotaxis. Integr. Biol. 2, 604–629. doi:10.1039/c0ib00049c

Ahmed, T., Shimizu, T.S., Stocker, R., 2010b. Bacterial Chemotaxis in Linear and Nonlinear Steady Microfluidic Gradients. Nano Lett. 10, 3379–3385. doi:10.1021/nl101204e

Ahmed, T., Stocker, R., 2008. Experimental verification of the behavioral foundation of bacterial transport parameters using microfluidics. Biophys. J. 95, 4481–4493.

Alvarez, L., Dai, L., Friedrich, B.M., Kashikar, N.D., Gregor, I., Pascal, R., Kaupp, U.B., 2012. The rate of change in Ca 2+ concentration controls sperm chemotaxis. J. Cell Biol. 196, 653–663. doi:10.1083/jcb.201106096

Asmar, N.H., 2004. Partial Differential Equations, 2nd ed. Pearson.

Bates, D., Maechler, M., Bolker, B., Walker, S., 2014. lme4: Linear mixed-effects models using Eigen and S4.

Bell, A.F., Crimaldi, J.P., 2015. Effect of steady and unsteady flow on chemoattractant plume formation and sperm taxis. J. Mar. Syst. 148, 236–248. doi:10.1016/j.jmarsys.2015.03.008

Beltrán, C., Galindo, B.E., Rodríguez-Miranda, E., Sánchez, D., 2007. Signal transduction mechanisms regulating ion fluxes in the sea urchin sperm. Signal Transduct. 7, 103–117. doi:10.1002/sita.200600129

Bentley, J.K., Shimomura, H., Garbers, D.L., 1986. Retention of a Functional Resact Receptor in Isolated Sperm Plasma Membranes. Cell 45, 281–288.

Birkhead, T., Moller, A. (Eds.), 1998. External Fertilizers, in: Sperm Competition and Sexual Selection. Academic Press, San Diego, California, pp. 177–191.

Böhmer, M., Van, Q., Weyand, I., Hagen, V., Beyermann, M., Matsumoto, M., Hoshi, M., Hildebrand, E., Kaupp, U.B., 2005. Ca2+ spikes in the flagellum control chemotactic behavior of sperm. EMBO J. 24, 2741–52. doi:10.1038/sj.emboj.7600744

Brokaw, C.J., 1957. Chemotaxis of bracken spermatozoids. J. Exp. Biol. 35, 192–196.

Brown, D.A., Berg, H.C., 1974. Temporal stimulation of chemotaxis in Escherichia coli. Proc. Natl. Acad. Sci. 71, 1388–92.

Burnett, L.A., Anderson, D.M., Rawls, A., Bieber, A.L., Chandler, D.E., 2011. Mouse sperm exhibit chemotaxis to allurin, a truncated member of the cysteine-rich secretory protein family. Dev. Biol. 360, 318–328. doi:10.1016/j.ydbio.2011.09.028

Chang, H., Kim, B.J., Kim, Y.S., Suarez, S.S., Wu, M., 2013. Different migration patterns of sea urchin and mouse sperm revealed by a microfluidic chemotaxis device. PLoS One 8, e60587. doi:10.1371/journal.pone.0060587

Clark, N.L., Aagaard, J.E., Swanson, W.J., 2006. Evolution of reproductive proteins from animals and plants. Reproduction 131, 11–22. doi:10.1530/rep.1.00357

Clark, N.L., Gasper, J., Sekino, M., Springer, S.A., Aquadro, C.F., Swanson, W.J., 2009. Coevolution of interacting fertilization proteins. PLoS Genet. 5, e1000570. doi:10.1371/journal.pgen.1000570

Clifton, A., 2015. WindRose [WWW Document]. Stack Overflow. URL http://stackoverflow.com/questions/17266780/wind-rose-with-ggplot-r

Cook, S.P., Brokaw, C.J., Muller, C.H., Babcock, D.F., 1994. Sperm Chemotaxis: Egg Peptides Control Cytosolic Calcium to Regulate Flagellar Responses. Dev. Biol. 165, 10–19.

Crean, A.J., Marshall, D.J., 2015. Eggs with larger accessory structures are more likely to be fertilized in both low and high sperm concentrations in Styela plicata (Ascidiaceae). Mar. Biol. 162, 2251–2256. doi:10.1007/s00227-015-2755-0

Crean, A.J., Marshall, D.J., 2008. Gamete plasticity in a broadcast spawning marine invertebrate. Proc. Natl. Acad. Sci. U. S. A. 105, 13508–13513. doi:10.1073/pnas.0806590105

Crimaldi, J.P., Zimmer, R.K., 2014. The physics of broadcast spawning in benthic invertebrates. Ann. Rev. Mar. Sci. 6, 141–65. doi:10.1146/annurev-marine-010213-135119

Darszon, A., Guerrero, A., Galindo, B.E., Nishigaki, T., Wood, C.D., 2008. Sperm-activating peptides in the regulation of ion fluxes, signal transduction and motility. Int. J. Dev. Biol. 52, 595–606. doi:10.1387/ijdb.072550ad

De Lisa, E., Salzano, A.M., Moccia, F., Scaloni, A., Di Cosmo, A., 2013. Sperm-attractant peptide influences the spermatozoa swimming behavior in internal fertilization in Octopus vulgaris. J. Exp. Biol. 216, 2229–37. doi:10.1242/jeb.081885

Eisenbach, M., 1999. Sperm chemotaxis. Rev. Reprod. 4, 56–66.

Engqvist, L., 2013. A general description of additive and nonadditive elements of sperm competitiveness and their relation to male fertilization success. Evolution 67, 1396–1405. doi:10.1111/evo.12024

Evans, J.P., Garcia-Gonzalez, F., Almbro, M., Robinson, O., Fitzpatrick, J.L., 2012. Assessing the potential for egg chemoattractants to mediate sexual selection in a broadcast spawning marine invertebrate. Proc. R. Soc. 279, 2855–2861. doi:10.1098/rspb.2012.0181

Evans, J.P., Sherman, C.D.H., 2013. Sexual selection and the evolution of egg-sperm interactions in broadcast-spawning invertebrates. Biol. Bull. 224, 166–183.

Farley, G.S., Levitan, D.R., 2001. The role of jelly coats in sperm-egg encounters, fertilization success, and selection on egg size in broadcast spawners. Am. Nat. 157, 626–636. doi:10.1086/320619

Fitzpatrick, J.L., Lüpold, S., 2014. Sexual selection and the evolution of sperm quality. Mol. Hum. Reprod. 20, 1180–1189. doi:10.1093/molehr/gau067

Fitzpatrick, J.L., Simmons, L.W., Evans, J.P., 2012. Complex patterns of multivariate selection on the ejaculate of a broadcast spawning marine invertebrate. Evolution (N. Y). 66, 2451–2460. doi:10.5061/dryad.307c3n10

Foltz, K.R., Lennarz, W.J., 1990. Purification and characterization of an extracellular fragment of the sea urchin egg receptor for sperm. J. Cell Biol. 111, 2951–2959. doi:10.1083/jcb.111.6.2951

Franke, E.S., Babcock, R.C., Styan, C.A., 2002. Sexual conflict and polyspermy under sperm-limited conditions: in situ evidence from field simulations with the free-spawning marine echinoid Evechinus chloroticus. Am. Nat. 160, 485–96. doi:10.1086/342075

Friedrich, B.M., Julicher, F., 2007. Chemotaxis of sperm cells. Proc. Natl. Acad. Sci. 104, 13256–13261. doi:10.1073/pnas.0703530104

Gage, M.J.G., Macfarlane, C.P., Yeates, S., Ward, R.G., Searle, J.B., Parker, G. a., 2004. Spermatozoal traits and sperm competition in Atlantic salmon. Curr. Biol. 14, 44–47. doi:10.1016/j.cub.2003.12.028

Garbers, D.L., Hardman, J.G., 1976. Effects of egg factors on cyclic nucleotide metabolism in sea urchins. J. Cyclic Nucleotide Res. 2, 59–70.

Garbers, D.L., Watkins, H.D., Hansbrough, J.R., Smith, A., Misono, K.S., 1982. The amino acid sequence and chemical synthesis of speract and of speract analogues. J. Biol. Chem. 257, 2734–2737.

Gray, J., 1928. The Effect of Egg-Secretions on the Activity of Spermatozoa. BJEB 362–365.

Guerrero, A., Espinal, J.J., Wood, C.D., Rendon, J.M., Carneiro, J., Martínez-Mekler, G., Darszon, A., Rendón, J.M., Carneiro, J., Martínez-Mekler, G., Darszon, A., 2013. Niflumic acid disrupts marine spermatozoan chemotaxis without impairing the spatiotemporal detection of chemoattractant gradients. J. Cell Sci. 126, 1477–1487. doi:10.1242/jcs.121442

Guerrero, A., Nishigaki, T., Carneiro, J., Tatsu, Y., Wood, C.D., Darszon, A., 2010. Tuning sperm chemotaxis by calcium burst timing. Dev. Biol. 344, 52–65.

Hansbrough, J.R., Garbers, D.L., 1981. Speract: purification and characterization of a peptide associated with eggs

that activates spermatozoa. J. Biol. Chem. 256, 1447–1452.

Harvey, E.B., 1956. The American Arbacia and Other Sea Urchins. Princeton University Press, Princeton, NJ.

Heck, D.E., Laskin, J.D., 2003. Ryanodine-Sensitive Calcium Flux Regulates Motility of Arbacia punctulata Sperm. Biol. Bull. 205, 185–186.

Hellberg, M.E., Dennis, A.B., Arbour-Reily, P., Aagaard, J.E., Swanson, W.J., 2012. the Tegula Tango: a Coevolutionary Dance of Interacting, Positively Selected Sperm and Egg Proteins. Evolution (N. Y). 66, 1681–94. doi:10.1111/j.1558-5646.2011.01530.x

Holt, W. V., Fazeli, a., 2015. Do sperm possess a molecular passport? Mechanistic insights into sperm selection in the female reproductive tract. Mol. Hum. Reprod. 21, 491–501. doi:10.1093/molehr/gav012

Hussain, Y.H., Guasto, J.S., Zimmer, R.K., Stocker, R., Riffell, J.A., 2016. Sperm chemotaxis promotes individual fertilization success in sea urchins. J. Exp. Biol. 1458–1466. doi:10.1242/jeb.134924

Jammalamadaka, S.R., Gupta, A. Sen, 2001. Topics in Circular Statistics. World Scientific Publishing Co, River Edge, NJ.

Johnson, D.W., Monro, K., Marshall, D.J., 2013. The maintenance of sperm variability: context-dependent selection on sperm morphology in a broadcast spawning invertebrate. Evolution (N. Y). 67, 1383–1395. doi:10.1111/evo.12022

Kashikar, N.D., Alvarez, L., Seifert, R., Gregor, I., Jäckle, O., Beyermann, M., Krause, E., Benjamin Kaupp, U., Kaupp, U.B., 2012. Temporal sampling, resetting, and adaptation orchestrate gradient sensing in sperm. J. Cell Biol. 198, 1075–91. doi:10.1083/jcb.201204024

Kaupp, U.B., Hildebrand, E., Weyand, I., 2006. Sperm chemotaxis in marine invertebrates — molecules and mechanisms. J. Cell. Physiol. 208, 487–494. doi:10.1002/jcp

Kaupp, U.B., Kashikar, N.D., Weyand, I., 2008. Mechanisms of Sperm Chemotaxis. Annu. Rev. Physiol. 70, 93–117.

Kaupp, U.B., Solzin, J., Hildebrand, E., Brown, J.E., Helbig, A., Hagen, V., Beyermann, M., Pampaloni, F., Weyand, I., 2003. The signal flow and motor response controling chemotaxis of sea urchin sperm. Nat. Cell Biol. 5, 109–117.

Kinoh, H., Shimizu, T., Fujimoto, H., Suzuki, N., 1994. Expression of a putative precursor mRNA for sperm-activating peptide I in accessory cells of the ovary in the sea urchin Hemicentrotus pulcherrimus. Roux's Arch. Dev. Biol. 381–388.

Kirkman-Brown, J.C., Sutton, K.A., Florman, H.M., 2003. How to attract a sperm. Nat. Cell Biol. 5, 93–6. doi:10.1038/ncb0203-93

Kopf, G.S., Tubb, D.J., Garbers, D.L., 1979. Activation of sperm respiration by a low molecular weight egg factor and 8-bromoguanosine 3'5'-monophosphate. J. Biol. Chem. 254, 8554–8560.

Kosman, E.T., Levitan, D.R., 2014. Sperm competition and the evolution of gametic compatibility in externally fertilizing taxa. Mol. Hum. Reprod. 20, 1190–1197. doi:10.1093/molehr/gau069

Kregting, L.T., Thomas, F.I.M., Bass, A.L., Yund, P.O., 2014. Relative Effects of Gamete Compatibility and Hydrodynamics on Fertilization in the Green Sea Urchin Strongylocentrotus droebachiensis. Biol. Bull. 227, 33–39.

Krug, P.J., Riffell, J.A., Zimmer, R.K., 2009. Endogenous signaling pathways and chemical communication between sperm and egg. J. Exp. Biol. 212, 1092–1100. doi:10.1242/jeb.027029

Lazova, M.D., Ahmed, T., Bellomo, D., Stocker, R., Shimizu, T.S., 2011. Response rescaling in bacterial chemotaxis. Proc. Natl. Acad. Sci. 108, 13870–13875. doi:10.1073/pnas.1108608108

Lessios, H.A., Lockhart, S., Collin, R., Sotil, G., Sanchez-Jerez, P., Zigler, K.S., Perez, A.F., Garrido, M.J., Geyer, L.B., Bernardi, G., Vacquier, V.D., Haroun, R., Kessing, B.D., 2012. Phylogeography and bindin evolution in Arbacia, a sea urchin genus with an unusual distribution. Mol. Ecol. 21, 130–144. doi:10.1111/j.1365-294X.2011.05303.x

Levitan, D.R., 2012. Contemporary evolution of sea urchin gamete-recognition proteins: experimental evidence of density-dependent gamete performance predicts shifts in allele frequencies over time. Evolution (N. Y). 66, 1722–1736. doi:10.5061/dryad.0k2469h8

Levitan, D.R., 2006. The relationship between egg size and fertilization success in broadcast-spawning marine invertebrates. Integr. Comp. Biol. 46, 298–311. doi:10.1093/icb/icj025

Levitan, D.R., 2004. Density-dependent sexual selection in external fertilizers: variances in male and female fertilization success along the continuum from sperm limitation to sexual conflict in the sea urchin Strongylocentrotus franciscanus. Am. Nat. 164, 298–309. doi:10.1086/423150

Levitan, D.R., 2002. Density-Dependent Selection on Gamete Traits in Three Congeneric Sea Urchins. Ecology 83, 464–479.

Levitan, D.R., 2000. Sperm velocity and longevity trade off each other and influence fertilization in the sea urchin Lytechinus variegatus. Proc. R. Soc. 267, 531–534. doi:10.1098/rspb.2000.1032

Levitan, D.R., 1996. Effects of gamete traits on fertilization in the sea and the evolution of sexual dimorphism. Nature 382, 153–155.

Levitan, D.R., Terhorst, C.P., Fogarty, N.D., 2007. The risk of polyspermy in three congeneric sea urchins and its implications for gametic incompatibility and reproductive isolation. Evolution (N. Y). 61, 2007–14. doi:10.1111/j.1558-5646.2007.00150.x

Lillie, F.R., 1915. Studies of fertilization: VII. analysis of variations in the fertilizing power of sperm suspensions of Arbacia. Biol. Bull. 28, 229–251.

Lillie, F.R., 1912. The production of sperm iso-agglutinins by ova. Science (80-.). 36, 527–530. doi:10.1126/science.36.929.527

Lishko, P. V., Botchkina, I.L., Kirichok, Y., 2011. Progesterone activates the principal Ca2+ channel of human sperm. Nature 471, 387–391.

Lund, U., Agostinelli, C., 2002. CircStats: Circular Statistics, from "Topics in Circular Statistics" (2001).

Lüpold, S., Pitnick, S., Berben, K.S., Blengini, C.S., Belote, J.M., Manier, M.K., 2013. Female mediation of competitive fertilization success in Drosophila melanogaster. Proc. Natl. Acad. Sci. 110. doi:10.1073/pnas.1300954110

Manier, M.K., Belote, J.M., Berben, K.S., Novikov, D., Stuart, W.T., Pitnick, S., 2010. Resolving mechanisms of competitive fertilization success in Drosophila melanogaster. Science (80-.). 328, 354–357. doi:10.1126/science.1187096

Metz, E.C., Gómez-Gutiérrez, G., Vacquier, V.D., 1998. Mitochondrial DNA and bindin gene sequence evolution among allopatric species of the sea urchin genus Arbacia. Mol. Biol. Evol. 15, 185–195.

Miller, R.L., 1997. Specificity of sperm chemotaxis among Great Barrier Reef shallow-water Holothurians and Ophiuroids. J. Exp. Zool. 279, 189–200. doi:10.1002/(SICI)1097-010X(19971001)279:2<189::AID-JEZ10>3.0.CO;2-B

Miller, R.L., 1985. Sperm chemo-orientation in the Metazoa, in: Metz, C. (Ed.), Biology of Fertilization, v.2: Biology of the Sperm. Elsevier Science, pp. 275–331.

Morita, M., Nishikawa, A., Nakajima, A., Iguchi, A., Sakai, K., Takemura, A., Okuno, M., 2006. Eggs regulate sperm flagellar motility initiation, chemotaxis and inhibition in the coral Acropora digitifera, A. gemmifera and A. tenuis. J. Exp. Biol. 209, 4574–9. doi:10.1242/jeb.02500

Narayanan, A.S., Anwar, R.A., 1969. The specificity of purified porcine pancreatic elastase. Biochem. J. 114, 11–17.

Nozawa, Y., Isomura, N., Fukami, H., 2015. Influence of sperm dilution and gamete contact time on the fertilization rate of scleractinian corals. Coral Reefs. doi:10.1007/s00338-015-1338-3

Oliver, M., Evans, J.P., 2014. Chemically moderated gamete preferences predict offspring fitness in a broadcast spawning invertebrate. Proc. R. Soc. 281, 20140148.

Palumbi, S.R., 1999. All males are not created equal: fertility differences depend on gamete recognition polymorphisms in sea urchins. Proc. Natl. Acad. Sci. 96, 12632–12637.

Pennington, J.T., 1985. The ecology of fertilization of echinoid eggs: the consequences of sperm dilution, adult aggregation, and synchronous spawning. Biol. Bull. 169, 417–430.

Pfeffer, W., 1903. The Physiology of Plants, 2, Volume ed. Clarendon Press.

Pichlo, M., Bungert-Plümke, S., Weyand, I., Seifert, R., Bönigk, W., Strünker, T., Kashikar, N.D., Goodwin, N., Müller, A., Pelzer, P., Van, Q., Enderlein, J., Klemm, C., Krause, E., Trötschel, C., Poetsch, A., Kremmer, E., Kaupp, U.B., 2014. High density and ligand affinity confer ultrasensitive signal detection by a guanylyl cyclase chemoreceptor. J. Cell Biol. 206, 541–57. doi:10.1083/jcb.201402027

Podolsky, R.D., 2001. Evolution of egg target size: an analysis of selection on correlated characters. Evolution (N. Y). 55, 2470–2478.

Qasaimeh, M.A., Gervais, T., Juncker, D., 2011. Microfluidic quadrupole and floating concentration gradient. Nat. Commun. 2.

R Core Team, 2013. R: A language and environment for statistical computing.

Ralt, D., Goldenberg, M., Fetterolf, P., Thompson, D., Dor, J., Mashiach, S., Garbers, D.L., Eisenbach, M., 1991. Sperm attraction to a follicular factor(s) correlates with human egg fertilizability. Proc. Natl. Acad. Sci. 88, 2840–2844.

Ramarao, C.S., Burks, D.J., Garbers, D.L., 1990. A single mRNA encodes multiple copies of the egg peptide speract. Biochemistry 29, 3383–3388.

Riffell, J.A., Krug, P.J., Zimmer, R.K., 2004. The ecological and evolutionary consequences of sperm

chemoattraction. Proc. Natl. Acad. Sci. 101, 4501–4506.

Riffell, J.A., Krug, P.J., Zimmer, R.K., 2002. Fertilization in the sea: the chemical identity of an abalone sperm attractant. J. Exp. Biol. 205, 1439–1450.

Rosen, W.G., 1962. Cellular Chemotropism and Chemotaxis. Q. Rev. Biol. 37, 242–259.

Rosman, J.H., Koseff, J.R., Monismith, S.G., Grover, J., 2007. A field investigation into the effects of a kelp forest (Macrocystis pyrifera) on coastal hydrodynamics and transport. J. Geophys. Res. 112, 1–16. doi:10.1029/2005JC003430

Rothschild, Lord, 1956. Fertilization. John Wiley & Sons, Inc, New York.

Sawada, H., Inoue, N., Iwano, M. (Eds.), 2014. Sexual Reproduction in Animals and Plants, Sexual Reproduction in Animals and Plants. Springer Japan, Tokyo. doi:10.1007/978-4-431-54589-7

Schmell, E.L.I., Earles, B.J., Breaux, C., Lennarz, W.J., William, J., Lennarz, W.J., 1977. Identification of a sperm receptor on the surface of the eggs of the sea urchin Arbacia punctulata. J. Cell Biol. 72, 35–46. doi:10.1083/jcb.72.1.35

Seltman, H.J., 2015. Experimental Design and Analysis. Carnegie Mellon University, Pittsburgh, PA.

Shiba, K., Baba, S.A., Inoue, T., Yoshida, M., 2008. Ca 2+ bursts occur around a local minimal concentration of attractant and trigger sperm chemotactic response. Proc. Natl. Acad. Sci. 105, 19312–19317.

Shimomura, H., Dangott, L.J., Garbers, D.L., 1986a. Covalent Coupling of a Resact Analogue to Guanylate Cyclase *. J. Biol. Chem. 261, 15778–15782.

Shimomura, H., Suzuki, N., Garbers, D.L., 1986b. Derivatives of speract are associated with the eggs of Lytechinus pictus sea urchins. Peptides 7, 491–495.

Simmons, L.W., Fitzpatrick, J.L., 2012. Sperm wars and the evolution of male fertility. Reproduction 144, 519–534. doi:10.1530/REP-12-0285

Simpson, J.L., Humphries, S., Evans, J.P., Simmons, L.W., Fitzpatrick, J.L., 2014. Relationships between sperm length and speed differ among three internally and three externally fertilizing species. Evolution (N. Y). 68, 92–104. doi:10.1111/evo.12199.This

Snook, R.R., 2005. Sperm in competition: not playing by the numbers. Trends Ecol. Evol. 20, 46–53. doi:10.1016/j.tree.2004.10.011

Spehr, M., Gisselmann, G., Poplawski, A., Riffell, J.A., Wetzel, C.H., Zimmer, R.K., Hatt, H., 2003. Identification of a testicular odorant receptor mediating human sperm chemotaxis. Science (80-.). 299, 2054–2058. doi:10.1126/science.1080376

Starkweather, J., 2010. Linear Mixed Effects Modeling using R. Univ. North Texas.

Strathmann, M.F., 1987. Reproduction and Development of Marine Invertebrates of the Northern Pacific Coast. University of Washington Press, Seattle, WA.

Strünker, T., Alvarez, L., Kaupp, U.B., 2015. At the physical limit — chemosensation in sperm. Curr. Opin. Neurobiol. 110–116. doi:10.1016/j.conb.2015.02.007

Suarez, S.S., Pacey, A.A., 2006. Sperm transport in the female reproductive tract. Hum. Reprod. Updat. 12, 23–37.

Suzuki, N., 1995. Structure, Function, and Biosynthesis of Sperm-Activating Peptides and Fucose Sulfate Glycoconjugate in the Extracellular Coat of Sea Urchin Eggs. Zoolog. Sci. 12, 13–27.

Suzuki, N., Garbers, D.L., 1984. Stimulation of sperm respiration rates by speract and resact at alkaline extracellular pH. Biol. Reprod. 30, 1167–74.

Suzuki, N., Shimomura, H., Radany, E.W., Ramarao, C.S., Ward, G.E., Bentley, J.K., Garbers, D.L., 1984. A peptide associated with eggs causes a mobility shift in a major plasma membrane protein of spermatozoa. J. Biol. Chem. 259, 14874–14879.

Swanson, W.J., Nielsen, R., Yang, Q., 2003. Pervasive adaptive evolution in mammalian fertilization proteins. Mol. Biol. Evol. 20, 18–20.

Swanson, W.J., Vacquier, V.D., 2002. The rapid evolution of reproductive proteins. Nat. Rev. Genet. 3, 137–144. doi:10.1038/nrg/733

Swanson, W.J., Yang, Z., Wolfner, M.F., Aquadro, C.F., 2001. Positive Darwinian selection drives the evolution of several female reproductive proteins in mammals. Proc. Natl. Acad. Sci. 98, 2509–2514.

Thomas, F.I.M., 1994. Physical Properties of Gametes in Three Sea Urchin Species. J. Exp. Mar. Bio. Ecol. 194, 263–84.

Thomas, F.I.M., Kregting, L.T., Badgley, B.D., Donahue, M.J., Yund, P.O., 2013. Fertilization in a sea urchin is not only a water column process: effects of water flow on fertilization near a spawing female. Mar. Ecol. Prog. Ser. 494, 231–240. doi:10.3354/meps10601

Tvedt, H.B., Benfey, T.J., Martin-Robichaud, D.J., Power, J., 2001. The relationship between sperm density, spermatocrit, sperm motility and fertilization success in Atlantic halibut, Hippoglossus hippoglossus.

Aquaculture 194, 191–200. doi:10.1016/S0044-8486(00)00516-0

Vacquier, V.D., 1998. Evolution of Gamete Recognition Proteins. Science (80-.). 281, 1995–1998. doi:10.1126/science.281.5385.1995

Vacquier, V.D., Moy, G.W., 1977. Isolation of bindin: the protein responsible for adhesion of sperm to sea urchin eggs. Proc. Natl. Acad. Sci. 74, 2456–2460.

van der Horst, G., Maree, L., 2013. Sperm form and function in the absence of sperm competition. Mol. Reprod. Dev. 81, 204–216. doi:10.1002/mrd.22277

Veitinger, T., Riffell, J.A., Veitinger, S., Nascimento, J.M., Triller, A., Chandsawangbhuwana, C., Schwane, K., Geerts, A., Wunder, F., Berns, M.W., Neuhaus, E.M., Zimmer, R.K., Spehr, M., Hatt, H., 2011. Chemosensory Ca2+ Dynamics Correlate with Diverse Behavioral Phenotypes in Human Sperm. J. Biol. Chem. 286, 17311–17325.

Vinauger, C., Lutz, E.K., Riffell, J. a, 2014. Olfactory learning and memory in the disease vector mosquito, Aedes aegypti. J. Exp. Biol. 217, 2321–2330. doi:10.1242/jeb.101279

Ward, G.E., Brokaw, C.J., Garbers, D.L., Vacquier, V.D., 1985. Chemotaxis of Arbacia punctulata spermatozoa to resact, a peptide from the egg jelly layer. J. Cell Biol. 101, 2324–2329.

Watkins, H.D., Kopf, G.S., Garbers, D.L., 1978. Activation of sperm adenylate cyclase by factors associated with eggs. Biol. Reprod. 19, 890–894.

Wilburn, D.B., Swanson, W.J., 2016. From molecules to mating: Rapid evolution and biochemical studies of reproductive proteins. J. Proteomics 135, 12–25. doi:10.1016/j.jprot.2015.06.007

Wood, C.D., Darszon, A., Whitaker, M., 2003. Speract induces calcium oscillations in the sperm tail. J. Cell Biol. 161, 89–101.

Xiang, X., Kittelson, A., Olson, J., Bieber, A., Chandler, D., 2005. Allurin, a 21 kD sperm chemoattractant, is rapidly released from the outermost jelly layer of the Xenopus egg by diffusion and medium convection. Mol. Reprod. Dev. 70, 344–60. doi:10.1002/mrd.20201

Yanagimachi, R., Cherr, G., Matsubara, T., Andoh, T., Harumi, T., Vines, C., Pillai, M., Griffin, F., Matsubara, H., Weatherby, T., Kaneshiro, K., 2013. Sperm attractant in the micropyle region of fish and insect eggs. Biol. Reprod. 88, 47. doi:10.1095/biolreprod.112.105072

Yeates, S.E., Diamond, S.E., Einum, S., Emerson, B.C., Holt, W. V., Gage, M.J.G., 2013. Cryptic choice of conspecific sperm controlled by the impact of ovarian fluid on sperm swimming behavior. Evolution (N. Y). 67, 3523–3536. doi:10.1111/evo.12208

Yoshida, M., Hiradate, Y., Sensui, N., Cosson, J., Morisawa, M., 2013. Species-specificity of sperm motility activation and chemotaxis: a study on ascidian species. Biol. Bull. 224, 156–165.

Yoshida, M., Kawano, N., Yoshida, K., 2008. Control of sperm motility and fertility: diverse factors and common mechanisms. Cell. Mol. Life Sci. 65, 3446–3457. doi:10.1007/s00018-008-8230-z

Yoshida, M., Yoshida, K., 2011. Sperm chemotaxis and regulation of flagellar movement by Ca2+. Mol. Hum. Reprod. 17, 457–465.

Yoshino, K., Takao, T., Shimonishi, Y., Suzuki, N., 1991. Determination of the amino acid sequence of an intramolecular disulfide linkage-containing sperm-activating peptide by tandem mass spectrometry. FEBS Lett. 294, 179–82.

Zigler, K.S., McCartney, M.A., Levitan, D.R., Lessios, H.A., 2005. Sea urchin bindin divergence predicts gamete compatibility. Evolution (N. Y). 59, 2399–2404.

Zimmer, R.K., Riffell, J.A., 2011. Sperm Chemotaxis, Fluid Shear, and the Evolution of Sexual Reproduction. Proc. Natl. Acad. Sci. 108, 13200–13205.

Zuur, A.F., Ieno, E.N., Walker, N.J., Saveliev, A.A., Smith, G.M., 2009. Mixed Effects Models and Extensions in Ecology with R, Statistics for Biology and Health. Springer New York, New York, NY. doi:10.1007/978-0-387-87458-6

Summary

Fertilization is a critical point in the life cycle of sexually-reproducing organisms, the link between generations. The phenomenon of sperm chemotaxis, in which sperm are guided to eggs by egg-derived chemical signals, has been well-studied in sea urchins for over a century, yielding insight into the peptide chemoattractants produced by eggs and the molecular mechanisms of the signaling cascade response in sperm. Sea urchins have been an excellent model for this work because of their viability in lab studies and their broadcast-spawning behavior which leaves few other pre-gamete-encounter variables to contend with. I was surprised to learn how much scientists in 1912 understood about fertilization in sea urchins but am also surprised at how much more we have to learn.

Previous work has identified egg-derived chemoattractants, elucidated the mechanism of sperm response, and documented the effects of chemoattractant on sperm behavior. However, we knew very little about the variability between individual female and male sea urchins and how differences in their gametes might affect chemoattraction and chemotaxis. My dissertation is a contribution to filling this gap – I investigated

(i) the differences in sperm chemotactic ability between individual males and how those differences change relative fertilization success,

(ii) the variability in chemoattractant production from eggs of individual females and how those differences contribute to sperm chemoattraction, and

(iii) the behavior and physiology of sperm in chemoattractant gradients to understand the constraints of chemotactic response.

I found that

(i) variability in sperm chemotactic ability correlates with the relative fertilization success

of individual males,

(ii) individual females vary in their production of sperm chemoattractants, which changes

the *in vivo* attractant gradient and potential sperm behavior, and

(iii) sea urchin sperm respond chemotactically to very low attractant concentrations but

also display individual differences in behavioral response.

The results of my work open the door to future studies such as: investigating the interactions

between multiple chemoattractants in a single species, seeing if the effects of sperm chemotaxis

on individual male fertilization success are more pronounced in competitive fertilization assays,

pinpointing the source of regulation of egg chemoattractant production, and determining the

effects of female differences in attractant production on their individual fertilization success. The

more we learn, the more questions arise; my dissertation has answered several questions about

sperm chemotaxis and the field has a long list of questions ahead.